

Novel functions of SUN1

Inaugural-Dissertation

zur

Erlangung des Doktorgrades

der Mathematisch-Naturwissenschaftlichen Fakultät

der Universität zu Köln



vorgelegt von

Ping Li

aus

Taiyuan, Shanxi, China

Köln, 2015

Berichterstatter: Prof. Dr. Angelika A. Noegel

Berichterstatter: Prof. Dr. Mirka Uhlova

Vorsitzender: Prof. Dr. Michael Nothnagel

Tag der mündlichen Prüfung: 29. 06. 2015

The present research work was carried out from October 2011 to February 2015 at the Centre for Biochemistry, Institute of Biochemistry I, Medical Faculty, University of Cologne, Cologne, Germany, under the supervision of Prof. Dr. Angelika A. Noegel.

Die vorliegende Arbeit wurde in der Zeit von Oktober 2011 bis Februar 2015 unter der Anleitung von Prof. Dr. Angelika A. Noegel am Biochemischen Institut I der Medizinischen Fakultät der Universität zu Köln angefertigt.

Contents

1. Introduction.....	1
1.1 The nuclear envelope	1
1.1.1 The LINC complex.....	2
1.1.1.1 <i>SUN domain proteins</i>	3
1.1.1.2 <i>KASH domain proteins</i>	4
1.1.2 Nuclear pore complexes (NPCs)	6
1.1.3 Lamins and other nuclear envelope proteins.....	7
1.2 Nuclear envelope and human disease	8
1.3 Nuclear envelope and mRNA export.....	9
1.3.1 mRNA transcription and processing	10
1.3.2 Targeting and translocating through the NPC.....	12
1.3.3 Releasing into the cytoplasm and linking to translation	12
1.4 Aims of this work	14
2. Results	15
2.1 Contribution of SUN1 mutations to the pathomechanism in muscular dystrophies	15
2.1.1 Patient information.....	15
2.1.2 The patient cells have defects in cell proliferation and cell size.....	16
2.1.3 The patient cells show differences in centrosome distance and senescence	17
2.1.4 Heat shock induces severe nuclear shape alterations in patient cells.....	19
2.1.5 Cell migration is altered in patient cells in an in vitro wound healing assay	20
2.1.6 Transcript and protein levels but not localization of LINC components and binding partners are altered in patient cells	21
2.1.7 Analysis of SUN1 mutations.....	24
2.1.8 The mutations in SUN1 affect the interactions with Emerin and Lamin A/C	27
2.2 Inner nuclear envelope protein SUN1 plays a prominent role in mammalian mRNA export.....	29
2.2.1 SUN1 and SUN2 interact with hnRNP F/H and hnRNP K/J	29

2.2.2 hnRNP F/H and hnRNP K accumulate in the nucleus by SUN1 depletion	31
2.2.3 RNA fluorescence in situ hybridization (FISH) reveals nuclear accumulation of poly(A)+RNA in SUN1 absent cells	32
2.2.4 SUN1 functions in mRNA export independent of the CRM1-dependent pathway	33
2.2.5 SUN1 associates with nuclear mRNP through a direct interaction with NXF1, a general mRNA export factor in mammals	36
2.2.6 SUN1 associates with the NPC through a direct interaction with Nup153, a nuclear FG nucleoporin at the NPC basket involved in mRNA export	38
3. Discussion	41
3.1 Contribution of SUN1 mutations to the pathomechanism in muscular dystrophies	41
3.2 Inner nuclear envelope protein SUN1 plays a prominent role in mammalian mRNA export.....	42
3.2.1 Both SUN1 and SUN2 interact with hnRNP F/H and hnRNP K/J which accumulate in the nucleus by SUN1 depletion.....	42
3.2.2 SUN1 is important for mRNA export	45
3.2.3 SUN1 functions in mRNA export independent of the CRM1-dependent export pathway	45
3.2.4 NXF1 mediates the association between SUN1 and mRNP.....	46
3.2.5 SUN1 hands the mRNP over to the NPC component Nup153	47
4. Summary.....	51
5. Materials and Methods	54
5.1 Materials	54
5.1.1 Human cells.....	54
5.1.2 Bacterial strains	54
5.1.3 Vectors and plasmids	54
5.1.4 Oligonucleotides.....	54
5.1.5 Enzymes	55
5.1.6 Kits	56
5.1.7 Antibiotics	56

5.1.8 Chemicals	56
5.1.9 Primary antibodies.....	58
5.1.10 Secondary antibodies.....	59
5.2 Molecular biological methods	59
5.2.1 Polymerase Chain Reaction (PCR)	59
5.2.2 Site-directed mutagenesis.....	60
5.2.3 Agarose gel electrophoresis of DNA	60
5.2.4 Ligation of DNA fragments	61
5.2.5 Preparation of chemically competent <i>E. coli</i> cells	61
5.2.6 Transformation of chemically competent <i>E. coli</i> cells.....	62
5.2.7 Blue-white selection of transformants.....	62
5.2.8 Colony PCR.....	62
5.2.9 DNA-Mini-preparation from <i>E. coli</i>	62
5.2.10 Restriction analysis of DNA	63
5.2.11 DNA-Midi/Maxi preparation-Pure Yield™ Plasmid System	63
5.2.12 Measurement of DNA and RNA concentrations.....	64
5.2.13 Isolation of total RNA with TRIzol®	64
5.2.14 cDNA synthesis.....	64
5.2.15 Quantitative Real Time PCR (qRT-PCR).....	65
5.3 Mammalian cell culture methods and transfections	65
5.3.1 Cell culture and transfection	65
5.3.2 Thawing cells	65
5.3.3 Freezing cells.....	66
5.3.4 RNAi	66
5.4 Cell biological assays.....	66
5.4.1 Cell proliferation, cell cycle and cell size measurements	66
5.4.2 Senescence-associated β -galactosidase assay	67
5.4.3 Heat stress experiment	67
5.4.4 Cell migration analysis and wound-healing assay	68
5.5 Immunological and protein chemical methods.....	68
5.5.1 Immunofluorescence	68
5.5.2 Protein lysates from mammalian cells and western blotting.....	69

5.5.3 Subcellular fractionation	70
5.5.4 Co-immunoprecipitation (Co-IP)	70
5.5.5 Purification of recombinant proteins from <i>E. coli</i>	71
5.5.6 GST pulldown assay.....	72
5.5.7 Poly(A)+RNA isolation-Oligo (dT) pulldown assay	72
5.5.8 In situ hybridization	73
6. Appendix.....	75
7. Abbreviations	77
8. References.....	79
Acknowledgement.....	94
Erklärung	96
Lebenslauf.....	97

1. Introduction

1.1 The nuclear envelope

In the cell, the genome is physically separated from the cytoplasm by the nuclear envelope (NE) (Fig. 1.1). The nuclear envelope contains a double membrane, the inner nuclear membrane (INM) and the outer nuclear membrane (ONM) that connect at nuclear pores and form surround the lumen (perinuclear space, PNS) which is the continuation of the endoplasmic reticulum (ER) lumen (Razafsky et al., 2014). While the ONM is an extension of the rough ER and studded with ribosomes, the INM is lacking ribosomes and includes over 60 putative transmembrane proteins which insert in the INM and interact through their nucleoplasmic domains with the nuclear lamina and/or chromatin (Schirmer et al., 2003).

The ONM and INM dynamically fuse to create pores and the nuclear pore complexes (NPCs) are embedded inside (Capelson et al., 2010). The NE serves as selective channels for bidirectional transport (Aitchison and Rout, 2012; Grossman et al., 2012). Small molecules, less than ~40 kDa, may pass through the NE unimpededly. In contrast, larger molecules require specific receptors to enter or exit the nucleus (Fried and Kutay, 2003).

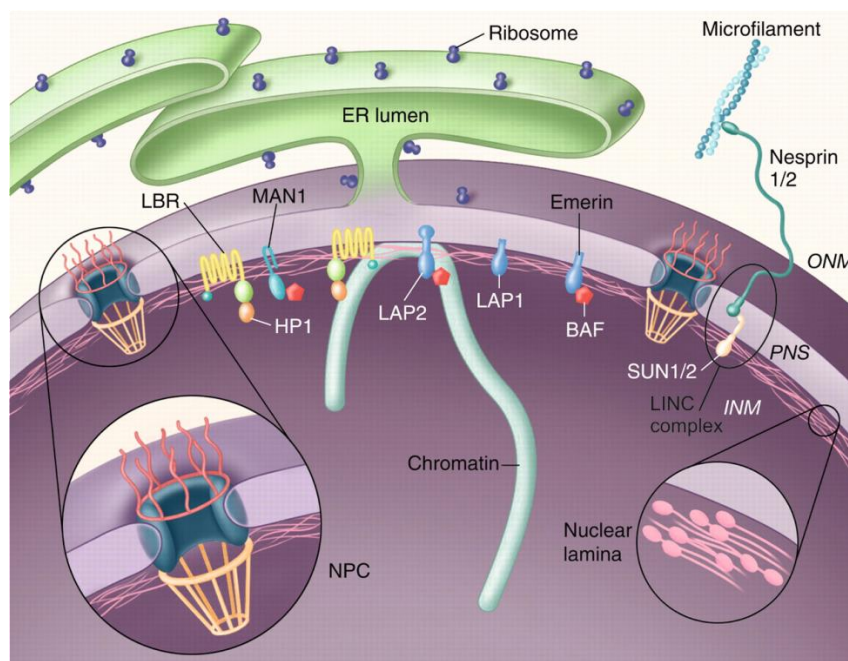


Figure 1.1 Organization of the nuclear envelope (modified from Stewart et al., 2007). The nuclear envelope consists of INM and ONM. Some selected INM proteins (LAP1, LAP2 and LBR) are shown which interact with HP1 and BAF to associate with chromatin. Lamins, the intermediate filament protein meshwork of the nucleus, and NPCs, formed by the ONM and INM fusion, are also shown. The LINC complex built by nesprin proteins in the ONM and SUN proteins in the INM is recognized as the linker of nucleoskeleton and cytoskeleton (Stewart et al., 2007).

1.1.1 The LINC complex

In eukaryotic cells, the nucleus is mechanically linked to the cytoskeleton by the LINC (Linker of Nucleoskeleton and Cytoskeleton) complex (Fig. 1.2). It is composed of SUN (Sad1 and UNC-84) domain protein in the INM and KASH (Klarsicht, ANC-1, and Syne homology) domain protein in the ONM. In the PNS, SUN and KASH domain proteins directly interact with each other to form a linker between the nucleo- and cytoskeleton through the NE. This interaction anchors the KASH domain protein in the ONM and prevents its diffusion into the ER. The N-terminus of KASH domain protein connects with the cytoplasm by interactions with different cytoskeletal proteins. Meanwhile, the N-terminus of SUN domain protein associates with the nucleoskeleton by interactions with A-type lamins, chromatin-binding proteins, and so on. These connections enable the LINC complex to mediate the communication and force transduction between nucleo- and cytoplasm. Briefly, LINC complex plays an important role in mechanical action and crosstalk between both sides of the NE (Chang et al., 2015; Rothballer and Kutay, 2013).

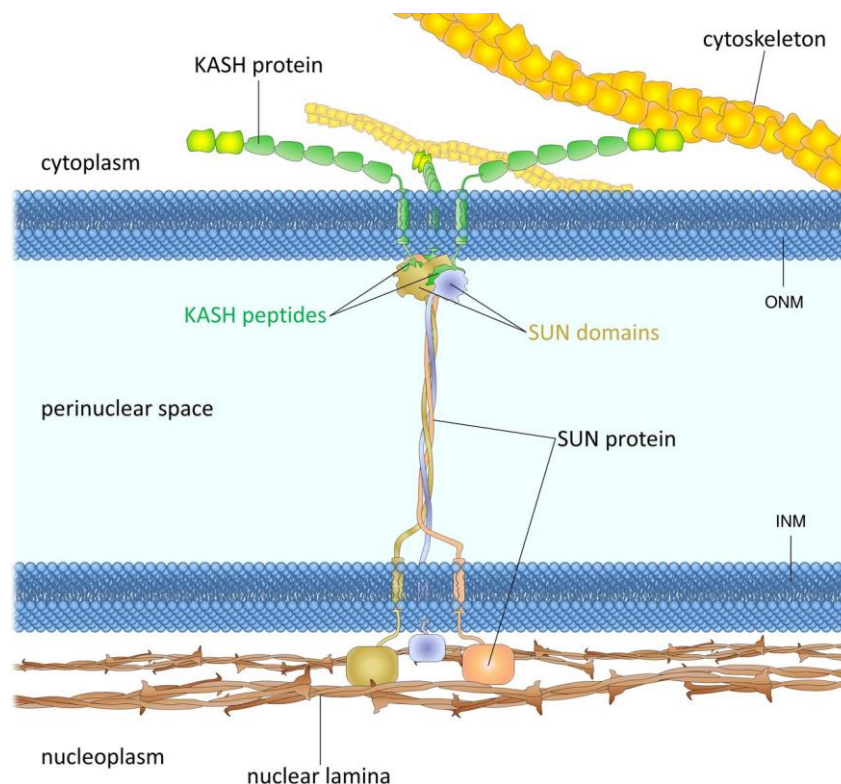


Figure 1.2 Schematic representation of the LINC complex (Chang et al., 2015). The LINC complex is composed of SUN domain protein and KASH domain protein. The homotrimeric SUN domains act as a tailored platform to provide the interaction with three KASH peptides. The N-termini of SUN protein and KASH protein interact with different elements on both sides of the NE respectively, enabling LINC complex to mediate the communication and force transduction between nucleo- and cytoplasm (Chang et al., 2015; Sosa et al., 2013).

1.1.1.1 SUN domain proteins

The INM components of LINC complexes are the SUN domain proteins. The SUN domain proteins are conserved type-II INM proteins and consist of N-terminus, coiled-coiled, transmembrane and SUN domain at the C-terminus in the lumen of NE (Mejat and Misteli, 2010; Tzur et al., 2006; Worman and Gundersen, 2006). SUN (Sad1 and UNC-84) proteins were originally identified in *S. pombe* (Sad1) (Hagan and Yanagida, 1995) and *Caenorhabditis elegans* (UNC-84) (Malone et al., 1999). Their remarkable feature is a ~200 amino acids containing domain at the C-terminus (Hagan and Yanagida, 1995).

Further, this region is named as SUN domain (Sad1-Unc84 homology, PFAM family PF03856), and found to be evolutionarily highly conserved from yeast to mammals: Mps3 in *S. cerevisiae* (Jaspersen et al., 2006); Sad1 in *S. pombe* (Hagan and Yanagida, 1995); Unc-84 and SUN1/MTF-1 (Matefin) in *C. elegans* (Malone et al., 1999) and Klaroid in *D. melanogaster* (Kracklauer et al., 2007) (Fig 1.3). So far, several SUN domain proteins have been reported in mammals including SUN1, SUN2, SUN3, SUN4 (SPAG4) and SUN5 (SPAG4L). The expression level of SUN1 and SUN2 are extensive in all tissues. However, for SUN3, the expression is special in testes and localization is restricted to the ER (Crisp et al., 2006). Similarly, SUN4 (SPAG4) is only found in spermatids, pancreas and testes (Shao et al., 1999) and SUN5 (SPAG4L) is uniquely expressed in testis as well (Frohnert et al., 2011).

Due to the aim of this project, we will emphasize the roles of SUN1 and SUN2 in mammals. The largest member of the SUN domain family SUN1 contains 812 amino acids corresponding to a molecular weight of ~90 kD, while SUN2 contains 717 amino acids with a molecular weight of ~80 kD. SUN1 and SUN2 display high homology up to 64% (Haque et al., 2006).

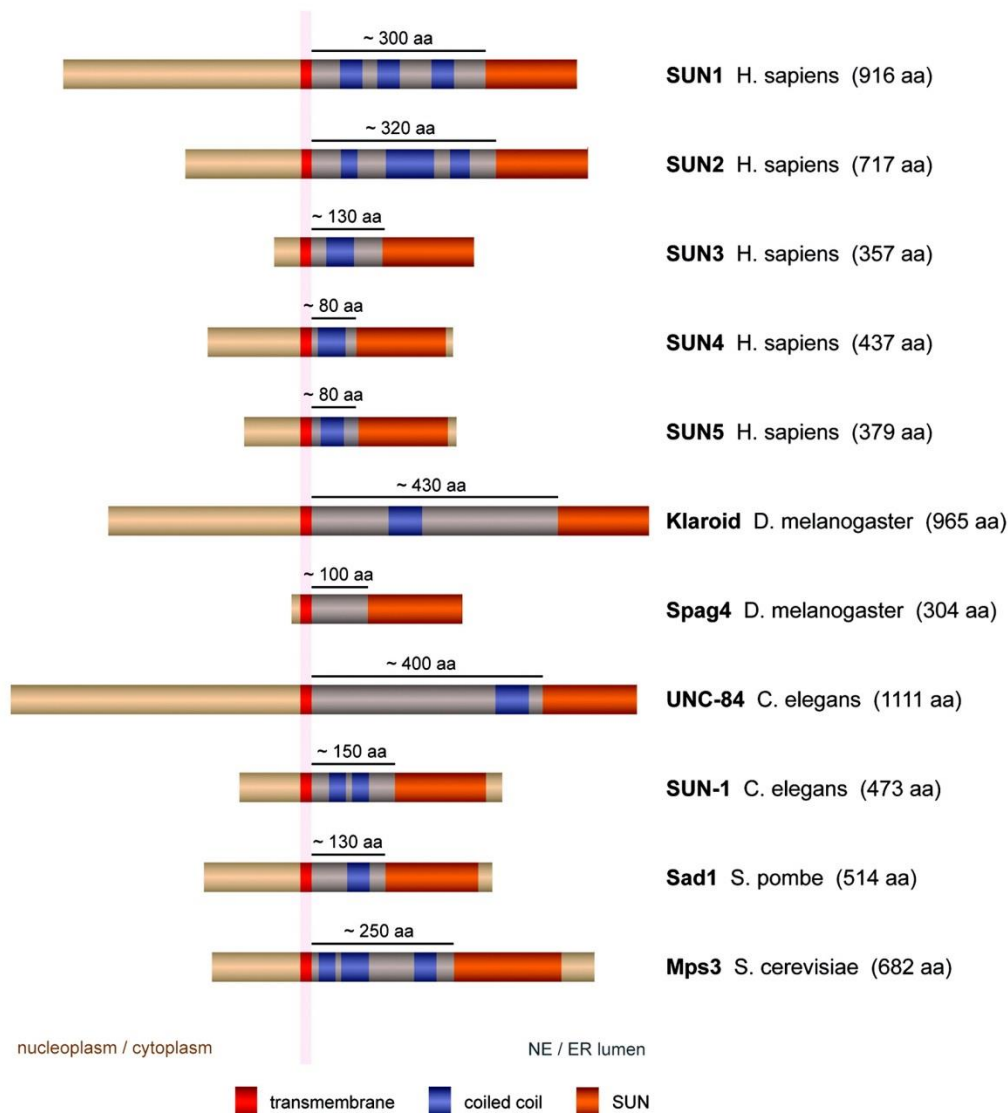


Figure 1.3 Evolutionarily highly conserved SUN domain proteins from yeast to mammals (Rothballer et al., 2013). All the SUN domain proteins contain the N-terminus (yellow) in the nucleoplasm, one transmembrane region (red) in the INM, and both the coiled coil region (blue) and the conserved SUN domain (orange) in the lumen of the NE/ER.

1.1.1.2 KASH domain proteins

The ONM components of the LINC complexes are the KASH domain proteins. The SUN domain interacts directly with the KASH domain in the PNS. The **KASH** (**K**larsicht/**A**nc-1, **S**yne **H**omology, PFAM family PF10541) domain is a transmembrane domain of ~60 amino acids followed by a luminal C-terminal extension of ~30 amino acids (Razafsky et al., 2014). Like SUN proteins, KASH domain proteins are also evolutionarily conserved and have been identified in *S. pombe* (Kms1/2), *S. cerevisiae* (Mps2), *C. elegans* (ZYG-12, UNC-83, ANC-1 and KDP-1), *D. melanogaster* (Klarsicht and Msp-300) and mammals (nesprin 1-4 and KASH5) (Mejat and Misteli, 2010; Morimoto et al., 2012).

In mammals, the KASH domain proteins are composed of nesprins 1-4 and KASH5 (Figure 1.4) encoded by five independent genes (*SYNE1-5*). Nesprins (**nuclear envelope spectrin-repeat proteins**) have many isoforms due to alternative splicing and transcription initiation (Apel et al., 2000; Morimoto et al., 2012; Roux et al., 2009; Wilhelmsen et al., 2005; Zhang et al., 2002). The expression levels of nesprin-1, -2 and -3 are comparatively high in all tissues. However, for nesprin-4, the expression is limited to secretory epithelial cells and hair cells of the inner ear (Roux et al., 2009), and KASH5 is specifically found in testis related to meiosis (Morimoto et al., 2012).

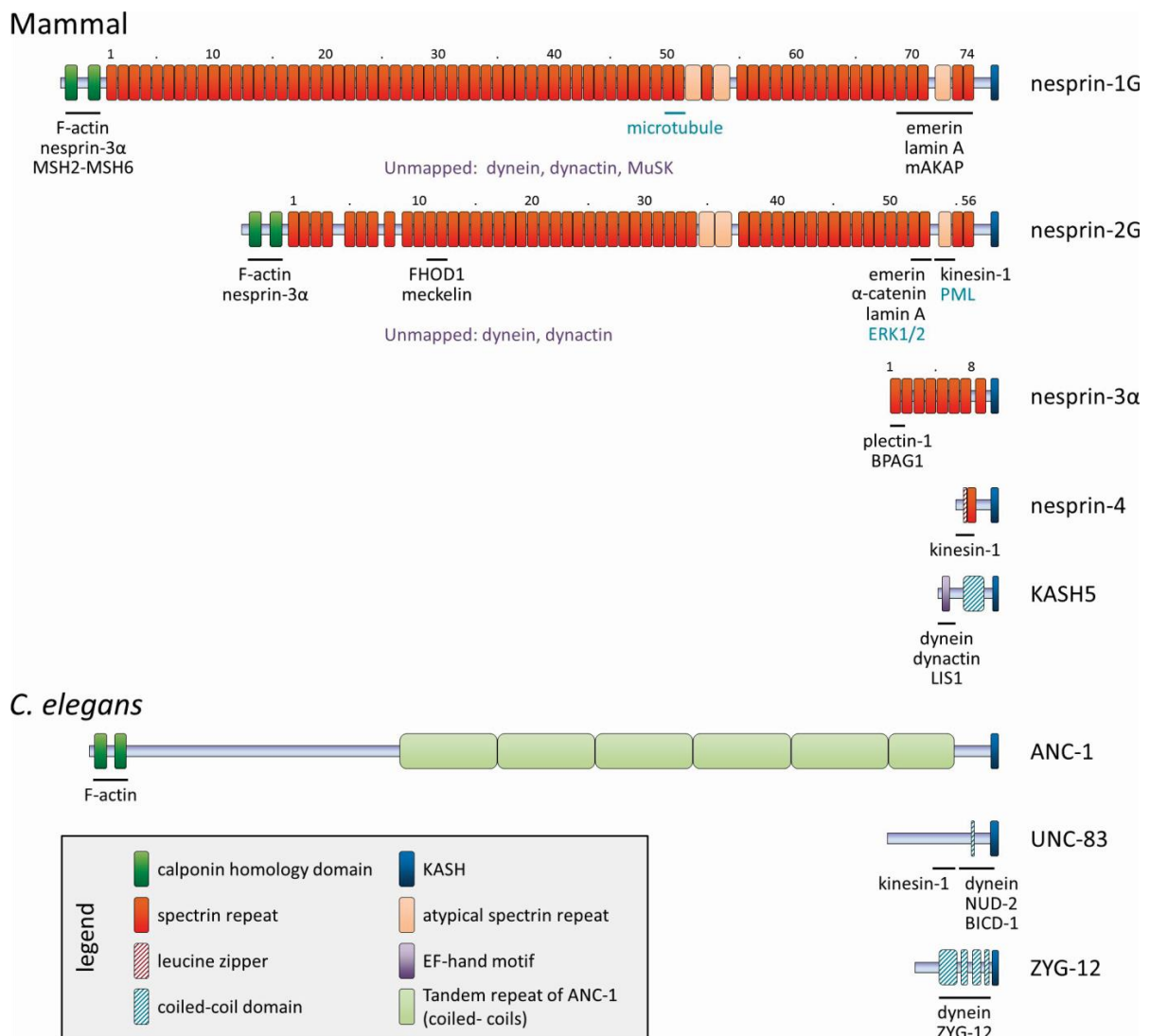


Figure 1.4 Overview of the KASH domain proteins and their interaction partners (Chang et al., 2015). The schematic of KASH domain proteins in mammals and *C. elegans* are shown. The binding regions for their interaction partners are indicated by the lines under the KASH proteins. “Unmapped” means the binding sites of these partners have not been identified. The CH domains in the giant KASH proteins (nesprin-1G, nesprin-2G, and ANC-1) is responsible for F-actin, microtubule motors, and signaling proteins binding. The interaction partners of some KASH domain missing isoforms are indicated in blue.

1.1.2 Nuclear pore complexes (NPCs)

The INM and ONM of the NE join and bend to form pores within which the NPCs embed (Wente and Rout, 2010). NPCs are large protein assemblies (~125 nm in diameter) with a molecular weight of 125 MDa in metazoa and 60 MDa in yeast and are constructed from multiple copies of ~30 different proteins named nucleoporins (Nups) (Kohler and Hurt, 2007). The NPC is an eightfold symmetrical cylindrical structure consisting of eight spokes surrounding a central tube and can be divided into three parts: the nuclear face, the central channel and the cytoplasmic face (Oeffinger and Zenklusen, 2012). The biggest part of the NPC is its central channel. Surrounding the central tube there are three main rings: two outer rings and one inner ring. The inner ring is located at the NPC's equator, and the two outer rings are separated by the inner ring at the nucleo- and cytoplasmic side, respectively. Both the nuclear side and the cytoplasmic side contain asymmetrical filamentous structures which link the NPC central channel to its molecular environment either in the nucleus or in the cytoplasm (Strambio-De-Castillia et al., 2010). According to the structure of the NPC, the Nups can be subdivided into four types: transmembrane Nups, core scaffold Nups, linker Nups and FG (Phe-Gly) Nups (Strambio-De-Castillia et al., 2010) (Figure 1.5).

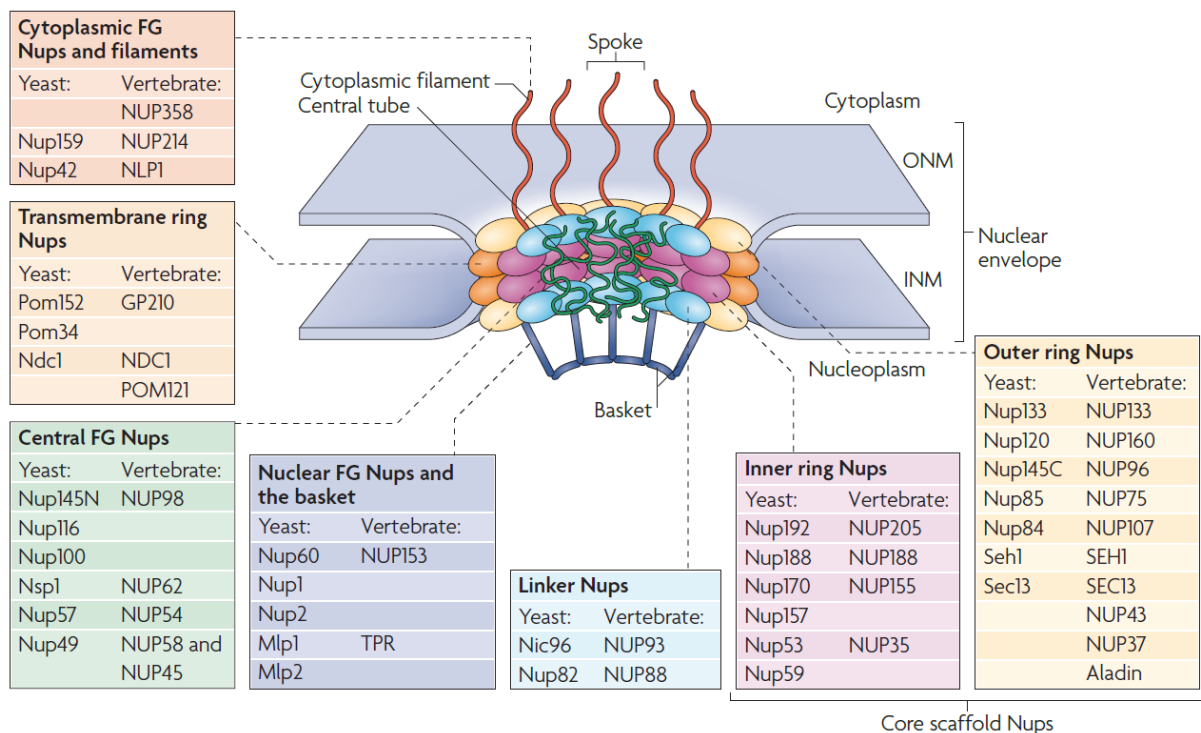


Figure 1.5 Schematic of the NPC (Strambio-De-Castillia et al., 2010). Each NPC is a symmetrical cylindrical structure comprising of eight spokes surrounding a central tube. The transmembrane ring structure made of transmembrane Nups anchor the NPC to the nuclear envelope. The core scaffold including the inner and the outer ring is constructed by the core scaffold Nups. The central FG (Phe-Gly) Nups locate at the surface of the

central tube from the nuclear to the cytoplasmic face. The linker Nups provide a connection between these FG Nups and the core scaffold of the NPC. Cytoplasmic filaments and the basket also made of FG Nups are the NPC-associated peripheral structures. For yeast and vertebrates, all Nups which have been identified in each NPC substructure are shown.

1.1.3 Lamins and other nuclear envelope proteins

In metazoan, the lamina is comprised of intermediate filament proteins called Lamins which are attached to the nuclear side of the INM (Brachner and Foisner, 2011) and are the major components of the nucleoskeleton (Dittmer and Misteli, 2011) (Figure 1.1). The nuclear lamina in mammals mainly include two types of lamins, A-type and B-type, which form a filamentous meshwork connecting with the INM. The A-type Lamins including lamins A, C, AΔ10, C2, and AΔ50 (also known as ‘progerin’) are generated by alternative splicing of *LMNA* (Bokenkamp et al., 2011; Dittmer and Misteli, 2011) while the B-type Lamins including lamins B1, B2 and B3 are encoded by different genes, *LMNB1* and *LMNB2* (Dittmer and Misteli, 2011; Schumacher et al., 2006). The nuclear lamina have several important roles such as connecting chromatin, interacting with signalling proteins and supporting epigenetic regulation, mechanotransduction, development, transcription, replication and DNA damage repair (Dechat et al., 2008; Dittmer and Misteli, 2011; Simon and Wilson, 2011).

LEM protein family members have been characterized along with other INM proteins (Wagner and Krohne, 2007). They are defined according to the presence of a common structural bihelical motif named as **LEM** [**LAP2** (lamina-associated polypeptide 2) / **emerin** / **MAN1**] domain (Laguri et al., 2001; Lin et al., 2000). In different experiments, the typical LEM domain always show strong interaction with BAF (barrier to autointegration factor) (Cai et al., 2001; Cai et al., 2007; Shumaker et al., 2001), an critical 10 kDa chromatin-associated protein identified in all metazoan (Margalit et al., 2007; Margalit et al., 2005; Zheng et al., 2000). Therefore, LEM domain proteins are considered to be dynamically associated with chromatin (Shimi et al., 2004), probably regulated by BAF phosphorylation (Bengtsson and Wilson, 2006; Gorjanacz et al., 2007; Nichols et al., 2006) and other unknown mechanisms so far (Figure 1.1).

1.2 Nuclear envelope and human disease

Due to the extensive cellular functions related to nucleo-cytoskeletal coupling, it is not surprised that mutations in LINC complex-associated proteins can result in a large number of human diseases (Isermann and Lammerding, 2013) (Figure 1.6). The majority of diseases are caused by mutations in the *LMNA* gene, encoding lamin A and C, collectively named laminopathies (Butin-Israeli et al., 2012; Worman, 2012). So far almost 400 different disease-causing mutations in A-type lamins have been identified, emphasizing their importance to cell and tissue biology and human physiology. The disease can affect specific tissues (striated muscle, adipose tissue, or peripheral nerves) or the whole body. To date, many laminopathies have been found including Emery-Dreifuss muscular dystrophy, dilated cardiomyopathy, limb-girdle muscular dystrophy, Charcot-Marie-Tooth, familial partial lipodystrophy or accelerated aging disorder Hutchinson-Gilford progeria syndrome (Schreiber and Kennedy, 2013). Clinically, overlapping phenotypes are also identified in these laminopathies (Ellis and Shackleton, 2011).

Diseases caused by mutations or gene duplications have been mapped to B-type lamins (Schreiber and Kennedy, 2013). Duplication of the *LMNB1* gene can result in adult onset leukodystrophy (Brussino et al., 2010; Molloy et al., 2012; Padiath et al., 2006; Schuster et al., 2011), or leukoencephalopathy (Brussino et al., 2009), characterized by demyelination in the central nervous system. Mutations in *LMNB2* cause increased sensitivity to acquired partial lipodystrophy, which involves a progressive loss of subcutaneous fat tissue (Gao et al., 2012; Hegele et al., 2006). The disease cause for the wide range of nuclear envelopathies is still unknown.

However, the mutations in emerin (*STA* or *EMD* gene), nesprin-1 (*Syne-1*) and nesprin-2 (*Syne-2*) can also affect striated muscle, resulting in Emery-Dreifuss muscular dystrophy and dilated cardiomyopathy, indicating a LINC complex-associated disease mechanism (Gundersen and Worman, 2013). Apart from these muscular disease, mutations in nesprin-1 can also cause autosomal recessive cerebellar ataxia (Gros-Louis et al., 2007) and arthrogyrosis (Attali et al., 2009), which is identified in congenital joint contractures resulting from reduced fetal movements. The expression of Nesprin-4 is restricted in secretory epithelial cells and hair cells of the inner ear (Roux et al., 2009), while its mutations can cause progressive high-frequency hearing loss and the phenotype also can be detected in mice deficient in either nesprin-4 or SUN1 (Horn et al., 2013). Among these diseases, cardiac and skeletal muscles are experienced especially high levels of mechanical stress; therefore,

nucleo-cytoskeletal coupling and nuclear mechanics might be important for the cause of the disease phenotype (Isermann and Lammerding, 2013; Schreiber and Kennedy, 2013).

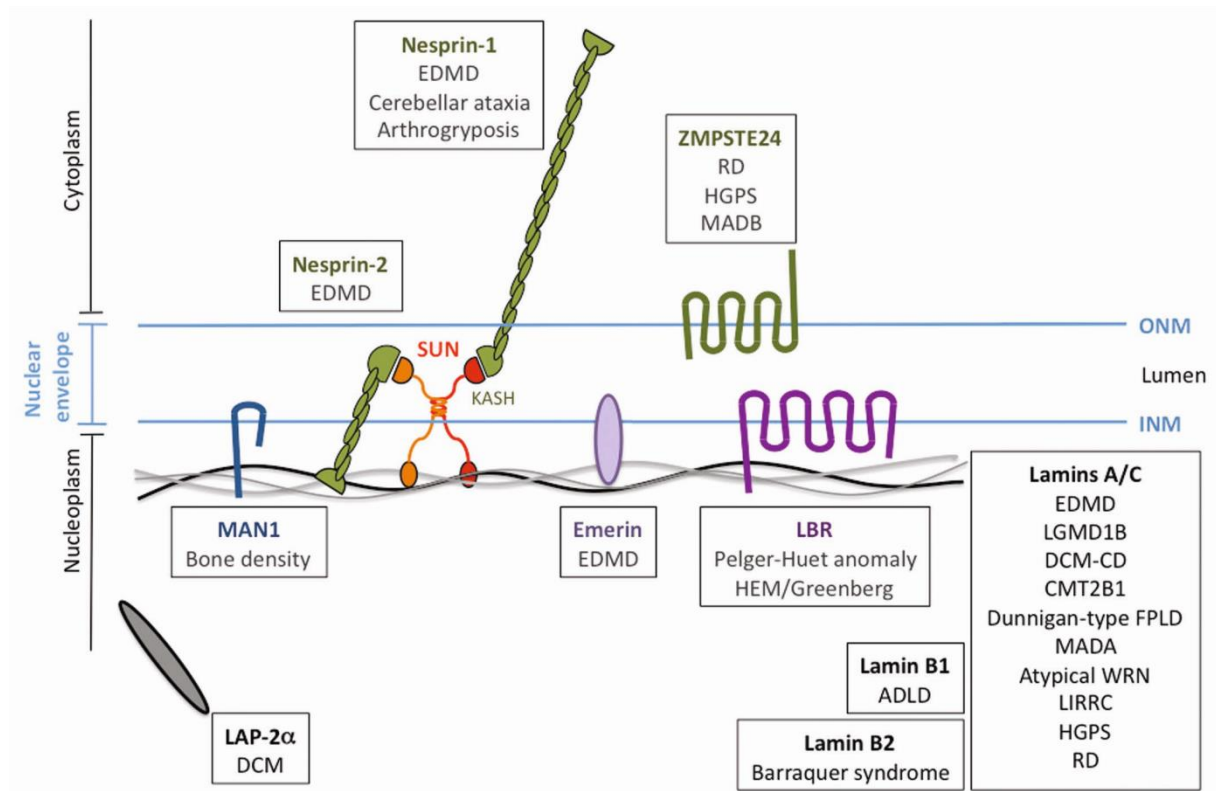


Figure 1.6 LINC complex-associated proteins involved human disease (Mejat and Misteli, 2010). “Envelopathies” means that the disease in human is caused by the mutations of the NE associated proteins. The names of the diseases caused by particular mutated proteins are shown.

1.3 Nuclear envelope and mRNA export

As we mentioned before, the nuclear envelope plays an important role in separating the inclusion of the nucleus from the cytoplasm. mRNA transcription takes place in the nucleus, while mRNA translation into functional protein happens in the cytoplasm (Hocine et al., 2010; Moore and Proudfoot, 2009). This spatial problem is settled by the efficient mRNA export from the nucleus into the cytoplasm (Natalizio and Wentz, 2013).

A crucial structure involved in the mRNA export process is the NPC present at the fusion point of the ONM and the INM (Capelson et al., 2010). The NPCs are embedded in the NE and have functions in selective material transport (Aitchison and Rout, 2012; Grossman et al.,

2012). For small molecules, like water, sugar and ions, the NPC channel is open and free for crossing, however, in case of bigger molecules (5-40 nm in diameter) such as proteins, rRNA and messenger ribonucleoprotein (mRNP), particular receptors are required for crossing the NPC (Aitchison and Rout, 2012; Guttler and Gorlich, 2011).

mRNA export is a multi-stage process in which the transcripts have to connect with the nucleoplasmic side of the NPC, the nuclear basket, translocate through the central channel, and be released from the cytoplasmic fibrils into the cytoplasm (Carmody and Wentz, 2009; Siddiqui and Borden, 2012; Strambio-De-Castillia et al., 2010). Therefore the nuclear export of mRNA transcripts can be divided into three different stages: first, pre-mRNA is packaged into mRNP complex after corrected transcription and processing; second, the mRNP targets and translocates through the central channel of NPC; third, the cytoplasmic fibrils release the mRNP into the cytoplasm for translation (Carmody and Wentz, 2009).

1.3.1 mRNA transcription and processing

Transcription is the first step of the mRNP formation. Many kinds of factors bind to the nascent mRNA transcript for helping transcriptional elongation. Some of the factors belong to heterogeneous nuclear ribonucleoproteins (hnRNPs) family. The hnRNPs are nuclear RNA-binding proteins with a high abundance in the cell. About 30 different hnRNPs have been found in human, while ~10 exist in *Saccharomyces cerevisiae* (Dreyfuss et al., 2002). The hnRNP proteins have various functions and accompany the mRNA at different stages during mRNP export (Dreyfuss et al., 2002). The nuclear restricted hnRNPs containing nuclear-retention signal are released from the mRNP and stay in the nucleus prior to export, while the shuttling hnRNPs accompany the mRNA through the NPC channel and into the cytoplasm, and then shuttle back to the nucleus (Carmody and Wentz, 2009; Dreyfuss et al., 2002) (Figure 1.7).

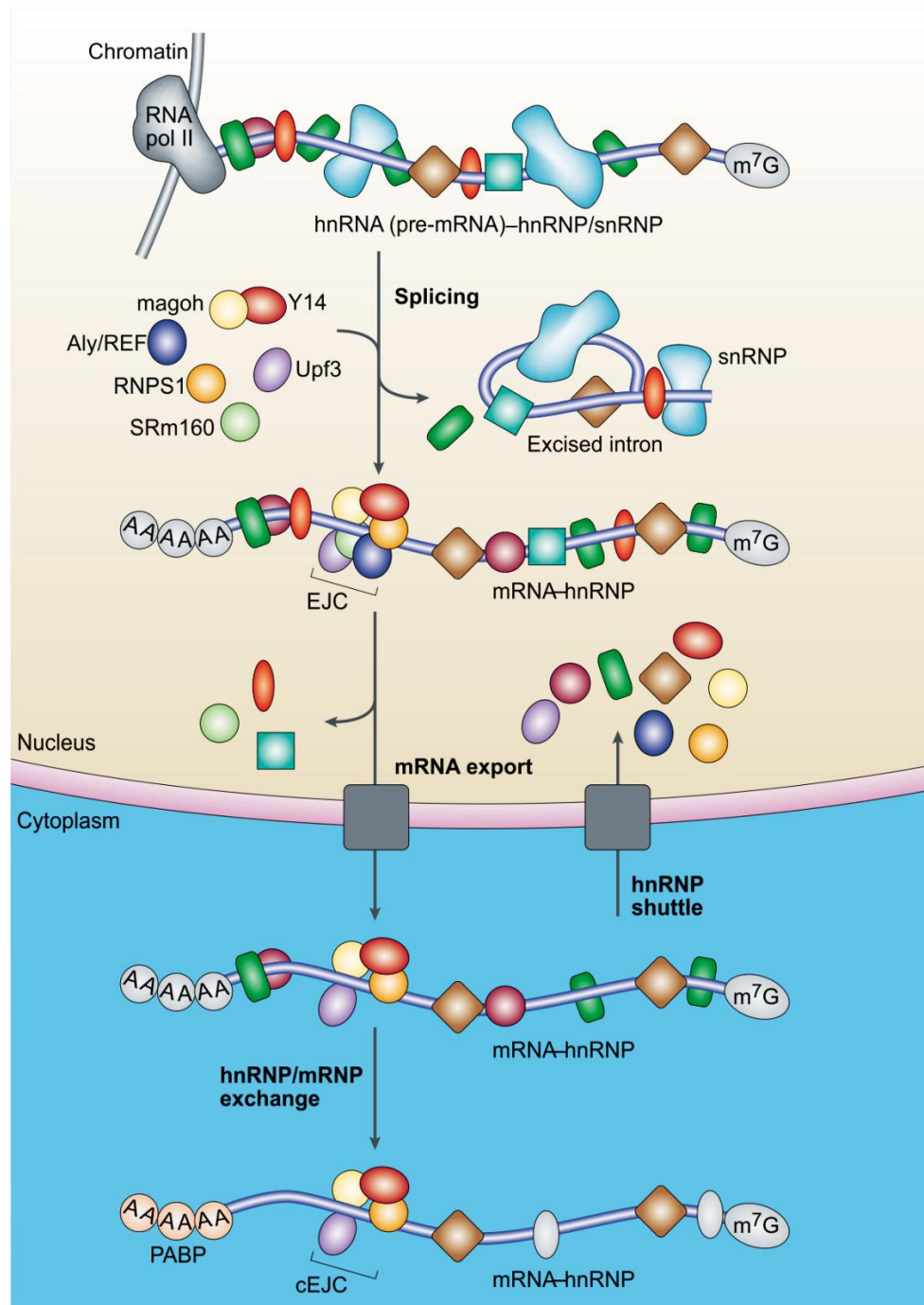


Figure 1.7 The hnRNPs and other factors required during mRNP export (Dreyfuss et al., 2002). Multifunction hnRNPs involved in transcription, processing, packaging, export and translation are shown. These hnRNPs accompany the mRNA at different steps during mRNP export. EJC, exon-exon junction complex; NMD, nonsense-mediated mRNA decay; RNA pol II, RNA polymerase II; snRNP, small nuclear ribonucleoprotein; PABP, poly(A)-binding protein; m⁷G, 5' 7- methylguanosine cap.

1.3.2 Targeting and translocating through the NPC

There are two major transport receptors involved in two distinct mRNA export pathways: NXF1 (nuclear RNA export factor 1, also known as TAP) and CRM1 (chromosome region maintenance 1, also known as exportin-1) (Carmody and Wentz, 2009; Culjkovic-Kraljacic and Borden, 2013; Kohler and Hurt, 2007; Natalizio and Wentz, 2013) (Figure 1.8). Based on the diversity of transport receptors, mRNA export can be roughly classified into two forms: bulk and specific export (Culjkovic-Kraljacic and Borden, 2013). Most of the constitutively expressed mRNAs are exported by the NXF1-dependent pathway (bulk export). There are at least three kinds of adaptor proteins, Aly/REF, GANP and SR (serine- and arginine-rich) proteins, attach NXF1 receptor and accelerate mRNA export (Culjkovic-Kraljacic and Borden, 2013; Wickramasinghe et al., 2010). By contrast, specialized subsets of mRNAs, uridine-rich small nuclear ribonucleoprotein particles (UsnRNAs), rRNAs, and signal recognition particle (SRP) RNA are exported by the CRM1-dependent pathway (specific export) (Natalizio and Wentz, 2013). Like NXF1, CRM1 also has multiple adaptors involved in mRNA export, such as HuR, eIF4E and NXF3 (Culjkovic et al., 2006; Hutten and Kehlenbach, 2007; Topisirovic et al., 2009; Yang et al., 2001).

1.3.3 Releasing into the cytoplasm and linking to translation

After passing through the central channel of the NPC, mRNP is released from the cytoplasmic fibrils to start translation which is the last step of the export (Carmody and Wentz, 2009). In the NXF1-dependent pathway, the mRNP cargo will be associated with the cytoplasmic fibrils of the NPC once it reaches the cytoplasmic face and then be released by these fibrils. Meanwhile, the export factors start recycling. The regulation of the process is crucial for the export efficiency. Nup358 (also referred to RanBP2) is one of the proteins forming the long fibrils at the cytoplasmic face of the NPC, providing the binding sites for NXF1 (Hutten and Kehlenbach, 2007; Wentz and Rout, 2010). In the CRM1-dependent pathway, the release of the mRNP into the cytoplasm requires the help from RanGAP (Ran GTPase-activating protein) and RanBP1 (or RanBP2) which enable GTP to be hydrolysed by Ran. The CRM1-cargo complex disassembles into mRNA and export factors, leaving mRNA to start translation and export factors to recycle (Hutten and Kehlenbach, 2007).

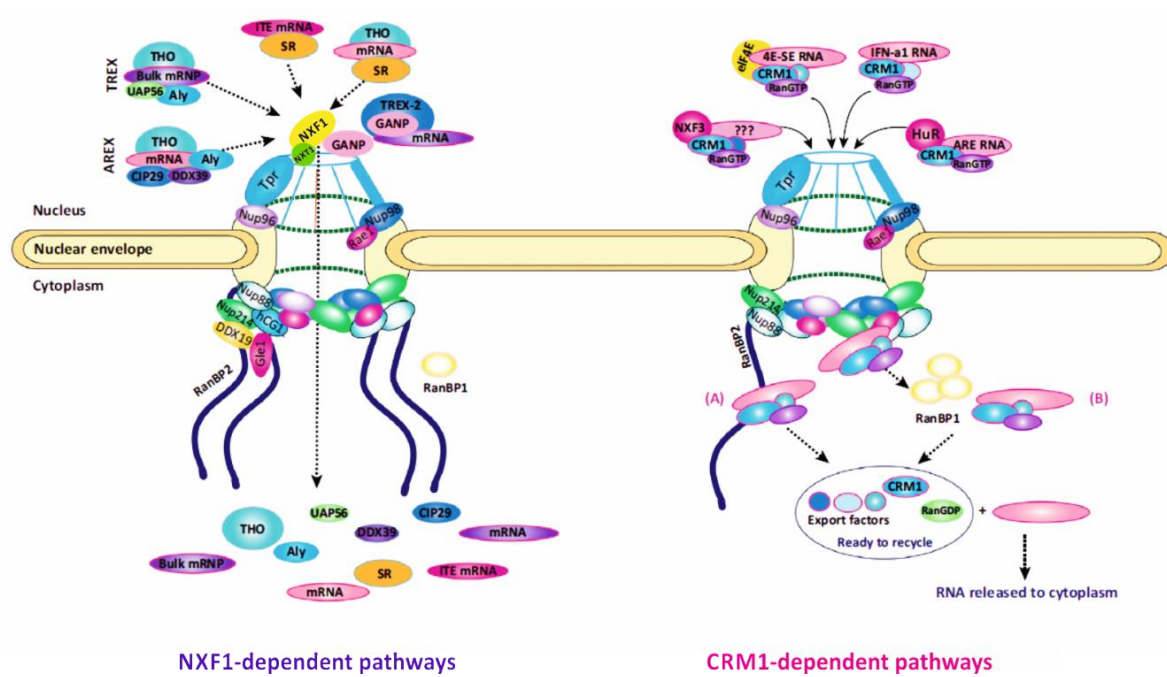


Figure 1.8 Overview of the NXF1-dependent and CRM1-dependent mRNA export pathways (Modified from Culjkovic-Kraljacic and Borden, 2013). The NPC-dependent mRNA export is divided into two main pathways: the NXF-dependent and the CRM1-dependent pathway. Based on the variety of the adaptor proteins, each export pathway can be subdivided into several branches. For instance, the NXF1-dependent pathway could be independently mediated by Aly/REF, GANP or SR proteins. Likewise, the CRM1-dependent pathway is categorized according to the involvement of HuR, eIF4E or NXF3 proteins. The main export factors involved in these pathways are shown.

1.4 Aims of this work

The LINC complex is well known for functions in mechanotransduction and more and more reports raise the association between the LINC components and human disease, particularly in the pathophysiology of EDMD (Emery-Dreifuss muscular dystrophy). SUN1 and SUN2 being crucial components of the LINC complex became our obvious candidates of investigation with respect to EDMD.

The first part of my project has two major objectives:

- **To examine the influence of SUN1 mutations in primary fibroblasts from two EDMD patients.**
 - Phenotypic characterization of the patient cells.
- **To address the molecular pathology underlying the disease.**
 - Study the defects of LINC components at the protein level, including the localization, expression and their interactions.

Until now, the role of SUN1 was mainly restricted to the functions in the LINC complex in concert with the KASH domain proteins.

The second part of my project expands the role of SUN1 and has a third objective:

- **To reveal whether SUN1 has additional functions in mammalian cells aside from its role in the LINC complex.**
 - Confirm the interaction of SUN1 with hnRNPs.
 - Conduct knockdown studies of SUN1 to biochemically characterize the importance of SUN1 in hnRNP-containing mRNA export.
 - Identify the interaction partners of SUN1 involved in mRNA export pathway.

2. Results

2.1 Contribution of SUN1 mutations to the pathomechanism in muscular dystrophies

2.1.1 Patient information

We used primary fibroblasts from two patients (Patients 1 and 2, passage 11) suffering from a muscular dystrophy compatible with the clinical phenotype of Emery-Dreifuss muscular dystrophy (EDMD). Patient 1, male, had a mutation in the X-linked emerin gene *EMD* (*STA*) (hemizygous p.L84Pfs*6 in NCBI CAG38773) and harbored an additional heterozygous mutation in the *SUN1* gene leading to an amino acid exchange in the amino terminus at position 203 (p.A203V in NCBI O94901). *SUN1* p.A203V was found in a reference population at a very low frequency of 0.00092 (*SUN1* p.A203Vrs144929525; 4/2180; 1000GENOMES:phase_1_ALL). The heterozygous *SUN1* mutation alone is not disease causing. As seen in the pedigree of patient 1, family members II-2 and II-3 are heterozygous for the *SUN1* p.A203V mutation only and phenotypically healthy (Figure 2.1). But in combination with the *EMD* mutation p.L84Pfs*6, a more severe EDMD phenotype is observed (Hoeltzenbein et al., 1999).

Patient 2, a female patient suffering from an unclassified muscular dystrophy (see Materials and Methods) harbored a heterozygous mutation in the LAP2 α gene *TMPO* (p.P426L in NCBI NP_003267) and a heterozygous mutation in the C-terminus of *SUN1* (p.A614V in 09491, corresponds to p.A718V in 09491-9 (NCBI)). The *SUN1* mutation was found in a reference population at a very low frequency of 0.00046 (*SUN1* p.A614V rs114701323; 1/2183; 1000GENOMES:phase_1_ALL).

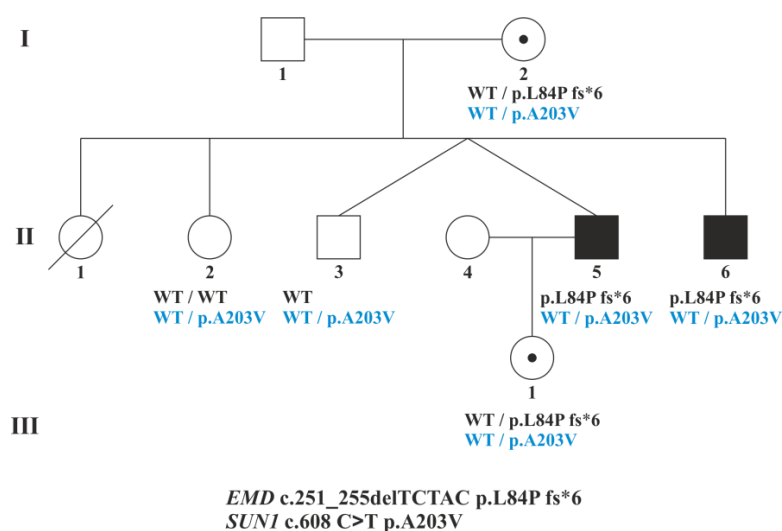
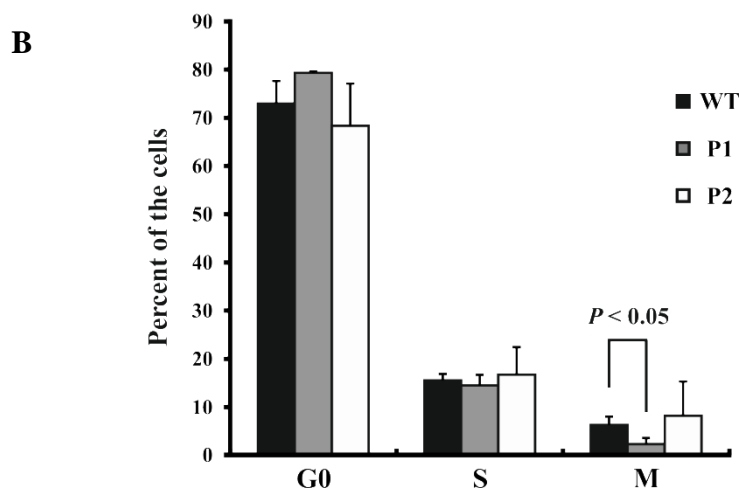
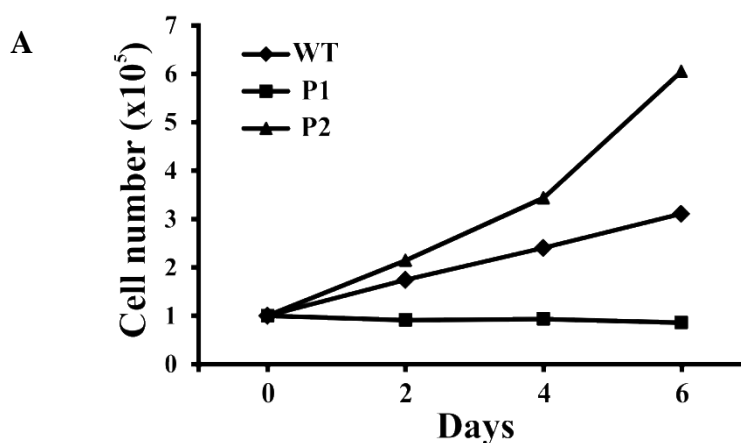


Figure 2.1 Segregation of the mutations *EMD* p.L84Pfs*6 and *SUN1* (p.A203V) in the pedigree of patient 1 (II-6). Females are represented as circles and males as squares. Affected males are black filled squares. Circles with a central dot symbolize female carriers. Cross slatched figures represent deceased individuals.

2.1.2 The patient cells have defects in cell proliferation and cell size

The contributions of the heterozygous mutations in SUN1 to the disease are not known. Therefore we carried out investigations on the cellular level to probe for alterations that are associated with diseases caused by mutations in components of the NE. To evaluate the proliferation potential of the EDMD patient cells, 1×10^5 patient and wild-type cells were seeded and counted every 48 h for a period of 6 days. The cells from patient P1 exhibited a remarkably reduced growth compared to the wild-type. In contrast, fibroblasts from patient P2 showed increased growth compared to wild-type (Figure 2.2A). The observed alterations may be caused by changes in the cell cycle phases. Therefore we checked the cell cycle distribution of exponentially growing control fibroblasts and fibroblasts from patients by flow cytometry and observed for P1 cells a significantly lower number of cells in M phase whereas wild-type and P2 cells did not significantly differ from each other (Figure 2.2B). Determination of the cell sizes revealed that P1 cells had an increased cell size compared to wild-type and P2 cells which were similar in size to wild type (Figure 2.2C).



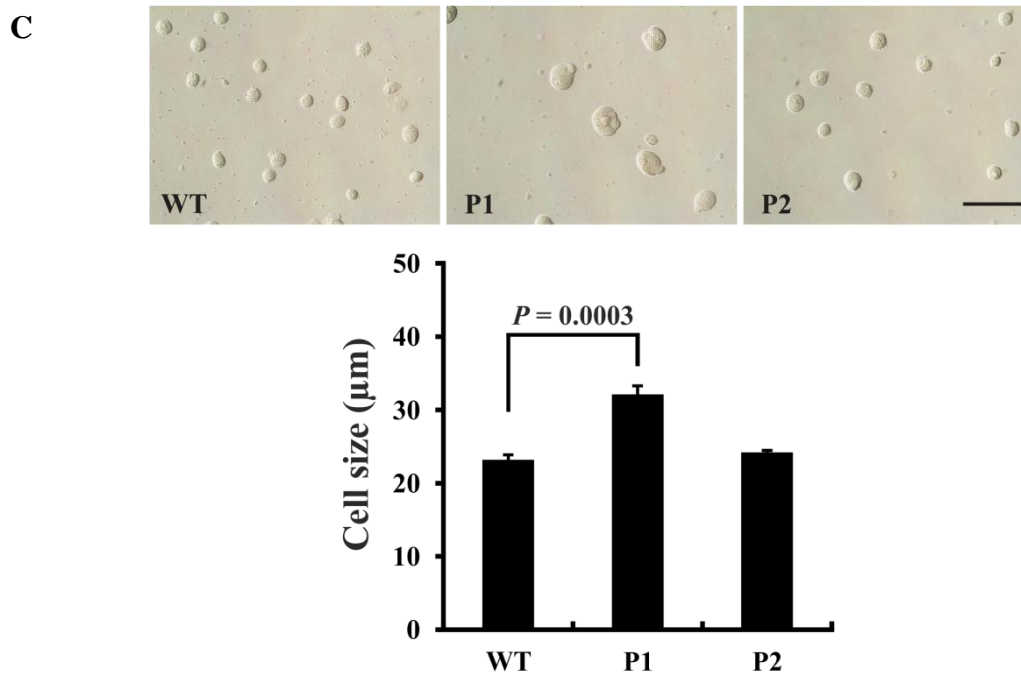


Figure 2.2 Defects in cell proliferation, cell cycle and cell size in EDMD patient cells. **A:** Cell proliferation of the wild-type and patient fibroblasts. 1×10^5 cells of each cell type were seeded. Cell numbers were determined every 48 h for a period of 6 days. **B:** Cell cycle analysis of wild-type and patient fibroblasts was done by flow cytometry. 5×10^5 cells each were used. **C:** Cell size of patient and wild-type fibroblasts. Bar: 100 μm . The values represent the mean \pm SD.

2.1.3 The patient cells show differences in centrosome distance and senescence

The centrosome plays a key role in cellular architecture by determining the position of several associated organelles, including the nucleus. Previous work indicated that nuclear envelope proteins like the LINC-proteins and emerin participate in centrosome-nucleus juxtaposition and mediate shuttling of nuclear and centrosomal proteins between these organelles (Salpingidou et al., 2007; Schneider et al., 2011; Zhang et al., 2009). Therefore we investigated the localization of the centrosome relative to the nucleus using antibodies against pericentrin (Figure 2.3A). The nucleus-centrosome distance was measured for 200 cells for each cell line using Leica LAS AF Lite software. In wild-type cells the mean distance of the nucleus to the centrosome was about 2.7 μm , for P2 cells we observed a decreased centrosome distance ($\sim 1.9 \mu\text{m}$), and for P1 cells the distance was significantly increased ($\sim 3.8 \mu\text{m}$) (Figure 2.3A).

An increased senescence has been reported for cells harbouring defects in components of the nuclear envelope (Le Dour et al., 2011). We queried how nuclear envelope mutations affected senescence and examined senescence-associated β -galactosidase (SA- β -Gal) in control and

patient cells (Figure 2.3B). In wild-type cells, less than 10 % of the cells were β -galactosidase positive, in P2 cells we observed staining in ~30 % and in P1 cells this number increased to 50 % (Figure 2.3B).

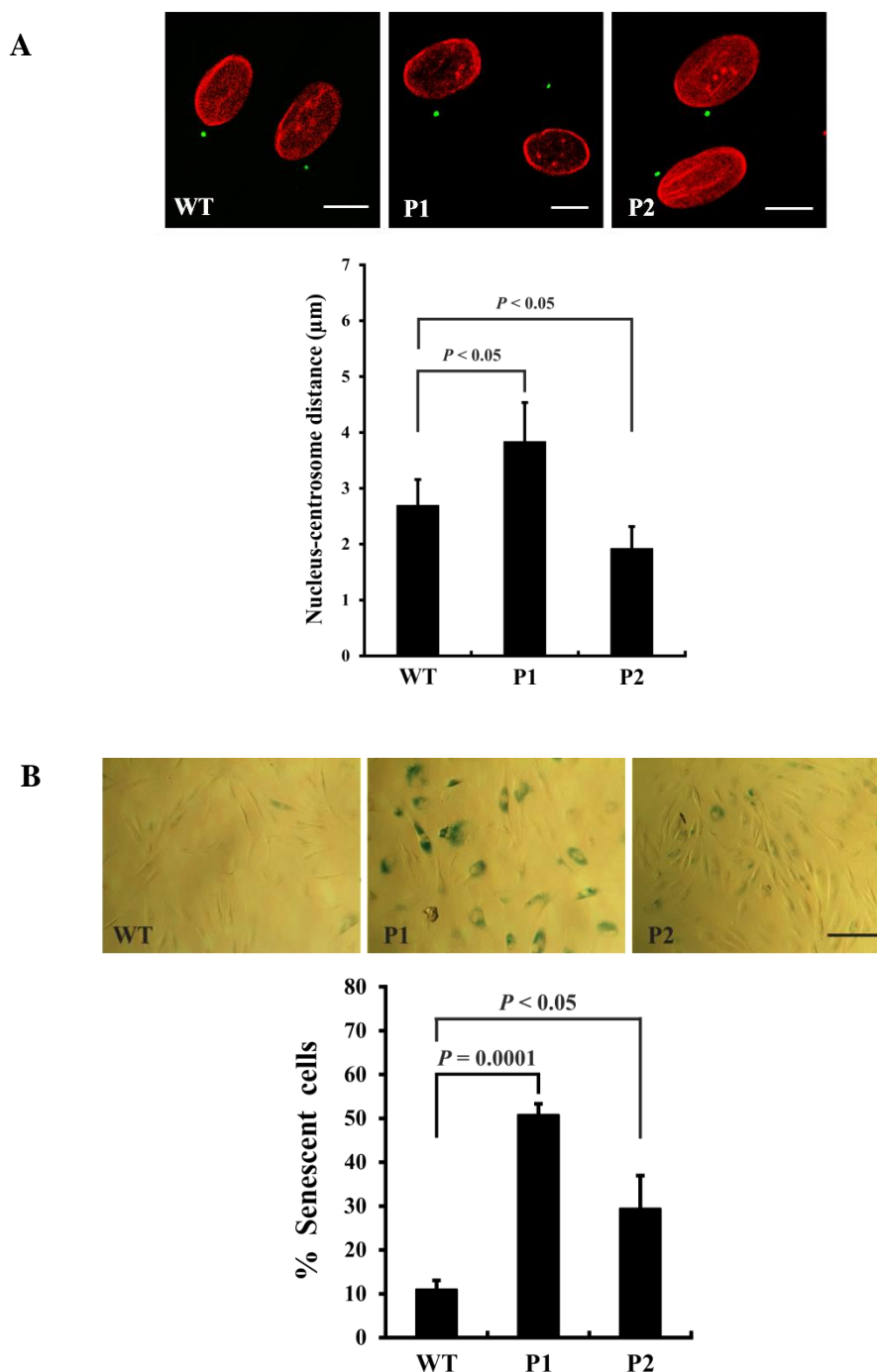
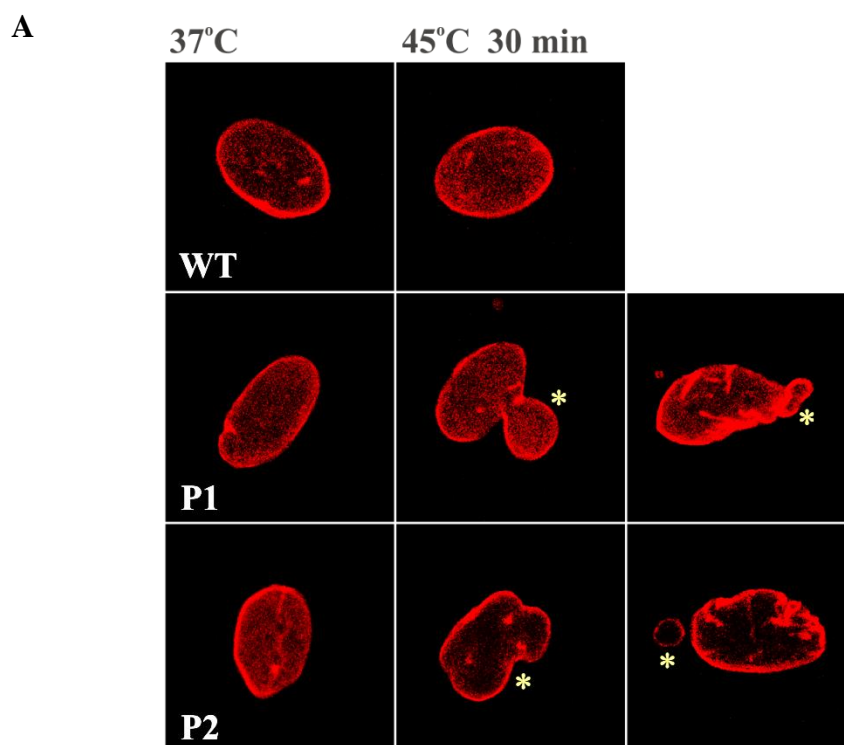


Figure 2.3 Alterations in centrosome distance and senescence. **A:** Nucleus-centrosome distance is altered in patient cells. Immunofluorescence analysis of wild-type and EDMD patient cells was performed by using Pericentrin antibodies to localize the centrosome and Lamin A/C antibodies to label the NE. Bar, 10 μ m. Evaluation is shown in the bar graph below. **B:** Visualization (upper panel) and quantification (lower panel) of senescence associated β -galactosidase show differences between wild-type and patient cells. Standard deviations are from three independent assays counting 400-500 cells in each experiment. The P values are indicated. Bar, 100 μ m.

2.1.4 Heat shock induces severe nuclear shape alterations in patient cells

Nuclei from laminopathy cells have an increased sensitivity to heat stress and deform upon a heat shock (Vigouroux et al., 2001). To evaluate the resistance of the NE to damage induced by heat stress, control and patient fibroblasts were subjected to heat shock treatment for 30 min at 45°C. Following the treatment, the cells were immediately fixed and stained for Lamin A/C to assess nuclear shape changes. Normally nuclei have an ellipsoid shape and Lamin A/C is homogeneously distributed along the NE. In wild-type cells Lamin A/C distribution was not dramatically altered upon heat stress whereas the number of deformed nuclei was increased. Patient fibroblasts showed an altered nuclear shape already in untreated cells. After heat treatment the number of cells with nuclear abnormalities increased further, however the difference to wild-type fibroblasts was not statistically significant. The NE of the nuclei was deformed and folds and pleats occurred (Figure 2.4A, B). These results suggest an alteration in the nuclear protein network that resulted in hypersensitivity to heat stress induced deformation. We also determined whether heat shock affected the centrosome positioning and stained for the centrosome marker pericentrin. We found that the nucleosome-centrosome distance was not altered in wild-type cells and slightly but not significantly increased in patient cells after heat shock (Figure 2.4C).



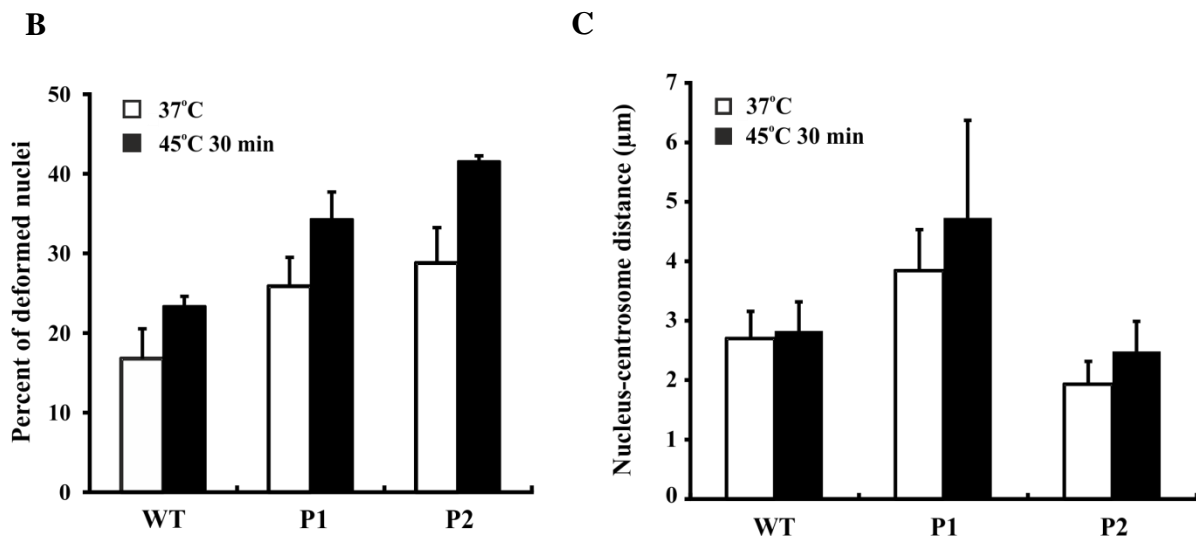


Figure 2.4 Heat shock induces severe nuclear shape alterations in EDMD fibroblasts. **A:** Wild-type and patient cells were subjected to heat shock treatment at 45^oC for 30 min and fixed immediately in ice cold methanol and immunolabeled for Lamin A/C. Nuclei of untreated cells (left column) and heat stressed cells nuclei (middle and right columns) as indicated on top are shown. Stars point out alterations. Bar, 10 μm. **B:** The numbers of deformed and disorganized nuclei prior to and after heat shock were determined. Between 300 to 500 cells were analyzed. **C:** Analysis of the nucleus centrosome distance after heat shock. The cells were stained for Lamin A/C and Pericentrin as centrosomal marker. 200 cells each were analyzed. The values represent the mean ±SD.

2.1.5 Cell migration is altered in patient cells in an in vitro wound healing assay

Earlier studies have demonstrated that mutations in key NE proteins can result in slower migration of fibroblasts (Houben et al., 2009; Lee et al., 2007; Luke et al., 2008). To investigate whether the mutations studied in this report also affect cell migration, wound healing assays were performed. We analysed the velocity of gap closure and determined the speed of single cells. We followed the gap closure over 20 h taking images every 15 min. After 15 h the P1 cells had migrated into the open area and nearly completely closed the gap. In case of wild-type and P2 cells the open area was wider (Figure 2.5A). After 20 h wild-type cells had closed the gap whereas gap closure was still not achieved after 20 h in case of P2 cells. Quantification of the speed with which individual cells moved supported this notion revealing a faster migration for P1 cells (0.384±0.05 μm/min). Wild-type and P2 cells exhibited a similar speed and migrated at 0.266±0.05 μm/min and 0.282±0.004 μm/min, respectively (Figure 2.5B).

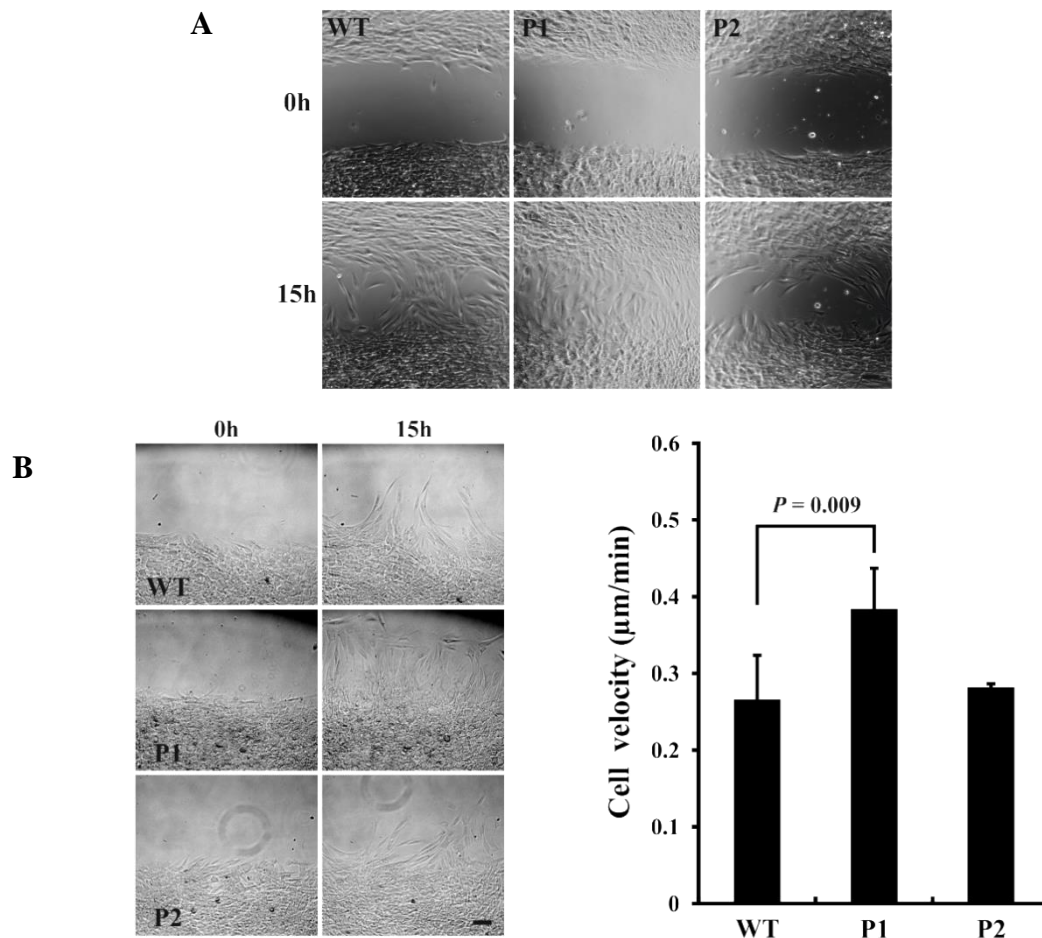
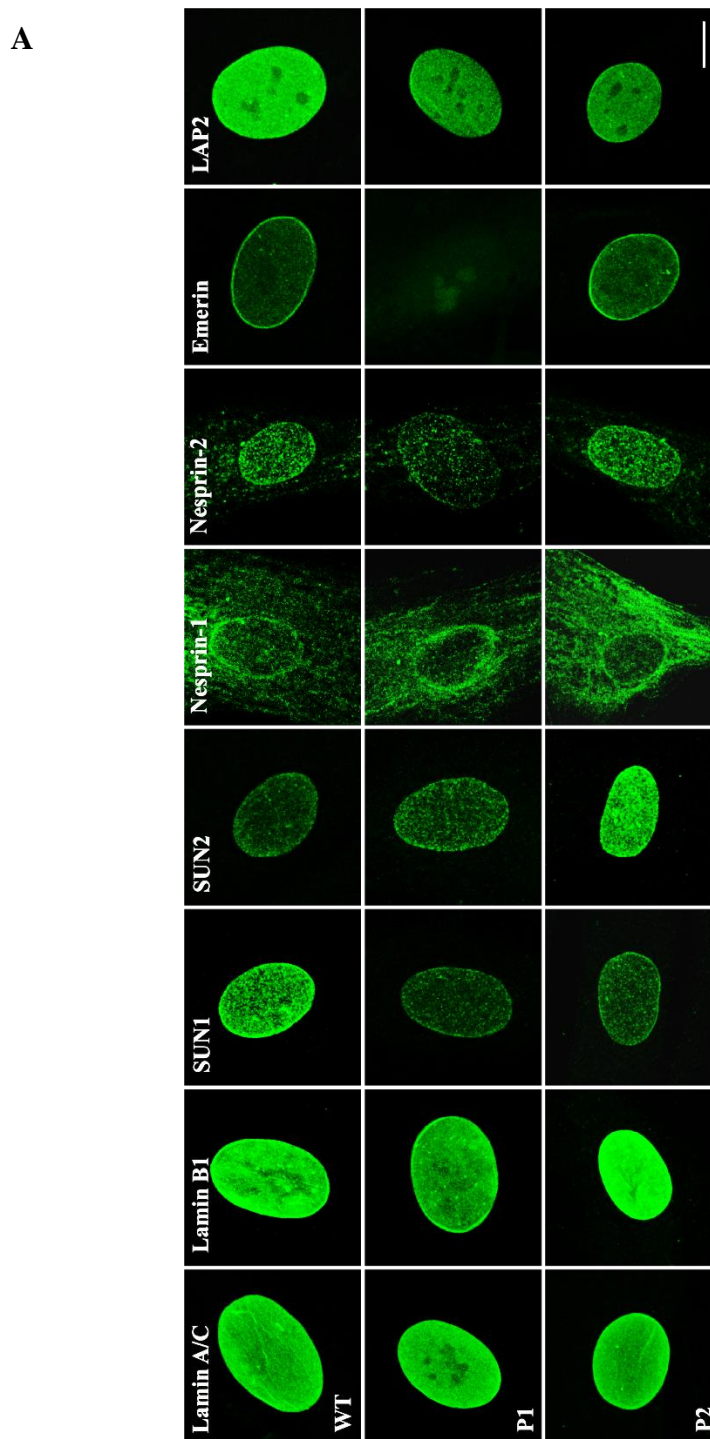


Figure 2.5 In vitro wound healing is altered in patient cells. **A:** Gap closure of wild-type and patient fibroblasts. Pictures from the 0 and 15 hour time points are shown. Cells were seeded at a density of 4×10^4 cells on each side of a culture insert. Inserts were removed to create a 500 μm gap between each side. The cell migration into the gap was followed over a period of 20 h under an inverted microscope with a live cell imaging system. **B:** The velocity of single cell migration. For analysis of the single cell motility, 100-130 cells were tracked using the manual tracking software component of the Image J program.

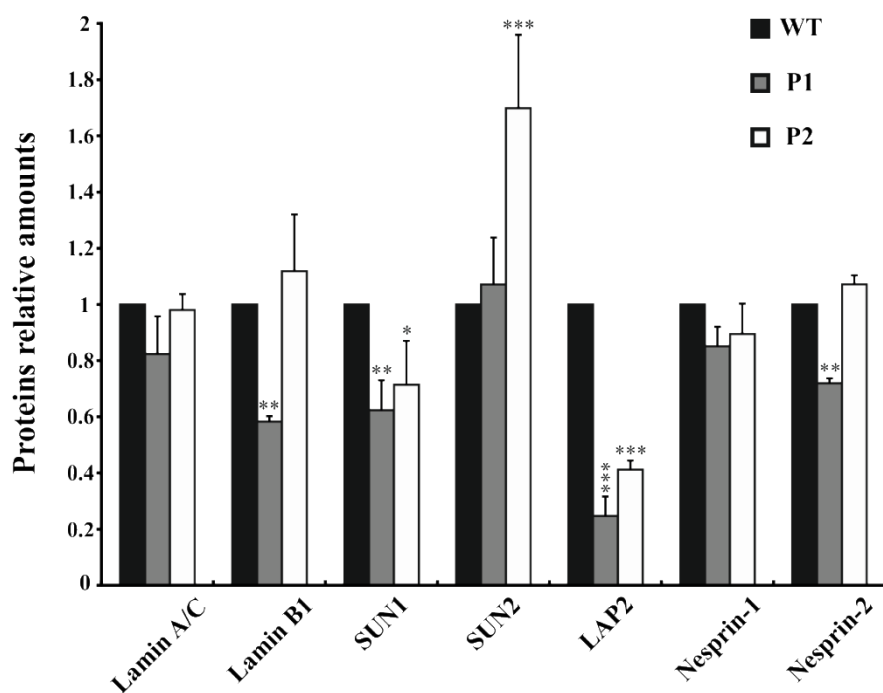
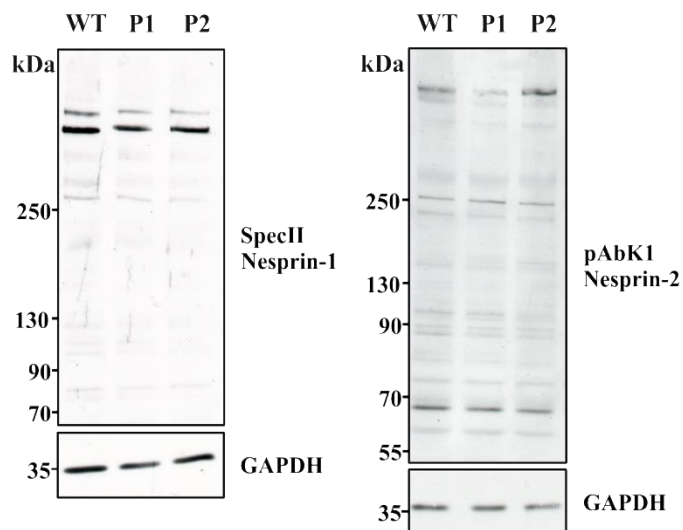
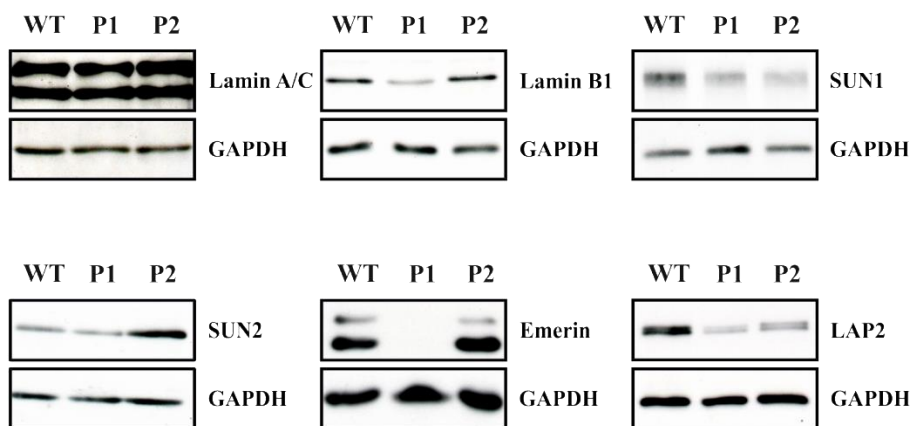
2.1.6 Transcript and protein levels but not localization of LINC components and binding partners are altered in patient cells

Based on the finding that the patients have mutations in SUN1 and other nuclear envelope proteins, we investigated the localization of LINC components and their binding partners by immunofluorescence. In particular we studied the distribution of Lamin A/C, Lamin B1, SUN1 and SUN2, Nesprin-1 and Nesprin-2, LAP2 and Emerin. All proteins were present at the NE (Figure 2.6A). The Nesprin-1 antibodies in addition stained filamentous structures in the cytoplasm which are presumably actin filaments (Padmakumar et al., 2004). In P1 cells Emerin was absent as expected (Figure 2.6A). A subsequent analysis of the protein levels

showed comparable expression for Lamin A/C in all cells, whereas Lamin B1 and Nesprin-2 amounts were significantly reduced in P1. For SUN1 and LAP2 we observed a reduction in both patient cells. SUN2 amounts were significantly higher in P2 cells (Figure 2.6B). Surprisingly, at the transcript level we observed an up-regulation in case of Lamin B1 and LAP2 for both patient cells and in case of Nesprin-2 for P1 cells as determined by qRT-PCR. No significant alterations were seen for SUN1 and SUN2 (Figure 2.6C; Table 1).



B



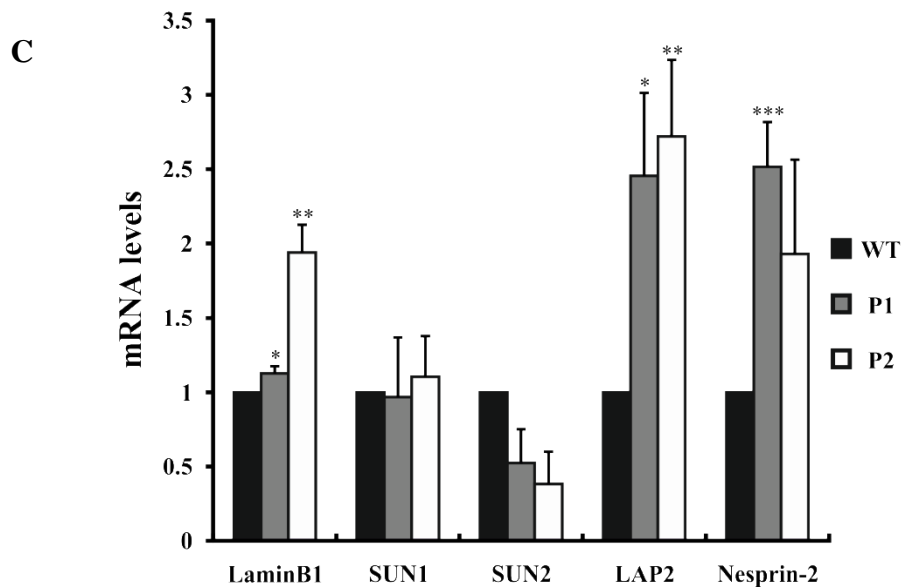


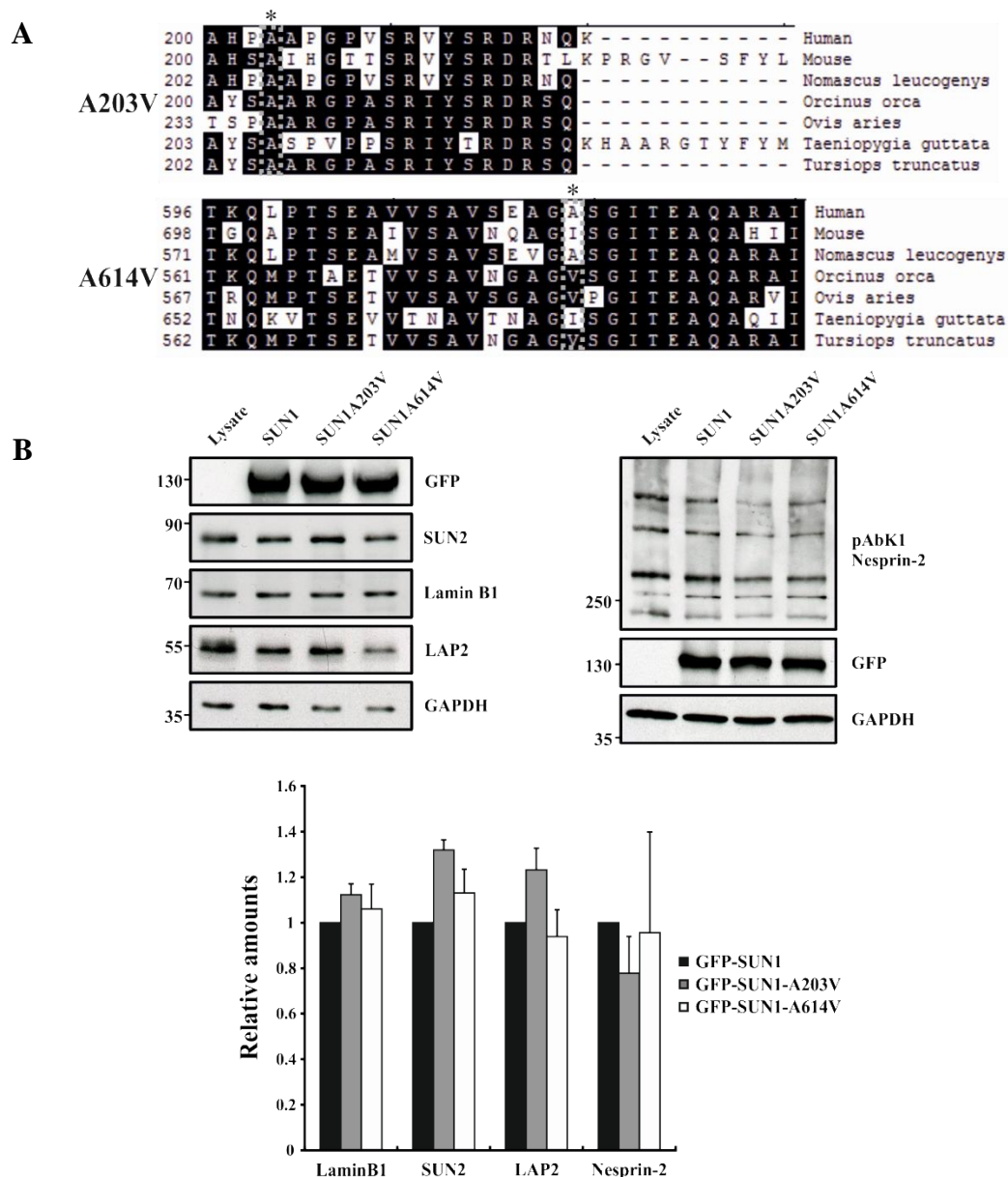
Figure 2.6 Localization, expression and transcript levels of LINC components and binding partners. A: Immunofluorescence analysis of LINC components and binding partners using appropriate antibodies. Bar, 10 μ m. **B:** Western blot analysis for several NE proteins. Whole cell lysates were separated by SDS-PAGE (12% acrylamide). For detection of Nesprin-1 and -2, 3-15% acrylamide gradient gels were used. For loading control GAPDH levels were determined by GAPDH antibodies. **C:** qRT-PCR analysis for detection of transcript levels. * $p < 0.05$, ** $p < 0.01$, *** $p < 0.001$.

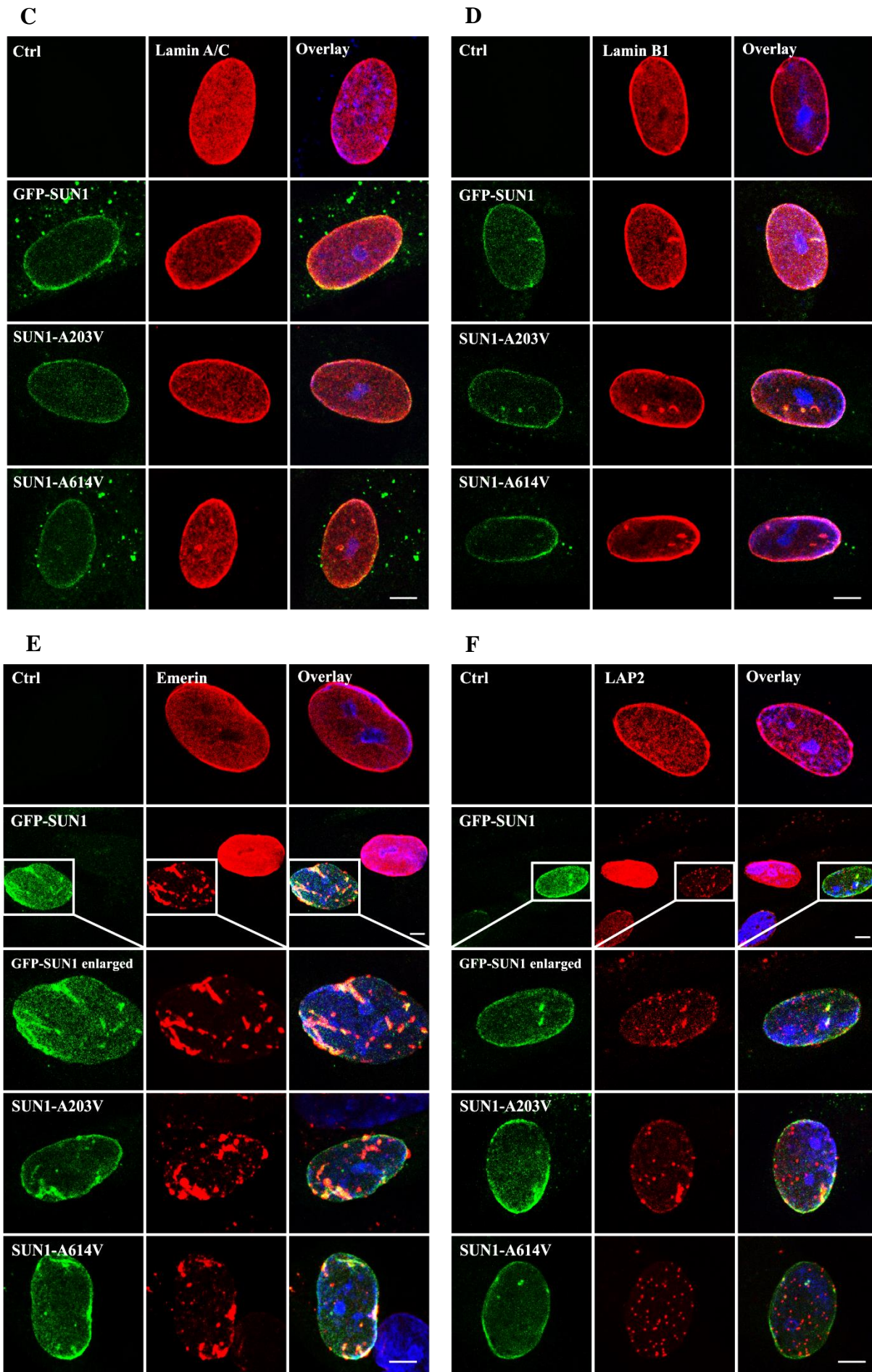
2.1.7 Analysis of SUN1 mutations

The Emery-Dreifuss muscular dystrophy P1 fibroblasts have a mutation p.A203V in the N-terminus of SUN1, and P2 fibroblasts have a SUN1 mutation p.A614V in the C-terminus. These mutations we considered possibly pathogenic, because they affect amino acids that are well conserved among SUN proteins from other species, in particular A203 is highly conserved (Figure 2.7A). In order to identify whether the SUN1 mutations are responsible for any of the observed defects of the patient cells we introduced these mutations into wild-type GFP-tagged SUN1 by site-directed mutagenesis and expressed the corresponding proteins in wild-type fibroblasts.

We found that GFP-SUN1, GFP-SUN1A203V and GFP-SUN1A614V were expressed at comparable levels and were present at the NE in the transfected cells. Next we focused on the expression levels of Lamin B1, SUN1, SUN2, LAP2 and Nesprin-2 by western blotting. We observed no significant differences between cells expressing the wild-type or mutant versions of SUN1 which suggested that the SUN1 mutations do not affect the amounts of the proteins (Figure 2.7B). Also, the localization pattern of these NE components appeared unperturbed with the exception of emerin and LAP2 (Figure 2.7C-G). In untransfected cells Emerin and

LAP2 antibodies labelled the NE. Ectopic expression of wild-type SUN1 and the mutant proteins led to a decrease of Emerin at the NE and a faint labelling was seen. In addition, Emerin positive aggregate like structures were observed at the NE. Occasionally these aggregates were also positive for GFP. Moreover, LAP2 positive dot like structures were also present at the NE with a faint labelling in cells expressing wild-type SUN1 and the mutant proteins (Figure 2.7E, F). We also noticed a down regulation of SUN2 in GFP-SUN1 overexpressing cells (Figure 2.7G). This result contradicts our findings obtained with patient cells. However, here we have overexpressed SUN1 which is not the case in the patient cell, further in the patient cell the situation is more complex as there is the additional heterozygous mutation in the LAP2 α gene.





G

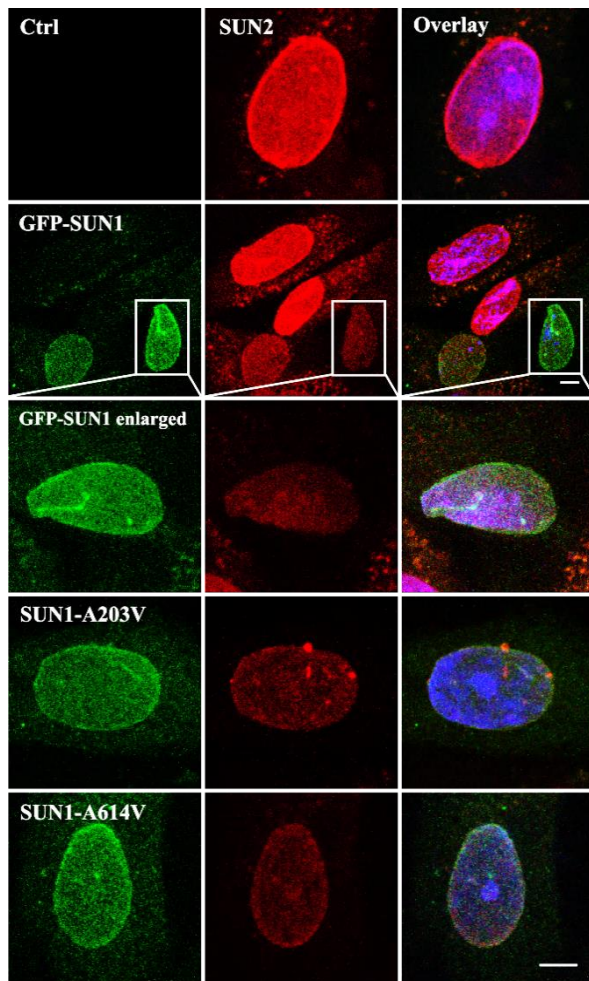


Figure 2.7 A: SUN1 mutations analysis and site-directed mutagenesis. Multiple alignment of amino acids for part of SUN1 shows conservation of Alanine residues at position 203 and position 614 for p.Ala203Val and p.Ala614Val. NCBI accession numbers are: HUMAN, O94901; MOUSE, Q9D666; *Nomascus leucogenys*, XM_003278674.2; *Orcinus orca*, XM_004269058.1; *Ovis aries*, XM_004021337.1; *Taeniopygia guttata*, XM_002191424.2; *Tursiops truncatus*, XM_004316169.1. **B:** Wild-type fibroblasts were transfected with GFP-SUN1, GFP-SUN1A203V and GFP-SUN1A614V plasmids and the expression of Lamin B1, SUN2, LAP2 and Nesprin-2 was checked by western blot analysis. **C-G:** Wild-type fibroblasts were transfected with GFP-SUN1, GFP-SUN1A203V and GFP-SUN1A614V plasmids and the expression and localization of Lamin A/C (C), Lamin B1(D), Emerin (E), LAP2 (F) and SUN2 (G) were studied by immunofluorescence. Bar: 5 μ m.

2.1.8 The mutations in SUN1 affect the interactions with Emerin and Lamin A/C

Although the NE components tested with the exception of Emerin and LAP2 had an unperturbed localization at the NE and unaltered amounts it might well be that the interactions between them were altered. We therefore performed co-immunoprecipitation and pulldown experiments and analyzed the interaction between the GFP-tagged SUN proteins and Emerin in human fibroblasts. We found that GFP-SUN1 and both GFP-SUN1A203V and GFP-SUN1A614V could co-immunoprecipitate Emerin (Figure 2.8A). A more quantitative analysis using densitometry revealed that the SUN1 mutant proteins precipitated less Emerin compared to WT SUN1, however, the difference was not significant (Figure 2.8A).

SUN proteins directly bind to Lamin although this interaction is not required for SUN1 localization at the NE. The interaction site in Lamin A was located in the tail region, in SUN1 an amino terminal region encompassing residues 1 to 138 was identified as interaction site (Haque et al., 2010; Simon and Wilson, 2013). We used GST-CT-Lamin A/C for pulldown

assays to check the interaction with SUN1 in wild-type and patient fibroblasts. In these experiments SUN1 wild-type was efficiently precipitated whereas both SUN1 mutant proteins were present in the precipitate in reduced amounts (Figure 2.8B). GST alone did not precipitate the proteins. The results suggested that the SUN1 mutations can affect the binding ability to Lamin A/C.

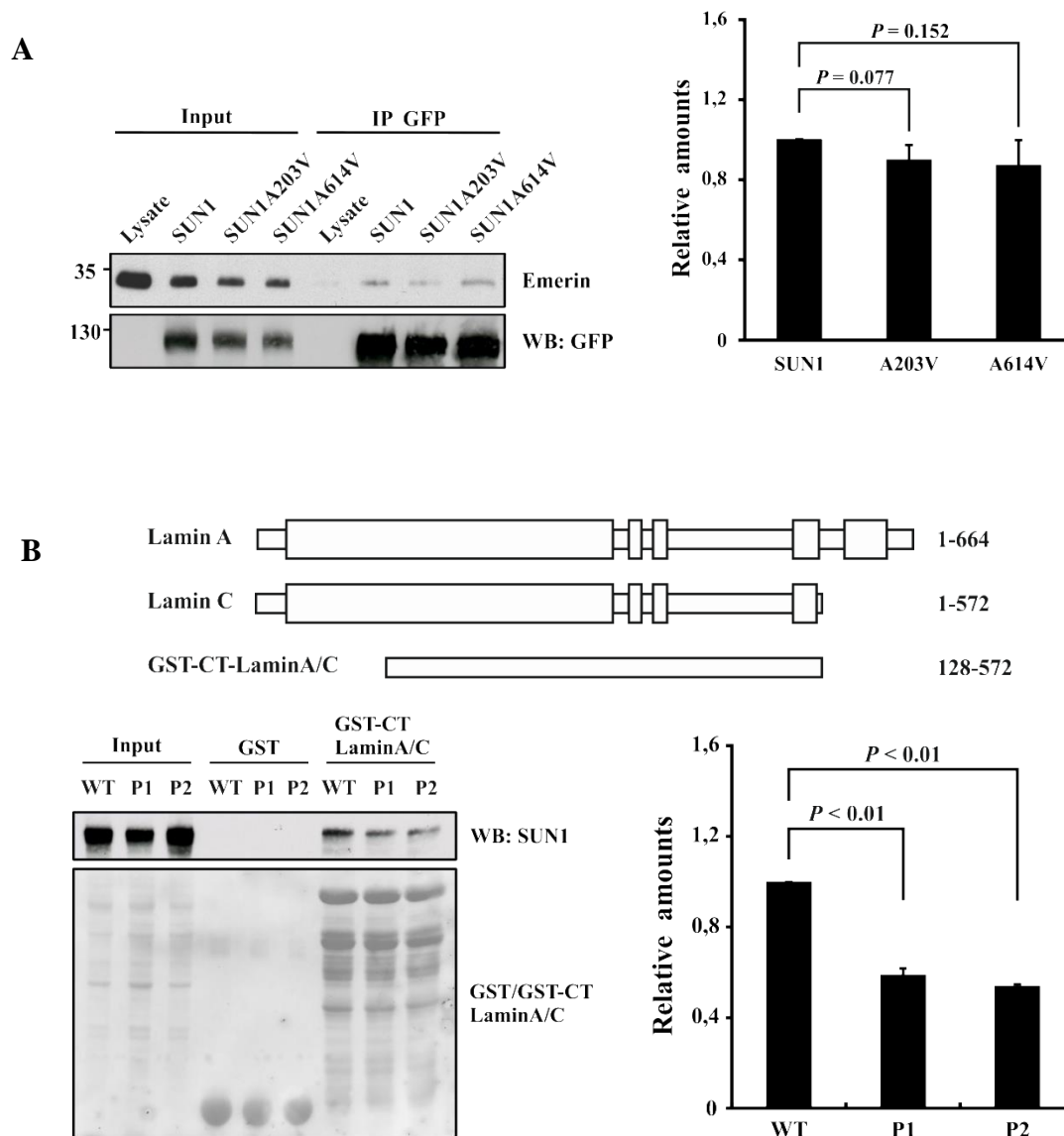
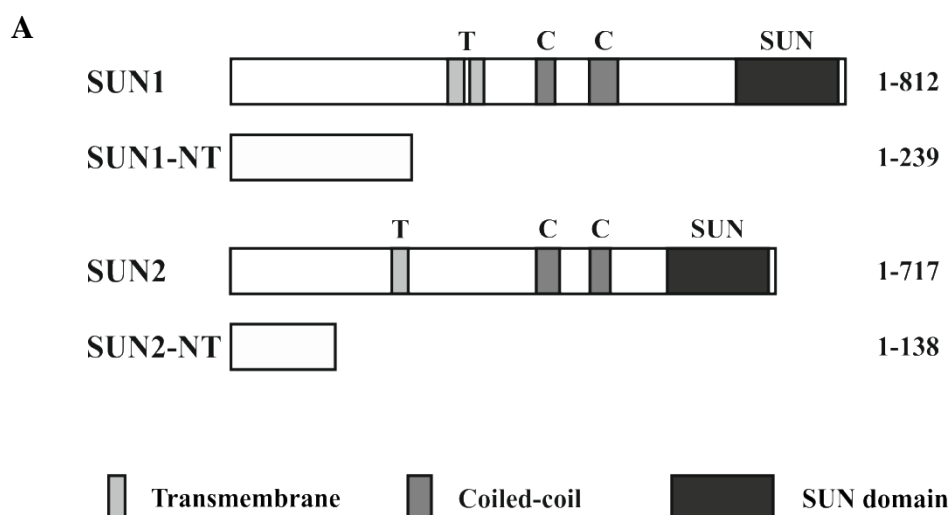


Figure 2.8 Interaction of SUN1 with Emerin and Lamin A/C. **A:** Co-immunoprecipitation of Emerin with GFP-SUN1, GFP-SUN1A203V and GFP-SUN1A614V. For immunoprecipitation polyclonal GFP antibodies were used. The immunoprecipitate was probed with Emerin and GFP specific antibodies (upper panel). The binding was quantified by scanning densitometry (lower panel). The P values are indicated. **B:** Lamin A/C interaction of mutant SUN1 in patient fibroblasts. The top panel shows a schematic of Lamin A/C and CT-Lamin A/C (residues 128-572) used as GST fusion protein (Libotte et al., 2005). For pulldown assays, GST and GST-CT-Lamin A/C were used to check the interaction with SUN1 in wild-type and patient fibroblasts (middle panel). The proteins were separated by SDS-PAGE (12% acrylamide). Scanning densitometry was used to determine the binding ability (lower panel).

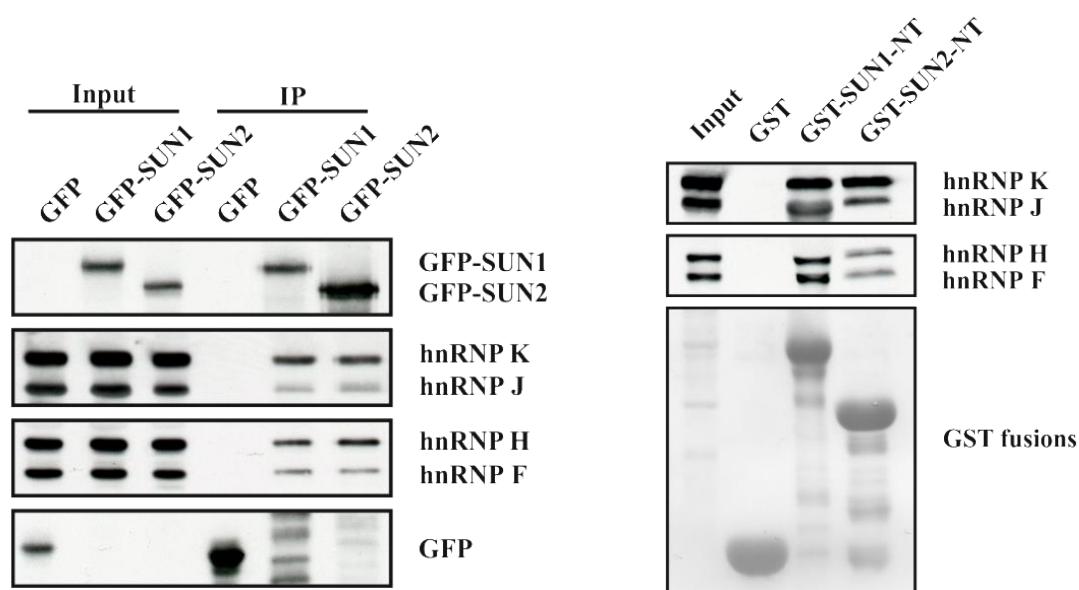
2.2 Inner nuclear envelope protein SUN1 plays a prominent role in mammalian mRNA export

2.2.1 SUN1 and SUN2 interact with hnRNP F/H and hnRNP K/J

In a previous study, in order to understand the role of SUN proteins, we screened for SUN interacting proteins by applying pulldown experiment and LC-MS analysis (Taranum et al., 2012). Many proteins taking part in gene regulatory processes were found. The hnRNPs, like hnRNP F/H and hnRNP K/J, are interesting candidates involved in RNA processing. To confirm the interaction between SUN1/2 and hnRNPs, we performed co-immunoprecipitation (Co-IP) and pulldown experiments. For Co-IP study, wild-type fibroblasts were transfected with GFP, GFP-SUN1 or GFP-SUN2 and both the GFP fusion proteins and their partners were immunoprecipitated by GFP-Trap beads. For pulldown assay, GST tagged the N-termini of SUN1 (residues 1-239) and SUN2 (residues 1-138) (Figure 2.9A) were directly incubated with the cell lysates and GST alone was used as negative control. All the samples were subjected to western blot analysis and probed with GFP monoclonal antibodies. Strong signals of hnRNP F/H and K/J were detected in both experiments confirming that hnRNP F/H and hnRNP K/J were associated with SUN1 and SUN2 (Figure 2.9B). We further examined the localization of the endogenous proteins by immunofluorescence. Consistent with previous studies, hnRNP F/H and hnRNP K/J were shown mainly in the nucleus and colocalized with both SUN1 and SUN2 along the inner nuclear envelope (Figure 2.9C).



B



C

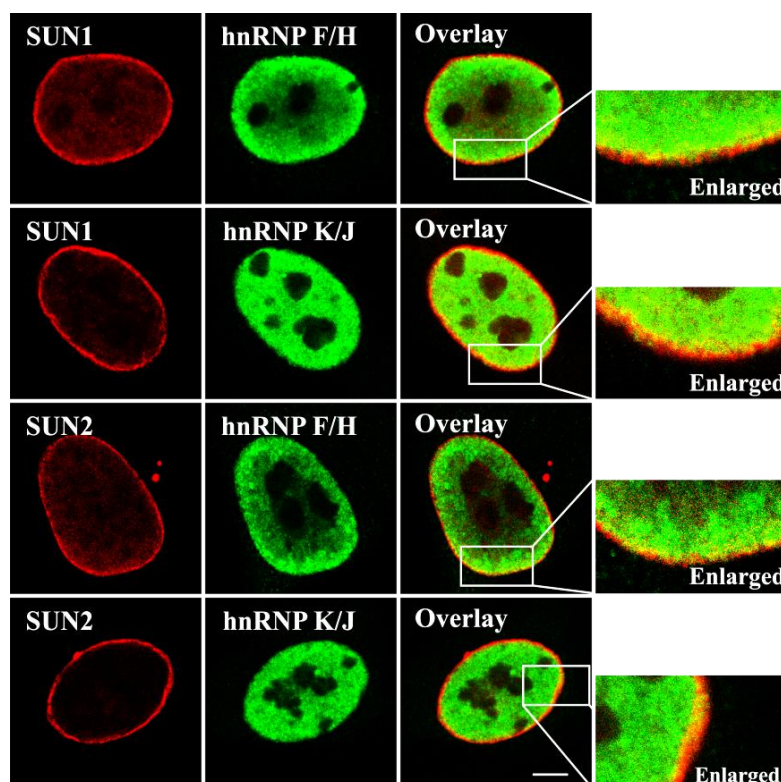
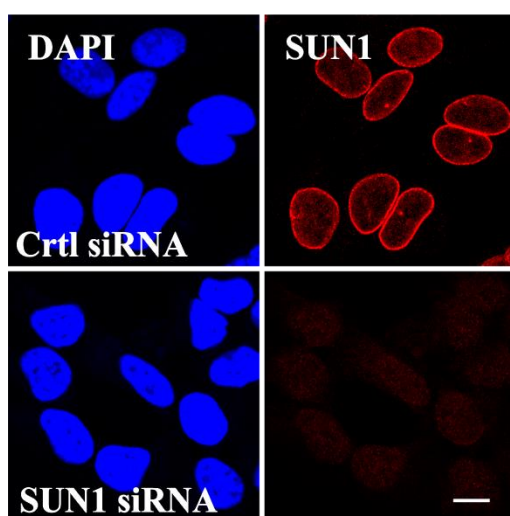


Figure 2.9 Interaction and colocalization of SUN1/2 and hnRNPs. **A:** Schematic of the full length and the N-termini of SUN1 and SUN2 used in this thesis. Transmembrane, coiled-coil and SUN domain are shown. **B:** Western blots analysis of Co-IP and pulldown between SUN1/2 and hnRNPs. For Co-IP, lysates from human fibroblasts expressing GFP alone, GFP-SUN1 or GFP-SUN2 were immunoprecipitated by using GFP-Trap beads and detected by GFP monoclonal antibodies. For pulldown experiment, GST, GST-SUN1-NT and GST-SUN2-NT were used and visualized by Ponceau S staining. The proteins were separated by SDS-PAGE (12% acrylamide) and the interactions were detected by hnRNP F/H and hnRNP K/J antibodies. **C:** Colocalization of endogenous SUN1/2 and hnRNP F/H or hnRNP K/J. HeLa cells were stained with required antibodies and analyzed by immunofluorescence. Bar: 5 μm .

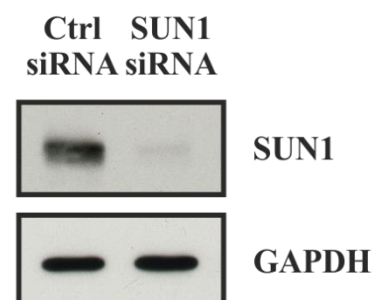
2.2.2 hnRNP F/H and hnRNP K accumulate in the nucleus by SUN1 depletion

The hnRNPs are RNA-binding proteins with a diverse function in gene regulation including nascent transcript packaging, alternative splicing, nucleocytoplasmic transport and translational regulation (Dreyfuss et al., 2002; Han et al., 2010). Considering that SUN1 and SUN2 are INM proteins, they might play a crucial role in hnRNP-associated nucleocytoplasmic transport. In order to verify our hypothesis, we performed small interfering RNA (siRNA)-mediated knockdown studies of SUN1. Immunofluorescence and western blot analysis confirmed the efficient knockdown of SUN1 in HeLa cells (Figure 2.10A, B). Immunofluorescence analysis by confocal microscopy of HeLa cells showed strong nuclear envelope staining for SUN1 in control siRNA cells and very weak staining of the nuclear interior in SUN1 siRNA cells (Figures 2.10A). Western blot analysis showed that SUN1 was absent from HeLa lysates after siRNA depletion (Figure 2.10B). To test whether depletion of SUN1 influences the distribution of hnRNPs, we performed subcellular fractionation in control and SUN1 knockdown cells (Figure 2.10C). SUN1 was only observed in the whole cell lysate and the nuclear fraction of control cells, and was not detectable in SUN1 knockdown cells. Lamin B1 and GAPDH were used as nuclear and cytosolic marker, respectively. Interestingly, based on the same level of Lamin B1 and GAPDH, both hnRNP F/H and K appeared decreased in the cytosolic fraction of SUN1 knockdown cells and increased in the nuclear fraction compared to control knockdown cells (Figure 2.10C).

A



B



C

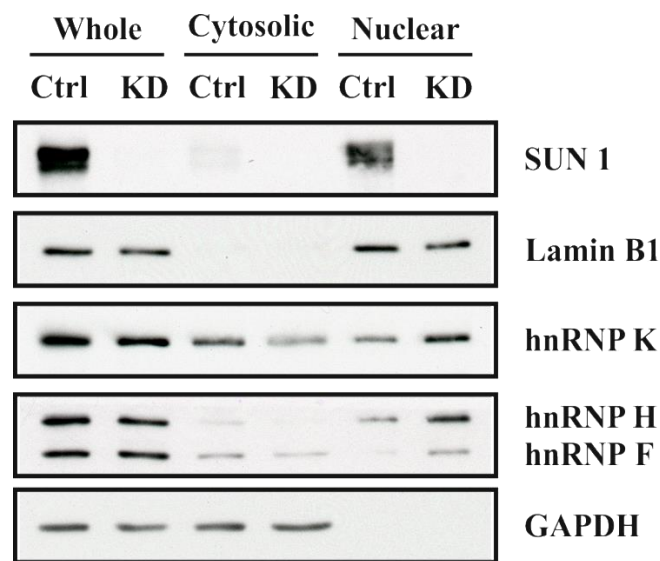


Figure 2.10 SUN1 depletion results in nuclear accumulation of hnRNPs. **A:** Immunofluorescence analysis with SUN1 antibodies of HeLa cells showed that SUN1 is localized at the NE in control cells and abolished in SUN1 siRNA cells. Nuclei are indicated by DAPI staining. Bar: 10 μ m. **B:** Western blot analysis of SUN1 expression level in control and SUN1 siRNA cells. GAPDH was used as loading control. **C:** Separation of nuclear and cytoplasmic proteins by subcellular fractionation in control and SUN1 knockdown cells. Lamin B1 and GAPDH were used as nuclear and cytosolic markers, respectively.

2.2.3 RNA fluorescence in situ hybridization (FISH) reveals nuclear accumulation of poly(A)+RNA in SUN1 absent cells

The shuttling hnRNP proteins are exported along with the mRNA to the cytoplasm during mRNA export and have functions in mRNA localization, stability, export, and/or translational regulation in the cytoplasm (Dreyfuss et al., 2002). One such shuttling hnRNP which we found to have interaction with SUN1 and SUN2 is hnRNP K, having a key role in translational regulation (Collier et al., 1998; Habelhah et al., 2001; Ostareck et al., 2001; Ostareck et al., 1997).

To investigate whether SUN1 plays a role in mammalian mRNA export, we examined the cellular distribution of poly(A)+RNA in control and SUN1 siRNA cells via RNA fluorescence in situ hybridization (FISH) with an oligo (dT) probe. In control cells, most poly(A)+RNA was cytoplasmic, except for a few discrete foci in the nucleus (Figure 2.11). In contrast, the SUN1 siRNA cells showed strong nuclear accumulation of poly(A)+RNA (Figure 2.11). Further, rescue of the mRNA export defect was performed by expressing a GFP tagged siRNA-resistant (R) SUN1 cDNA (GFP-SUN1^R) under siRNA treatment condition. We found that the expression of GFP-SUN1^R with SUN1 siRNA partially rescued the mRNA

export defect confirming that the SUN1 knockdown phenotype was not due to off-target effects (Figure 2.11).

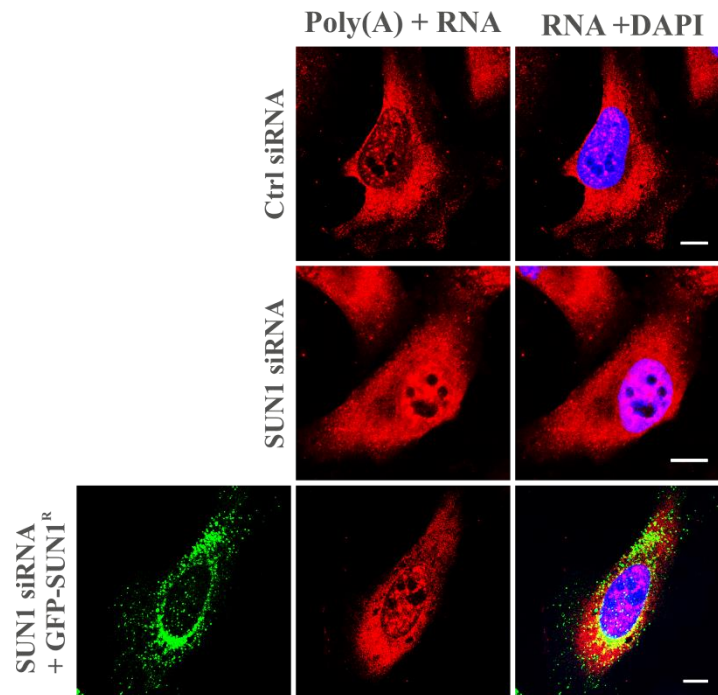


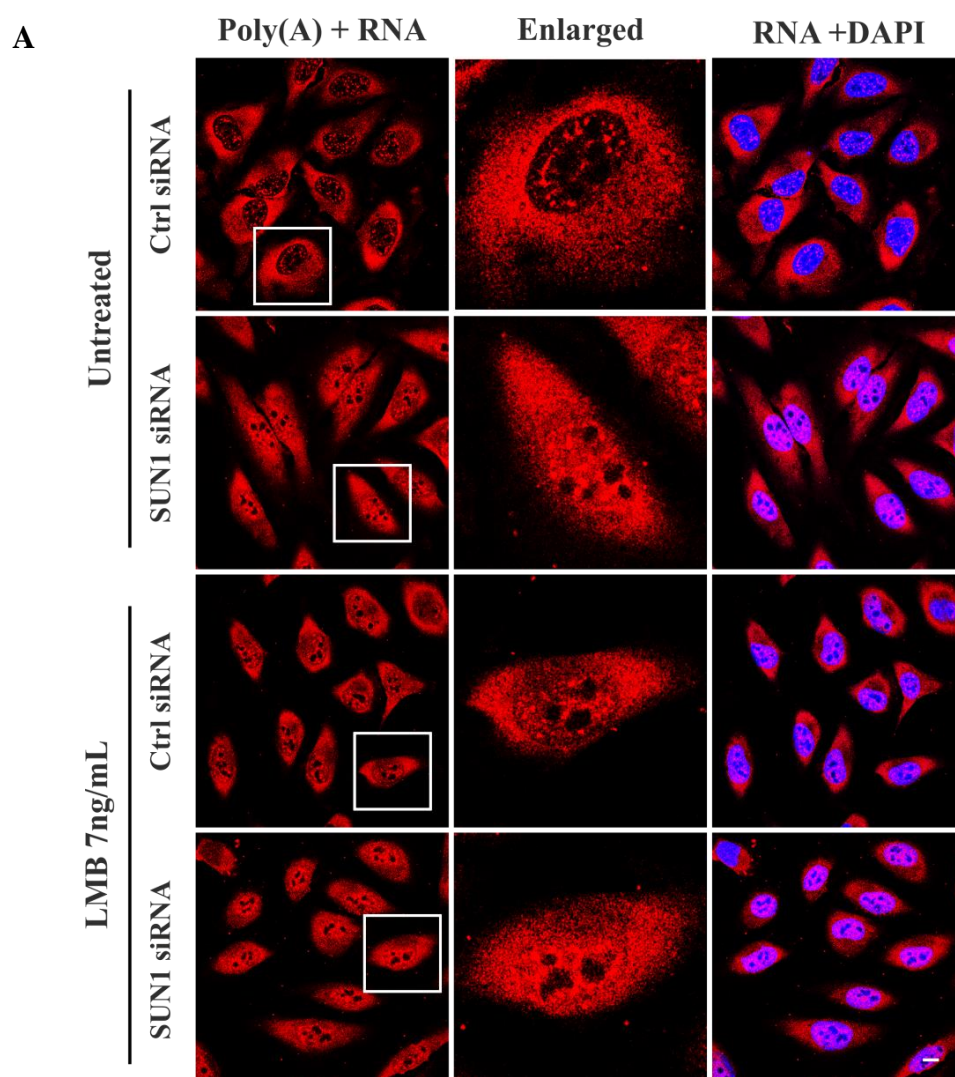
Figure 2.11 SUN1 depletion results in nuclear accumulation of poly(A)+RNA. RNA FISH showed poly(A)+RNA accumulation in the nucleus of SUN1-depleted cells after 72 h of siRNA transfection (upper two panels). For rescue experiment, HeLa cells were transfected with a GFP-SUN1^R expression vector and processed for poly(A)+RNA detection by FISH after 24 h and 72 h siRNA treatment, respectively (last panel). Bar: 10 μ m.

2.2.4 SUN1 functions in mRNA export independent of the CRM1-dependent pathway

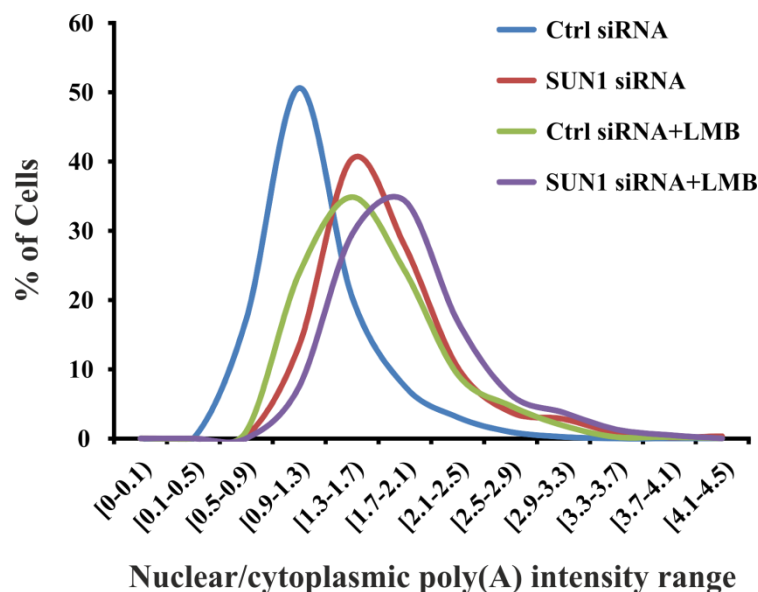
As we introduced before, mRNA export can be roughly divided into two forms: bulk and specific export according to the different export receptors (Culjkovic-Kraljacic and Borden, 2013). Most of the constitutively expressed mRNAs are exported by the NXF1-dependent pathway (bulk export), Whereas specialized subsets of mRNAs, UsnRNAs, rRNAs, and SRP RNA are exported by the CRM1-dependent pathway (specific export) (Natalizio and Wentz, 2013). Additionally, Leptomycin B (LMB) is a direct inhibitor of CRM1 and can directly block the CRM1-dependent pathway (Kudo et al., 1998).

SUN1 depletion resulting in nuclear accumulation of poly(A)+RNA indicates that SUN1 is involved in mRNA export. To further find out which mRNA export pathway requires SUN1, we compared the distribution of poly(A)+RNA in both LMB untreated and treated cells under siRNA condition (Figure 2.12A). For each trial, the nuclear/cytoplasmic (N/C) ratio of the

poly(A)+RNA distribution was determined by measuring the fluorescence intensity. Without LMB treatment, the N/C ratios of most control siRNA cells are centered at the range of [0.9-1.3) with a mean value of ~ 1.15 . In contrast, the N/C ratios of most SUN1 siRNA cells are centered at the range of [1.3-1.7) with a mean value of ~ 1.63 (Figure 2.12B, C). The shift in the range and the increase of the mean N/C ratio reflect higher nuclear accumulation of poly(A)+RNA upon SUN1 depletion. After treatment with 7 ng/ml of LMB, the N/C ratio ranges of both control and SUN1 siRNA cells were significantly shifted to [1.3-1.7) and [1.7-2.1) with an increased mean value up to ~ 1.56 and ~ 1.84 , respectively (Figure 2.12B,C). For control siRNA, the remarkable increase of the N/C ratio after LMB treatment revealed that the drug treatment worked under our experimental conditions. Strikingly, for SUN1 siRNA, the shift of the N/C ratio range and the increase in the mean value indicate that LMB treatment can cause additional nuclear accumulation of poly(A)+RNA above that caused by SUN1 depletion suggesting that SUN1 plays a role in mRNA export independent of the CRM1-dependent pathway.



B



C

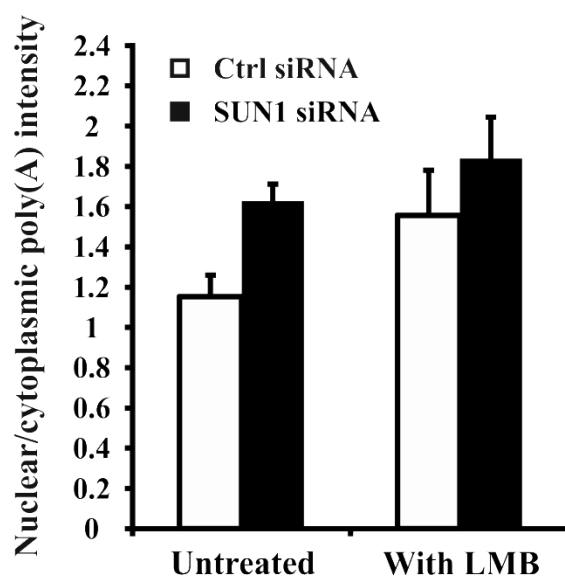


Figure 2.12 Comparison of the nuclear accumulation of poly(A)+RNA caused by SUN1 depletion and LMB treatment. **A:** RNA FISH showed the distribution of poly(A)+RNA in both LMB untreated and treated cells under siRNA condition. The treatment was performed by adding 7ng/ml of LMB for 2 h after 72 h siRNA transfection. Bar: 10 μ m. **B:** The nuclear/cytoplasmic (N/C) ratio of the poly(A)+RNA distribution was determined by measuring fluorescence intensity, and the percentages of cells in each N/C ratio intensity range were shown. For each condition ~500 cells were analysed. **C:** The mean nuclear/cytoplasmic (N/C) ratio of LMB untreated and treated cells under siRNA condition.

2.2.5 SUN1 associates with nuclear mRNP through a direct interaction with NXF1, a general mRNA export factor in mammals

Based on our results we assume that SUN1 might be involved in the NXF1-dependent mRNA export pathway (bulk export). After transcription and processing, the formation of the mRNP complex is the first step of mRNA export in eukaryotic cells (Carmody and Wenthe, 2009). To test whether SUN1 is associated with mRNP, we harvested the nuclear poly(A)+RNPs from mammalian nuclei with Dynabeads[®] Oligo (dT)₂₅. Endogenous SUN1 specifically copurified with the poly(A) fraction as did NXF1 (Figure 2.13A). Moreover, SUN2, hnRNP K and hnRNP H were also observed in the poly(A) fraction, but not hnRNP F (Figure 2.13A). These results indicate that SUN1 associates with NXF1-containing nuclear mRNP, either directly or indirectly through other proteins.

NXF1, also known as TAP, is a general metazoan mRNA export factor to transport mRNP through the NPC (Gruter et al., 1998; Stutz and Izaurralde, 2003). In order to find out how SUN1 associates with mRNP and functions in the NXF1-dependent mRNA export pathway, we performed several studies. Western blot analysis showed that NXF1 was down regulated when SUN1 is absent from HeLa cell lysates after SUN1 depletion compared to control siRNA. GAPDH was used as a loading control (Figure 2.13B). Moreover, endogenous NXF1 was pulled down from HeLa cell lysates by both GST tagged N-terminal SUN1 and SUN2 (Figure 2.9A and 2.13C). Consistently, endogenous SUN1 was precipitated by GST tagged full length NXF1 as well (Figure 2.13D). GST was used as negative control. A direct interaction study between NXF1 and GST-SUN1-NT was performed by pulldown of thrombin cleaved purified NXF1. NXF1 was detected by NXF1 antibodies in the GST-SUN1-NT precipitate (Figure 2.13E). These results indicate that SUN1 interacts directly with NXF1 in vitro and the N-termini of SUN1 and SUN2 are responsible for the binding. Further, immunofluorescence studies showed that NXF1 uniformly localized in the nucleus of GFP- and GFP-SUN1-overexpressing cells (Figure 2.13F). GFP-SUN1 localized along the nuclear envelope as previously reported (Li et al., 2014). However, most strikingly, overexpressed GFP-SUN1-NT was not able to localize at the nuclear envelope; instead, it formed aggregate-like structure both within and outside the nucleus (Figure 2.13F). Additionally, strong staining of NXF1 was observed along these GFP-SUN1-NT aggregate-like structures and only faint staining was seen in the nucleus as compared to untransfected cells (Figure 2.13F). These results indicate that SUN1 presumably associates with mRNP cargo through a direct interaction with NXF1 in the nucleus, and the N-terminus of SUN1 (1-239) is responsible for this connection.

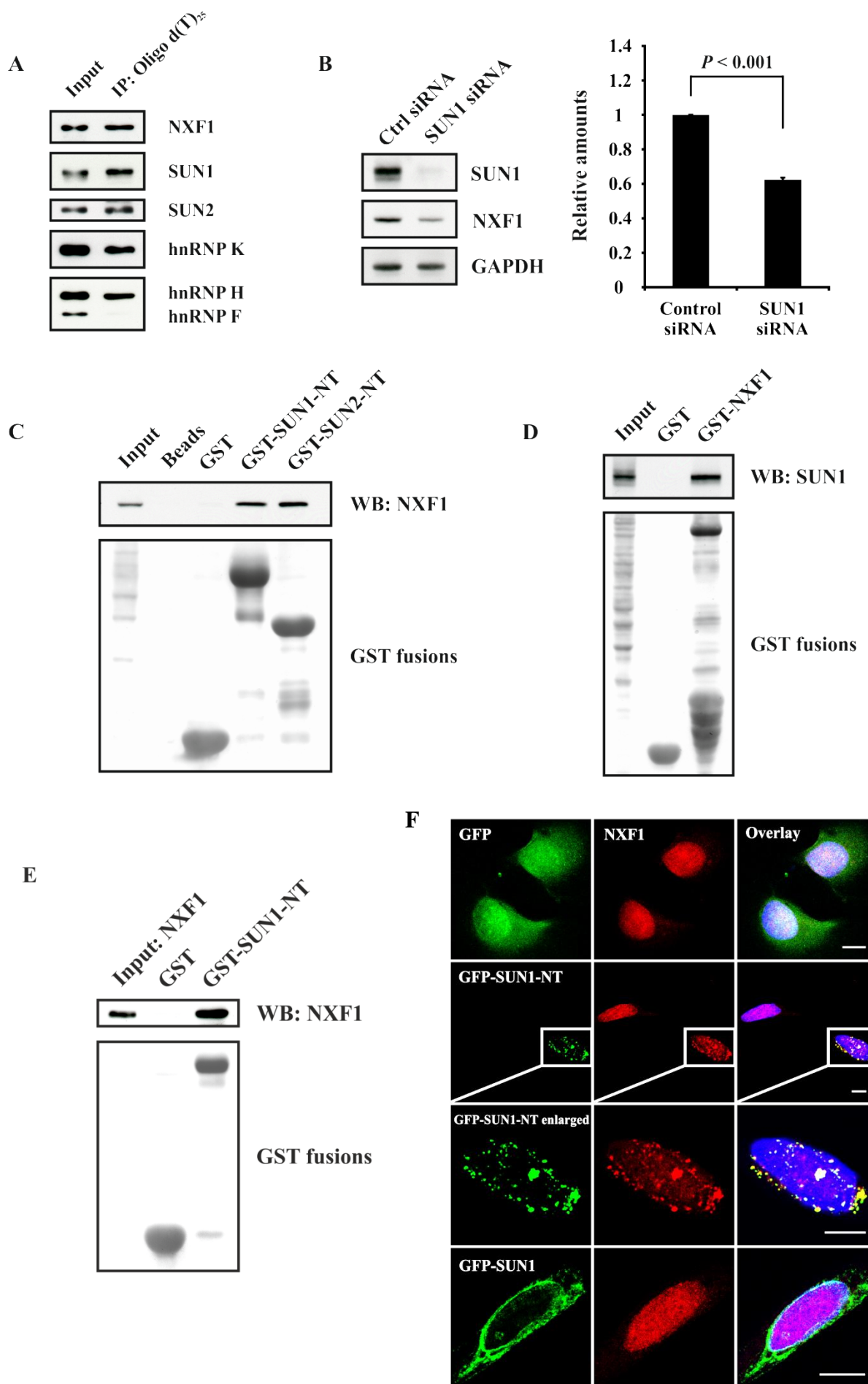


Figure 2.13 SUN1 associates with mRNP and mRNA export component NXF1. **A:** SUN1 interacts with nuclear poly(A)+RNPs. Nuclear poly(A)+RNA purified from soluble nuclear extract of HeLa cells was analysed by western blotting for associated proteins. **B:** Western blot analysis showed the down regulation of NXF1 in SUN1 depleted HeLa cell lysates. GAPDH was used as loading control. The expression level was quantified by scanning densitometry (right panel). **C:** The N-termini of SUN1 and SUN2 interact with NXF1. Endogenous NXF1 was pulled down from HeLa cell lysates by GST tagged N-termini of SUN1 and SUN2. **D:** NXF1 interacts with SUN1. Endogenous SUN1 was precipitated by GST tagged full length NXF1. **E:** The N-terminus of SUN1 directly interacts with NXF1 released from the GST part after thrombin cleavage. **F:** Immunofluorescence showed the altered localization of NXF1 in GFP-, GFP-SUN1-NT- and GFP-SUN1-overexpressing cells. Bar: 10 μ m. For all pulldown experiments, proteins were separated by SDS-PAGE (12% acrylamide) and the GST fusion proteins were visualized by Ponceau S staining. GST was used as negative control.

2.2.6 SUN1 associates with the NPC through a direct interaction with Nup153, a nuclear FG nucleoporin at the NPC basket involved in mRNA export

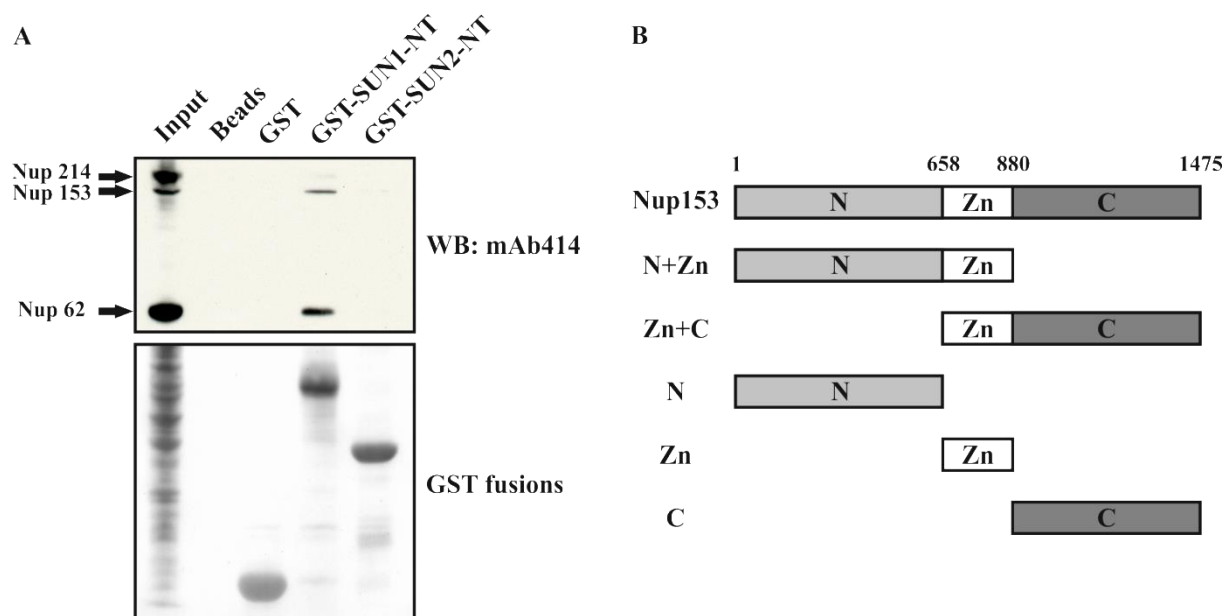
Our observation that SUN1 interacts directly with NXF1, that it is present at the nuclear envelope, suggests a role for SUN1 in mammalian mRNA export whereby SUN1 recruits NXF1-containing mRNP onto the nuclear envelope and hands it over to the NPC. One prediction of this hypothesis is that SUN1 depletion should reduce the association of NXF1 and NPC. However, SUN1 depletion reduced the amount of NXF1, showed in figure 2.13B.

Furthermore, previous reports highlighting the association of SUN1 and NPC revealed that SUN1 is important for NPC assembly in early steps of interphase and for its distribution across the nuclear surface (Chang et al., 2015; Liu et al., 2007; Talamas and Hetzer, 2011). To further confirm the association between SUN1 and NPC, we performed pulldown experiment. Western blot analysis showed that endogenous Nup62, Nup153 and a faint band of Nup214 were observed in GST-SUN1-NT precipitates by using mAb414 antibodies (Figure 2.14A). Surprisingly, these nucleoporins were not precipitated by GST-SUN2-NT. However, this is consistent with the previous results that SUN1 but not SUN2 colocalizes with Nup153 and NPC (Liu et al., 2007; Lu et al., 2008). These results indicate that SUN1 associates with the NPC via either direct or indirect interaction with a subset of nucleoporins, such as Nup62, Nup153 and Nup214.

To date, apart from vertebrate pore proteins Nup98, Nup133, Nup160, Tpr, and CAN/Nup214, Nup153 has been involved in the export of mRNA (Dimaano and Ullman, 2004; Kohler and Hurt, 2007). Moreover, compared to Nup62 and Nup214, GST tagged SUN1 N-terminus showed a preference for Nup153, given that there was much lower amount of Nup153 present in the input lysates (Figure 2.14A). Thus, we extended our interaction

studies to SUN1 and Nup153. According to the domain structure of Nup153, we used a series of plasmids which coded for the N-terminus, Zinc finger and C-terminus of Nup153 for pulldown experiment (Figure 2.14B). Endogenous SUN1 was precipitated by all GST fusion proteins which contain either N-terminal or C-terminal sequences, but not by the Zinc finger alone (Figure 2.14C). This result indicates that Nup153 interacts with SUN1, and that both the N- and C-terminus are important for this binding. Further, a direct interaction study between Nup153 and GST-SUN1-NT was performed by pulldown using PreScission protease cleaved purified Nup153-Zn+C fragment. A strong signal of Nup153-Zn+C was detected by Nup153 antibodies in the GST-SUN1-NT precipitate (Figure 2.14D). GST alone was used as negative control. Therefore, SUN1 associates with the NPC through Nup153, which is a nuclear FG nucleoporin at the NPC basket and plays an important role in mRNA export.

Additionally, it was reported that Nup153 is highly mobile and present at different parts of the pore as well as in the interior of the nucleus (Daigle et al., 2001; Griffis et al., 2004). This strongly supports our hypothesis that SUN1 recruits NXF1-containing mRNP onto the NE and hands it over to the NPC.



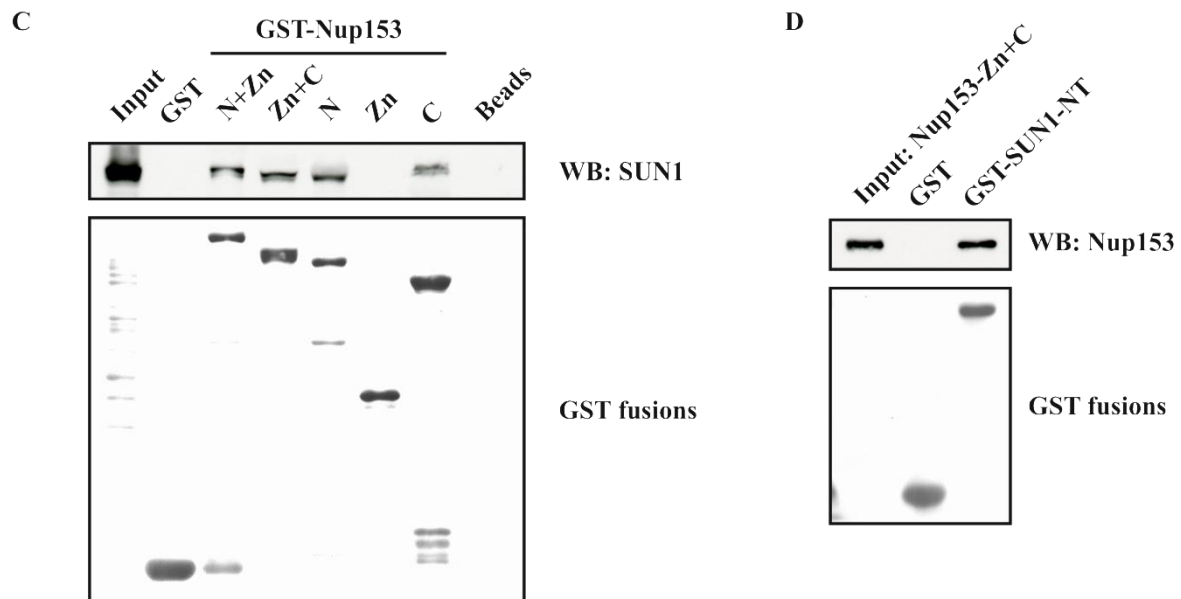


Figure 2.14 SUN1 interactions with Nup153, a nuclear FG nucleoporin involved in mRNA export. **A:** The N-terminus of SUN1 interacts with Nup62, Nup153 and Nup214. Western blot analysis showed that endogenous Nup62, Nup153 and a faint band of Nup214 were present in the precipitate of GST-SUN1-NT but not GST-SUN2-NT by using mAb414 antibodies. **B:** The predicted domain structure and a schematic of several Nup153 polypeptides which contain N-terminus, Zinc finger and/or C-terminus. **C:** Both the N- and C-terminus of Nup153 interact with SUN1. The pull-down experiment showed that endogenous SUN1 was precipitated by all GST fusion proteins which contain either N-terminus or C-terminus of Nup153, but not by Zinc finger sequences alone. **D:** The N-terminus of SUN1 directly interacts with Nup153-Zn+C fragment which was obtained by PreScission protease cleavage and detected by Nup153 antibodies. In all the pull-down experiments, proteins were separated by SDS-PAGE (12% acrylamide) and the GST fusion proteins were visualized by Ponceau S staining. GST was used as negative control.

3. Discussion

3.1 Contribution of SUN1 mutations to the pathomechanism in muscular dystrophies

The analysis of the patient cells revealed defects in several cellular properties that have been also associated with mutations in other NE components. This is explained by the complex nature of the NE and the many interactions its components undergo. We compared our observations with data available in the literature and found that in both cases most of the alterations, which we observed can be linked to laminopathic mutations to various degrees (Table 1). In regard to the wound healing experiment and single cell motility P1 cells exhibited a unique behavior and showed a faster gap closure and increased cell motility. By contrast, Lamin A/C and Nesprin-2 deficient cells have decreased wound closure and single cell motility (Hale et al., 2008; Rashmi et al., 2012). Alterations in cell cycle progression, which is discussed as one of the disease causing mechanisms were seen in laminopathies and were associated with loss of SUN1 and SUN2 as well (Lei et al., 2012; Pratt et al., 2011).

SUN proteins are central components of the LINC complex, which connects the nucleus to the cytosol through interactions with cytoskeletal elements such as F-actin and intermediate filaments. It is a major mediator of cellular mechanosensing and an important element of the physical pathways that transduce mechanical cues to the nucleus. Based on their central role they are also potential candidates in laminopathies although no mutations have been directly linked to this group of diseases. All SUN mutations that have been described so far were exclusively reported for different cancer cells [Ensembl database: www.ensembl.org; (Shan et al., 2013)]. Recent findings indicated that down regulation of SUN1 in *Lmna* deficient mice ameliorated the disease phenotype (Chen et al., 2012).

SUN proteins exist as oligomers; moreover, SUN1 and SUN2 can interact with each other and form heterooligomers (Lu et al., 2008; Xiong et al., 2008). Structural analysis of the KASH SUN complex has revealed the molecular details of the interaction between the SUN domain of SUN2 and the C-terminal sequence of Nesprin-2 (Sosa et al., 2012; Wang et al., 2012; Zhou et al., 2012). The SUN domain forms a trimer and binds to three Nesprin molecules. The complex is stabilized by an interchain disulphide bond between a conserved cysteine in the KASH domain and a cysteine in the SUN domain. The coiled coil regions of SUN form a triple helix which is responsible for the trimer formation. The mutation A614V is not present in the structure solved but precedes it by 2 amino acids. The impact of the mutation on formation of the triple helix and its stability is therefore not clear. However, in previous work

we have shown that sequences preceding the SUN domain interact with the KASH domain of Nesprins as well and an effect of this mutation on LINC complex formation is likely (Padmakumar et al., 2005). In fact, upon ectopic expression of the mutant protein in wild-type fibroblasts the interactions at the NE with Emerin are disturbed and both patient fibroblasts exhibited reduced interaction with Lamin A/C (Tables 1-2). The upregulation of SUN2 in the P2 patient cells may ameliorate some of the laminopathic characteristics, which are less severe compared to the P1 patient cells (Table 1).

The N-terminal domain of SUN1 faces the nucleoplasm. It provides an interaction site for Lamin A (residues 1-138) and Emerin and Nesprin-2 (residues 209-302) (Haque et al., 2010). Furthermore, the N-terminal domain also binds to chromatin (Xiong et al., 2008). The A203V mutation in SUN1 is not contained in these binding sites; however the mutant protein when expressed in wild-type fibroblasts or from both patient fibroblasts showed an impaired interaction with Emerin and Lamin A/C (Tables 1-2).

Taken together, our results highlight the interactions at the NE. Mutations in the *EMD* and *TMPO* gene in combination with mutations in SUN1 have an impact on several components of the network and affect both cellular properties as well as expression levels of NE proteins which themselves then can result in changes thus revealing various interdependencies.

3.2 Inner nuclear envelope protein SUN1 plays a prominent role in mammalian mRNA export

3.2.1 Both SUN1 and SUN2 interact with hnRNP F/H and hnRNP K/J which accumulate in the nucleus by SUN1 depletion

The double membrane of the nucleus physically separates the nucleus from the cytoplasm, whereas the LINC complex composed of conserved SUN and KASH domain proteins of the NE mechanically bridges the nucleoskeleton and cytoskeleton. SUN1 and SUN2 are INM components of the LINC complexes with a conserved Sad1/UNC-84 homology SUN-domain at the C-terminus.

The hnRNPs are RNA-binding proteins that associate with nascent transcripts produced by RNA polymerase II, and other RNA complexes (Dreyfuss et al., 1993). In human cells, about 30 different hnRNPs associate with pre-mRNAs in the nucleus. These proteins (hnRNP A1-U) with a molecular weight of ~34-120 kDa are highly abundant in the nucleus (Dreyfuss et al., 2002; Pinol-Roma and Dreyfuss, 1993). They affect multiple aspects of pre-mRNA processing and mRNA metabolism including the packaging of nascent transcripts, alternative

splicing, nucleocytoplasmic transport and translational regulation. Although they have some common characteristics, they differ from each other in domain composition and functional properties (Han et al., 2010).

The hnRNP F/H include hnRNP F, H1 (H), H2 (H) and H3 (2H9) and have highly similar sequence, structure and binding preferences. All the hnRNPs contain RBDs (RNA binding domain), however, compared to most hnRNPs, hnRNP F/H have different RBDs named as qRRMs (quasi-RNA recognition motif) (Honore et al., 1995). Moreover, hnRNP F/H specifically bind to poly(G) *in vitro* which is a characteristic different from others (Matunis et al., 1994). The hnRNP F/H are well known for their function in the regulation of alternative splicing, whereby the binding sites of hnRNP F/H improve the splicing of an enlarged intron and modulate the selection of splice-sites (Martinez-Contreras et al., 2006).

In eukaryotic cells, pre-mRNAs are synthesized in the nucleus by RNA polymerase II and after series of processing they are transported to the cytoplasm for translation. Therefore, another key difference between the hnRNPs is that some of them shuttle between the nucleus and the cytoplasm (Pinol-Roma and Dreyfuss, 1992). This was originally assumed as a means of transporting mRNA into the cytoplasm and there are evidences supporting the link between hnRNPs transport and mRNA export. First, it was reported that a subset of hnRNPs, including hnRNP A1, A2, D, E, I and K, continuously shuttle, accompanied by some mRNA export factors, between the nucleus and the cytoplasm (Michael et al., 1995b; Pinol-Roma and Dreyfuss, 1992; Pinol-Roma and Dreyfuss, 1993). Second, mRNA translocating through the NPC is directly associated with shuttling hnRNPs (Visa et al., 1996). Third, hnRNP A1 with a nuclear export signal (NES) has been identified as a direct player involved in mRNA export (Izaurrealde et al., 1997; Michael et al., 1995a).

One of such shuttling hnRNPs related to our finding is hnRNP K. The structure of hnRNP K is grossly different from the others in that it contains three KH (K homology) domains rather than RRM (RNA recognition motifs) or RRM-like domains. Due to its special structure, hnRNP K plays an important role in many aspects of mRNA metabolism, including mRNA silencing (Ostareck et al., 2001; Ostareck et al., 1997), transcription (Lynch et al., 2005; Stains et al., 2005), splicing (Expert-Bezancon et al., 2002), regulation of mRNA stability (Fukuda et al., 2009) and translation (Habelhah et al., 2001; Mukhopadhyay et al., 2009). Therefore, hnRNP K functions in mRNA processing within the nucleus, and then accompanies the mRNA until it translocates through the NPC into the cytoplasm for participating in translation regulation, indicating that hnRNP K might be involved in mRNA export as well.

SUN1 and SUN2 are conserved type-II INM proteins and consist of an N-terminal, coiled-coiled, transmembrane and SUN domain at the C-terminus which directly interacts with a KASH domain to form LINC complex in the lumen of the NE (Mejat and Misteli, 2010; Tzur et al., 2006; Worman and Gundersen, 2006). Obviously, the N-termini of SUN1 and SUN2 are responsible for the association with the nucleoskeleton and other nuclear events. Therefore, we used the N-terminus of SUN protein for pulldown and LC-MS analysis so as to find new interacting partners (Taranum et al., 2012). Our results that the N-termini of SUN1 and SUN2 interact with hnRNP F/H and hnRNP K/J *in vitro* suggest that the N-termini of SUN proteins might be associated with mRNA biogenesis according to the functions of hnRNP F/H and hnRNP K/J. *In vivo*, these hnRNPs can be precipitated by full length GFP-SUN1 and GFP-SUN2 indicating that SUN1 and SUN2 interact with hnRNP-mRNA complexes in the nucleus. Considering that SUN1 and SUN2 are anchored in the INM, they might play a crucial role in mRNA biogenesis at a late stage, such as mRNA export. Consistently, immunofluorescence analysis showed that endogenous SUN1 and SUN2 colocalized with hnRNP F/H and hnRNP K/J only at the NE.

The hnRNP proteins accompany mRNP at different stages during mRNP export (Dreyfuss et al., 2002). Before an mRNP translocates through the NPC, the nuclear restricted hnRNPs containing nuclear-retention signals start to get released from the mRNP and stay in the nucleus, whereas the shuttling hnRNPs will accompany the mRNA through the NPC channel and into the cytoplasm (Carmody and Wentz, 2009; Dreyfuss et al., 2002) (Figure 1.7). Therefore, the shuttling hnRNPs become an important marker reflecting the efficiency of mRNA export. One such well known shuttling hnRNP involved in our study is hnRNP K (hnRNP F/H were unknown until now), which interacts with both SUN1 and SUN2.

Knockdown is a general tool for studying the function of proteins. To confirm our hypothesis that SUN proteins are involved in mRNA export, we performed knockdown studies of SUN1 using siRNA. Based on the efficient SUN1 knockdown, we can see remarkably altered distributions of hnRNPs by performing subcellular fractionation experiment in control and SUN1 knockdown cells. Our results showed that all the studied hnRNPs, especially hnRNP K, accumulated in the nuclear fraction and reduced in the cytosolic fraction as compared to negative controls, indicating that SUN1 depletion affects the nucleocytoplasmic transport of a shuttling hnRNP protein, hnRNP K, supposed to be a marker of mRNA export. Besides, Lamin A/C, an interaction partner of SUN1, was reported to interact with hnRNP E1 (Zhong et al., 2005), another well-known shuttling hnRNP protein (Chkheidze et al., 1999; Dreyfuss

et al., 2002; Kiledjian et al., 1995), that strongly supports our hypothesis that SUN1 functions in mRNA export via either direct or indirect interactions.

3.2.2 SUN1 is important for mRNA export

In previous studies, nuclear mRNA export in higher eukaryotes was studied mainly using two methods, microinjection of specific antibodies into *Xenopus* oocytes and overexpression transfection assays in mammalian cells. Although both methods are powerful for analysing poly(A)+RNA in vivo, there exist still limitations. For example, one needs to purify the protein of interest and produce specific antibodies for injection. Based on these methods, one can find out whether a protein of interest promotes or inhibits nuclear mRNA export, but cannot tell whether this protein is essential for this pathway. Later on, the discovery of RNAi solved these problems in higher eukaryotes by transiently silencing of specific gene.

Our observations that hnRNP F/H and hnRNP K accumulate in the nucleus after SUN1 depletion provide a clue that SUN1 might participate in hnRNP involved mRNA export. To directly find out whether SUN1 is important for mammalian mRNA export, we performed RNA FISH analysis after SUN1 knockdown. Our results showed that the poly(A)+RNA distribution was altered in SUN1 knockdown cells, whereby poly(A)+RNA strongly accumulated in SUN1 depleted nucleus compared to the control. Further, a rescue study performed in mRNA export deficient cells confirmed that SUN1 depletion resulted in an mRNA export defect. The defective phenotype was not due to off-target effects. Thus, we conclude that SUN1 has an important role in mRNA export.

3.2.3 SUN1 functions in mRNA export independent of the CRM1-dependent export pathway

Recently, mRNA export has been roughly divided into two forms: bulk and specific export according to the different export receptors (Culjkovic-Kraljacic and Borden, 2013). The export receptor NXF1 mediates the export of most constitutively expressed mRNAs, named as NXF1-dependent pathway (bulk export). Another export receptor, CRM1, mediates the export of specialized subsets of mRNAs, UsnRNAs, rRNAs, and SRP RNA, named as CRM1-dependent pathway (specific export) (Natalizio and Wentz, 2013). Obviously, we have to ask what kind of mRNAs require SUN1 for export and in which export pathway SUN1 is involved.

For answering these questions, specific inhibitors are required to block one of the pathways. Luckily, LMB, a well-known inhibitor of CRM1, is available which can directly block the CRM1-dependent pathway (Herold et al., 2003; Kudo et al., 1998). Therefore, we used LMB to block the CRM1-dependent export under RNAi condition and compared the distribution of poly(A)+RNA in both LMB untreated and treated cells. For each trial, the nuclear/cytoplasmic (N/C) ratio of the poly(A)+RNA distribution was determined by measuring fluorescence intensity. Without LMB treatment, the N/C ratios of most control siRNA cells are centered at the range [0.9-1.3] with a mean value of ~1.15 which is similar as previously reported in HeLa control cells (Folkmann et al., 2013). Interestingly, the N/C ratios of SUN1 siRNA cells were increased up to ~1.63 reflecting higher nuclear accumulation of poly(A)+RNA. After treatment with 7 ng/ml of LMB, the N/C ratios of both control- and SUN1 siRNA-transfected cells were significantly increased with the mean value up to ~1.56 and ~1.84, respectively. In control siRNA cells, the increase after LMB treatment means that the drug treatment worked under our experimental conditions. Most surprisingly, in SUN1 siRNA cells, the further increase after LMB treatment indicates that LMB caused additional nuclear accumulation of poly(A)+RNA apart from that due to SUN1 depletion. Therefore, we conclude from the additional accumulation that SUN1 plays a role in mRNA export independent of the CRM1-dependent pathway, which in turn suggests SUN1 might participate in the NXF1-dependent pathway.

3.2.4 NXF1 mediates the association between SUN1 and mRNP

In higher eukaryotes, NXF proteins exist as a protein family encoded by the amplification of *nxf* genes. There is only one NXF protein encoded by yeast genome, Mex67p, but there are two NXFs in *Caenorhabditis elegans* and four in *Drosophila melanogaster* and *Homo sapiens*. However, the best known NXF protein is NXF1 (Mex67p in yeast) which has an essential role in bulk mRNA export (reviewed in (Izaurrealde, 2002)).

Based on previous results we assume that SUN1 might be involved in the NXF1-dependent mRNA export pathway. In eukaryotic cells, the formation of mRNP complex is the first step of mRNA export (Carmody and Wentz, 2009). Oligo dT pulldown experiment showed that endogenous SUN1 and NXF1 specifically copurified with the poly(A) fraction, as did SUN2, hnRNP K and hnRNP H, but not hnRNP F, suggesting SUN1 associates with NXF1-containing nuclear mRNP, either directly or indirectly through other proteins.

Since the essential role of NXF1 in mRNA export is well established in different species, we supposed that SUN1 associates with mRNP complex through the connection with NXF1. In

order to prove this point, several studies related to SUN1 and NXF1 were designed and implemented. Interestingly, the results indeed reveal that SUN1 is directly related to NXF1 in many ways. For instance, SUN1 depletion down regulates the expression level of NXF1, SUN1 and NXF1 directly interact with each other *in vitro* and NXF1 exhibits aggregate-like staining along with GFP-SUN1-NT. Importantly, the N-terminus of SUN1 is essential for these associations. These results highlight our hypothesis that SUN1 associates with mRNP cargo through a direct interaction with NXF1 which is recruited to the mRNP in the nucleus prior to export.

3.2.5 SUN1 hands the mRNP over to the NPC component Nup153

The second step in mRNA export is the mRNP targeting and translocating through the central channel of the NPC. Considering our finding that SUN1 directly interacts with NXF1 and that it is present at the NE, we assume that SUN1 supports mRNA export by recruiting NXF1-containing mRNP onto the NE and then hands it over to the NPC. Therefore, we continued our studies towards a connection between SUN1 and NPC. Although several reports indicate that SUN1 is important for the assembly and distribution of the NPC (Chang et al., 2015; Liu et al., 2007; Talamas and Hetzer, 2011), there is no evidence related to SUN1 and NPC-mediated mRNA export. In order to find out what is the connection between SUN1 and NPC, we performed several protein-protein interaction studies *in vitro*. The results showed that SUN1 but not SUN2 interacted with Nup62, Nup153 and Nup214 detected by mAb414 antibodies and that SUN1 exhibited a preference for Nup153. These results indicate that SUN1 associates with the NPC through either direct or indirect interaction with a subset of nucleoporins, such as Nup62, Nup153 and Nup214.

Nup153 is named for its predicted mass (Galy et al., 2003; Harborth et al., 2001) as is for most nucleoporins, localized at the nuclear basket of the NPC (Sukegawa and Blobel, 1993) and composed of the N-terminal, Zinc finger and C-terminal domain. The N-terminal domain (1–610) of Nup153 is unique and contains three overlapping regions involved in Nup153 localization and RNA binding, that are a nuclear envelope targeting cassette (NETC, 2–144), nuclear pore associating region (NPAR, 39–339) and a RNA binding domain (250–400) (Bastos et al., 1996; Enarson et al., 1998). The zinc finger domain (650–880) contains four C2–C2 type zinc fingers which have been reported to associate with DNA (Sukegawa and Blobel, 1993), and they are similar to those found in Nup358 (Wu et al., 1995; Yokoyama et al., 1995). The C-terminal domain of Nup153 contains FG repeats similar to several other nucleoporins, where F is phenylalanine, and G is glycine (Denning et al., 2003).

To date, apart from vertebrate pore proteins Nup98, Nup133, Nup160, Tpr, and CAN/Nup214, Nup153 has been identified to associate with mRNA export (Dimaano and Ullman, 2004; Kohler and Hurt, 2007). Nup153 is unique among the vertebrate pore proteins since it contains an RNA binding domain (250–400) which has the ability to directly bind to RNA (Dimaano et al., 2001). The RNA binding ability of Nup153 is conserved in *Drosophila*, *Xenopus* and human proteins (Dimaano et al., 2001), and it was found to preferentially bind single-stranded RNA, that refers to mRNA (Ball et al., 2004).

Thus, we extended our interaction studies to SUN1 and Nup153. According to the domain structure of Nup153, a series of polypeptides which contain the N-terminal, Zinc finger and/or C-terminal domain were used in the experiment. The results showed that Nup153 interacts directly with SUN1, and both the N- and C-terminus are important for this binding. Therefore, we concluded that SUN1 associates with the NPC through a direct interaction with Nup153 which plays an important role in mRNA export.

Additionally, it was reported that Nup153 is highly mobile and presents at different parts of the pore as well as in the interior of the nucleus (Daigle et al., 2001; Griffis et al., 2004). This strongly supports our hypothesis that SUN1 recruits NXF1-containing mRNP onto the NE and then hands it over to the NPC.

One prediction of our hypothesis is that SUN1 hands the mRNP over to the NPC component Nup153. Therefore there should be some connections between mRNP and Nup153. Indeed, these connections exist. Nup153 is able to recognize two parts of the mRNP, a single-stranded stretch of mRNA and the mRNA export receptor NXF1 which can interact with the C-terminal region of Nup153 (Bachi et al., 2000). Moreover, SUN1 hands the mRNP over to Nup153 for which several ways can be imagined. First, Nup153 interacts with NXF1 which could lead to a release of mRNP from SUN1, however this is in conflict with our finding that SUN1 directly interacted with Nup153; second, Nup153 interacts with SUN1 to set free the NXF1-containing mRNP and transfer it to Nup153, but this also looks rather unlikely considering that SUN1 showed a preference for NXF1 in the presence of Nup153 (data not shown); third, Nup153 simultaneously interacts with SUN1 and NXF1 leading to mRNP release from SUN1 and a direct transfer to Nup153. Such a scenario would well agree with our data.

Once the mRNP targets the NPC, it starts to translocate through the central channel of the NPC and be released into the cytoplasm for translation. Interestingly, Nup153 might be still involved in this process. There is evidence that Nup153 is not only localized at the nuclear basket of the NPC. Immuno-gold labelled antibodies and epitope-tagged versions of Nup153

were used for the examination. The N-terminal epitope tag was detected at the nuclear coaxial ring, while the C-terminus was distributed both in the basket and on the cytoplasmic side of the pore, suggesting that the C-terminal region is flexible and is not fixed at a point within the pore (Fahrenkrog et al., 2002). Similarly, several FG-rich domains were measured by biophysical methods and the results showed that these regions are natively unfolded and exist in a balance between many conformations (Denning et al., 2003). Additionally, Nup153 shuttles between the nuclear and cytoplasmic faces of the NPC since it contains an M9 shuttling domain, M9-type NLS, at the N-terminus (Nakielny et al., 1999). Thus, Nup153 might support mRNP to translocate through the NPC by its C-terminus.

Taken together, mRNA is transcribed by RNA polymerase II, packaged into mRNP by hnRNPs and other RNA binding proteins, then spliced and processed to form mature mRNA (mRNP). The mRNP is labelled by NXF1 in the nucleus and recruited onto the NE by the INM protein SUN1. Prior to the export from the NPC, the nuclear restricted hnRNPs and other RNA binding proteins are released from the mRNP and stay in the nucleus, whereas the shuttling hnRNPs accompany the mRNA into the cytoplasm. Finally, SUN1 hands over the mRNP to the NPC component Nup153, which most likely translocates the mRNP cargo through the NPC either directly by itself or indirectly together with other proteins.

This is consistent with a model for SUN1 functions in mammalian mRNA export whereby SUN1, acting as a docking point, recruits NXF1-containing mRNP onto the NE, and hands it over to the NPC component Nup153 which enables the nuclear mRNA export to be performed systematically (Figure 3.1).

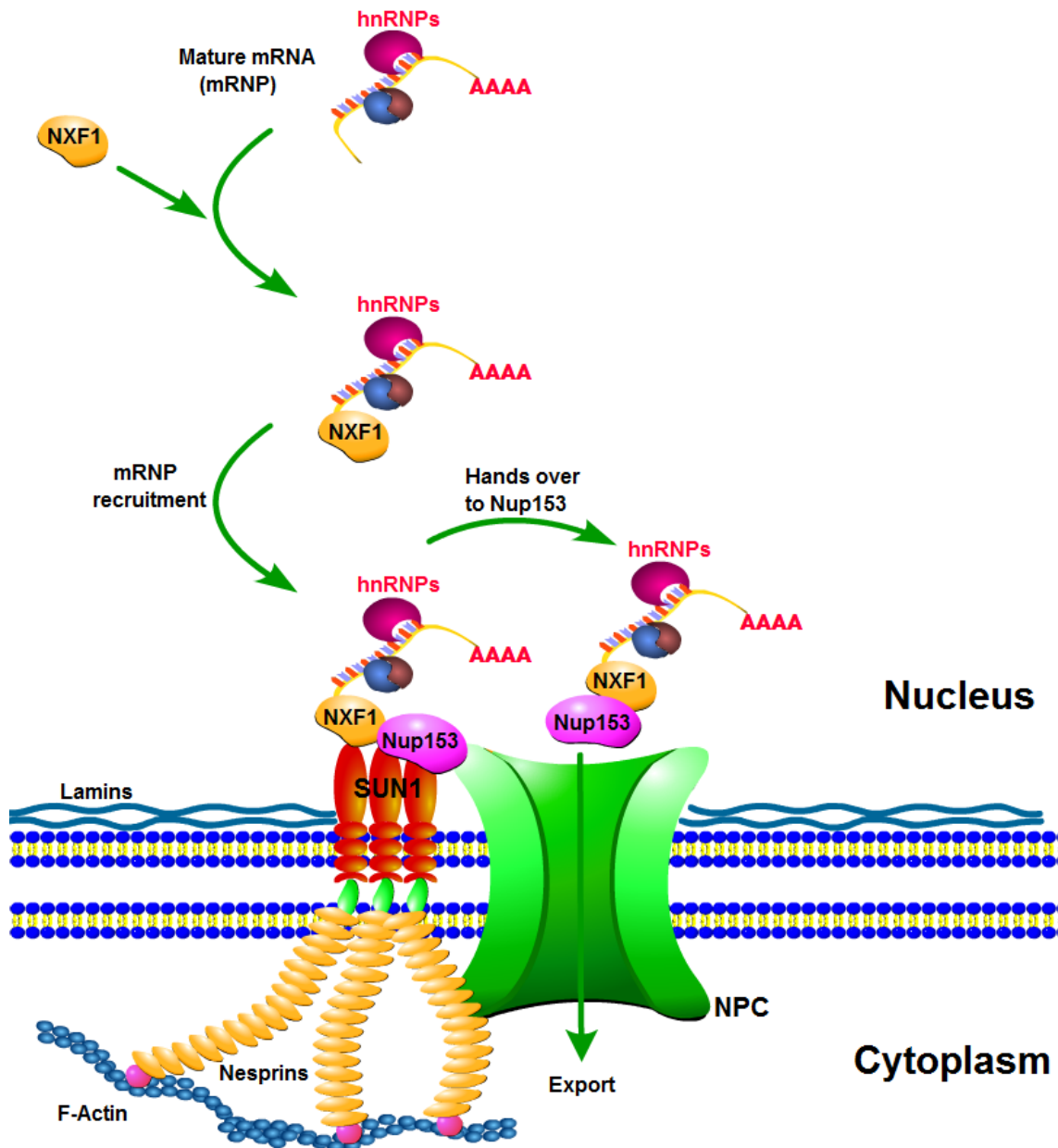


Figure 3.1: A model of SUN1 functions in mammalian mRNA export. We propose that SUN1 acts as a docking point to recruit NXF1-containing mRNP onto the NE and hands it over to Nup153.

4. Summary

Mutations in several genes encoding nuclear envelope associated proteins cause Emery-Dreifuss muscular dystrophy (EDMD). We analyzed fibroblasts from a patient who had a mutation in the EMD gene (p.L84Pfs*6) leading to loss of Emerin and a heterozygous mutation in SUN1 (p.A203V). The second patient harbored a heterozygous mutation in LAP2alpha (p.P426L) and a further mutation in SUN1 (p.A614V). p.A203V is located in the N-terminal domain of SUN1 facing the nucleoplasm and situated in the vicinity of the Nesprin-2 and Emerin binding site. p.A614V precedes the SUN domain which interacts with the KASH domain of Nesprins in the periplasmic space and forms the center of the LINC complex. At the cellular level we observed alterations in the amounts for several components of the nuclear envelope (NE) in patient fibroblasts and further phenotypic characteristics generally attributed to laminopathies such as increased sensitivity to heat stress. The defects were more severe than observed in EDMD cells with mutations in a single gene. In particular, in patient fibroblasts carrying the p.A203V mutation in SUN1 the alterations were aggravated. Moreover, both patient fibroblasts exhibited reduced interaction of SUN1 with Lamin A/C and when expressed ectopically in wild-type fibroblasts the SUN1 mutant proteins exhibited reduced interactions with Emerin as well.

Nuclear export of mRNPs through the NPC can be roughly classified into two forms: bulk and specific export, involving an NXF1-dependent pathway and CRM1-dependent pathway, respectively. Here, we show that mammalian cells require SUN1 for efficient nuclear mRNP export. The results show that both SUN1 and SUN2 interact with hnRNP F/H and hnRNP K/J. SUN1 depletion inhibits the mRNP export, with accumulations of both hnRNPs and poly(A)+RNA in the nucleus. LMB treatment indicates that SUN1 functions in mRNA export independent of the CRM1-dependent pathway. SUN1 mediates mRNA export through its association with mRNP complex by a direct interaction with NXF1. Overexpression of GFP fused SUN1 N-terminus leads to the formation of GFP-SUN1-NT positive aggregates which contain NXF1. Additionally, SUN1 associates with the NPC through a direct interaction with Nup153, a nuclear pore component involved in mRNA export. Taken together, our results reveal that the INM protein SUN1 has additional functions aside from being a central component of the LINC complex and that it is an integral component of the mammalian mRNA export pathway suggesting a model whereby SUN1 recruits NXF1-containing mRNP onto the nuclear envelope, and hands it over to Nup153.

Zusammenfassung

Mutationen in Genen für verschiedene Kernhülle assoziierte Proteine verursachen Emery-Dreifuss muskuläre Dystrophie (EDMD). Wir haben Fibroblasten eines Patienten mit einer Mutation im EDM Gen (p.L84Pfs*6), die zum Verlust von Emerin führt, analysiert. Dieser Patient ist zusätzlich heterozygot für eine Mutation im SUN1 Gen (p.A203V). Ein zweiter Patient ist heterozygot für eine Mutation im LAP2alpha Gen (p.P426L) und hat eine zusätzliche Mutation im SUN1 Gen (p.A614V). Die p.A203V Mutation verursacht einen Aminosäureaustausch in der N-terminalen Domäne von SUN1, welche sich im Nucleoplasma in der Nähe der Bindestelle von Nesprin-2 und Emerin befindet. Die p.A614V Mutation befindet sich vor der SUN Domäne, welche mit der KASH Domäne von Nesprinen im perinukleären Raum interagiert und die zusammen das Zentrum des LINC-Komplexes bilden. Auf zellulärem Niveau weisen die Fibroblasten des Patienten Änderungen in den Mengen mehrerer Bestandteile der Kernhülle auf, weiterhin sind für Laminopathien charakteristische phänotypische Eigenschaften wie eine erhöhte Empfindlichkeit gegenüber Hitzestress zu beobachten. Diese Schäden waren schwerwiegender als in EDMD Zellen mit Mutationen in nur einem Gen. Insbesondere Patienten-Fibroblasten mit der p.A203V-Mutation im SUN1 Gen weisen schwerere Defekte auf. Zusätzlich hierzu interagiert das SUN1 Protein in den Fibroblasten beider Patienten schwächer mit Lamin A/C. Die mutierten SUN1 Proteine zeigten ebenfalls eine reduzierte Interaktion mit Emerin nach ektopischer Expression in Wildtyp-Fibroblasten.

Der Export von messenger Ribonukleoproteinen (mRNPs) aus dem Zellkern wird in zwei Gruppen eingeteilt: unspezifischer NXF1-abhängiger Export und spezifischer CRM1-abhängiger Export. Wir zeigen hier, dass Säugerzellen SUN1 benötigen, um einen effektiven mRNP Export durchzuführen. Sowohl SUN1 als auch SUN2 interagiert mit hnRNP F/H und HnRNP K/J. Knock-down der SUN1 Expression hemmt den mRNP Export und hat eine Anhäufung von hnRNPs und poly(A)+RNA im Zellkern zur Folge. Zusätzlich zeigte die Behandlung der Zellen mit LMB, dass die den mRNA Export betreffende Funktion von SUN1 von CRM1 unabhängig ist. Durch Assoziation mit mRNP Komplexen und durch eine direkte Interaktion mit NXF1 vermittelt SUN1 den Export von mRNP aus dem Zellkern. Die Überexpression der SUN1 N-terminalen Domäne als GFP-Fusionsprotein führt zur Bildung von GFP-positiven Aggregaten, in die NXF1 rekrutiert wird. Zusätzlich, interagiert SUN1 direkt mit Nup153, einer Komponente des Kernporenkomplexes, welche am mRNA Export beteiligt ist.

Zusammengenommen zeigen unsere Ergebnisse eine Rolle von SUN1 im mRNA Export und implizieren ein Model, in dem SUN1 NXF1 enthaltende mRNP-Komplexe zur Kernhülle rekrutiert und diese an Nup 153 übergibt.

5. Materials and Methods

5.1 Materials

5.1.1 Human cells

HeLa	Human cervical cancer cell line
Wild-type fibroblast	Human primary fibroblasts from skin
Patient fibroblast	Human primary fibroblasts from skin

5.1.2 Bacterial strains

<i>E. coli</i> XL1-Blue	(Bullock <i>et al.</i> , 1987)
<i>E. coli</i> ArcticExpress RIL	Stratagene GmbH

5.1.3 Vectors and plasmids

pGEM-T Easy	Promega
pGEX-4T-1	GE Healthcare GmbH
pEGFP-C2	Clontech
GFP-SUN1	(Lu <i>et al.</i> , 2008)
GST-SUN2-NT	(Taranum <i>et al.</i> , 2012)
Sun2-V5-His	(Lu <i>et al.</i> , 2008)
GST-CT-ΔLamin A/C	(Libotte <i>et al.</i> , 2005)
GST-Nup153-(N, N+Zn, Zn, Zn+C, C)	Prof. Birthe Fahrenkrog (Institute for Molecular Biology and Medicine, Université Libre de Bruxelles, Charleroi, Belgium)
GST-NXF1	Prof. Stuart A Wilson (Department of Molecular Biology and Biotechnology, University of Sheffield, Sheffield, UK)

5.1.4 Oligonucleotides

Oligonucleotides used in this thesis were ordered from Sigma and are listed below.

Gene	Sequence
Lamin B1 (qRT)	Fw 5'-CGAAAGATGCAGCTCTTGCTACTGCAC-3'
	Rv 5'-CTCACTTGGGCATCATGTTGCTCTCTC-3'
SUN1 (qRT)	Fw 5'-GAGTGGACGTGCAAGTCAGAGAAATGG-3'
	Rv 5'-AGTACTCAAGATGCTGCCACCACCAGA-3'

Materials and Methods

SUN2 (qRT)	Fw	5'-GGACCTTGAAGAGGAAATCCAGCAACA-3'
	Rv	5'-CGAGCCTCTTCCTTCACTGTCTTCCAC-3'
LAP2 (qRT)	Fw	5'-AAGAGTGAGTTGGTCGCCAACAATGTG-3'
	Rv	5'-TGGTTGTTCCCACAATAGGACCAGGAT-3'
Nesprin-2 (qRT)	Fw	5'-AAGATTTAATGGCCTTGCAGGGAACC-3'
	Rv	5'-GGGTAAAAGGACCGGGCAAAGTTGT-3'
SUN1 siRNA		5'-UUACCAGGUGCCUUCGAAA-3'
GFP-SUN1 A203V	Fw	5'-GTGCTCACGGCGCACCCCGTGGCCCCCGGGCCCGTGTCG-3'
	Rv	5'-CGACACGGGCCCCGGGGGCCACGGGGGTGCGCCGTGAGCAC-3'
	Sq	5'-ACAACGGCTTCTCCTGCAGCAACT-3'
GFP-SUN1 A614V	Fw	5'-GCTGTGAGCGAGGCGGGGGTGTCTGGAATAACAGAGGCG-3'
	Rv	5'-CGCCTCTGTTATTCCAGACACCCCCGCCTCGCTCACAGC-3'
	Sq	5'-TGCGGAACGTCACCCACCACGTTT-3'
GFP/GST- SUN1-NT(1-239)	Fw	5'-GAATTCATGGATTTTTCTCGGCTTCACATGTACAGT-3'
	Rv	5'-GAATTCCTCGAGGGTCCCTGCCCGACCGGGGTGCGCGTC-3'
GFP-SUN1 ^{R-3}	Fw	5'-GATTTCTTGGCTGAATGTGTTTCTTCTAACGAGATGCCTTCG AAACATCTG-3'
	Rv	5'-CAGATGTTTCGAAGGCACTCTCGTTAGAAAGAAACACATTCAG CCAAGAAATC-3'
GFP-SUN1 ^{R-6}	Fw	5'-AATGTGTTTCTTCTAACGAGATGTCTACGTAACATCTGCAAG TTTTTAGTCTTG-3'
	Rv	5'-CAAGACTAAAACTTGCAGATGTTACGTAGACATCTCGTTA GAAGAAACACATTC-3'

5.1.5 Enzymes

Taq polymerase	GE Healthcare GmbH
T4 DNA	ligase Life technologies™ Corp.
Restriction endonucleases	New England Biolabs
Ribonuclease A (RNase A)	Sigma Aldrich Corp.
Calf Intestinal Alkaline Phosphatase (CIP)	Boehringer
<i>Pfu</i> DNA Polymerase	Promega
PreScission protease	GE Healthcare GmbH
Thrombin	Amersham
Trypsin	Invitrogen

5.1.6 Kits

pGEM-T easy Cloning Kit	Promega
NucleoSpin Extraction Kit	Macherey Nagel
Pure Yield™ Plasmid System	Promega
Qiagen Midi- and Maxi-prep	Qiagen
M-MLV reverse transcriptase RNase H Minus-kit	Promega
QuantiTect™ SYBR® Green PCR Kit	Qiagen
CLB-Transfection™ System	Lonza

5.1.7 Antibiotics

Ampicillin	Sigma Aldrich Corp.
Kanamycin	Sigma Aldrich Corp.
Penicillin/Streptomycin	Biochrom
Gentamycin (G418)	GE Healthcare GmbH

5.1.8 Chemicals

1kb plus DNA ladder	Promega
1,4-Dithiothreitol (DTT)	Gerbu Biotechnik GmbH
4',6-diamidino-2-phenylindole (DAPI)	Sigma Aldrich Corp.
5-Bromo-4-chlor-3-indolyl-β-D-galactopyranosid (X-Gal)	Carl Roth
Acetic acid (98-100 %)	Sigma Aldrich Corp.
Acrylamide	National Diagnostics Inc.
Agarose (Electrophoresis Grade)	Life technologies™ Corp.
Ammonium peroxide sulfate (APS)	Carl Roth
β-Mercaptoethanol	Sigma Aldrich Corp.
Boric acid	Merck KGaA
Bovine serum albumin (BSA)	Sigma Aldrich Corp.
Bromphenolblue (Na-Salt)	Serva Electrophoresis
Calcium chloride	Merck KGaA
Chloroform	Sigma Aldrich Corp.
Cobalt chloride	Sigma Aldrich Corp.
Complete mini protease inhibitor cocktail	Sigma Aldrich Corp.
Coomassie-Brilliant-Blue R250	Serva

Materials and Methods

DAPI	Sigma Aldrich Corp.
Deoxyribonucleotide triphosphates (dNTP)	Sigma Aldrich Corp.
Dextran sulfate	Sigma Aldrich Corp.
Diazabicyclooctane (DABCO)	Sigma Aldrich Corp.
Dimethylformamide (DMF)	Sigma Aldrich Corp.
Dimethylsulfoxide (DMSO)	Merck KGaA
Dulbecco's Modified Eagle's Medium (DMEM)	Pan biotech
Dynabeads [®] Oligo (dT) ₂₅	Life technologies [™] Corp.
Ethanol (98-100 %)	Riedel de Haen
Ethidium bromide	Sigma Aldrich Corp.
Ethylen diamine tetra acetic acid (EDTA)	Merck KGaA
Fetal calf serum (FCS)	Biochrom
Formaldehyde	Sigma Aldrich Corp.
Formamide	Merck KGaA
Gelvatol	Pfizer Inc.
Glycine	Sigma Aldrich Corp.
Herring sperm DNA	Fluka
Isopropanol	Sigma Aldrich Corp.
Isopropyl-D-thiogalactopyranoside (IPTG)	Loewe Biochemica GmbH
Leptomycin B	Sigma Aldrich Corp.
Low molecular weight (LMW) protein marker	GE Healthcare GmbH
Luminol	Sigma Aldrich Corp.
Magnesium chloride	Merck KGaA
Methanol	Sigma Aldrich Corp.
N,N,N',N'-Tetramethylethylenediamine (TEMED)	Merck KGaA
Nonylphenyl-polyethyleneglycol (NP-40)	Sigma Aldrich Corp.
N-[2-Hydroxyethyl] piperazine-N'-2 -ethanesulfonic acid (HEPES)	Biomol GmbH
p-cumaric acid	Sigma Aldrich Corp.
PageRuler Plus Prestained Protein Ladder	Thermo Scientific Inc.
Phenol	Carl Roth
Phenylmethylsulphonylfluoride (PMSF)	Sigma Aldrich Corp.
Polyoxyethylene-sorbitan monolaurate (Tween-20)	Sigma Aldrich Corp.
Polyvinyl alcohol	Sigma Aldrich Corp.

Materials and Methods

Ponceau S Concentrate	Sigma Aldrich Corp.
Potassium acetate	Sigma Aldrich Corp.
Potassium chloride	Sigma Aldrich Corp.
Potassium dihydrogen phosphate	Sigma Aldrich Corp.
Sodium acetate	Merck KGaA
Sodium chloride	Sigma Aldrich Corp.
Sodium dodecyl sulfate (SDS)	Serva Electrophoresis
Sodium hydroxide	Sigma Aldrich Corp.
t-octylphenoxypolyethoxyethanol (Triton X-100)	Sigma Aldrich Corp.
Tris (hydroxymethyl) aminomethane	Sigma Aldrich Corp.
tRNA	Roche
Trypan blue	Sigma Aldrich Corp.
Vanadyl ribonucleoside complexes	Sigma Aldrich Corp.
X-Gal (5-bromo-4-chloro-3-indolyl- β -D-galactopyranoside)	Roth

5.1.9 Primary antibodies

Rabbit polyclonal anti-pAbK1	(Libotte et al., 2005)
Rabbit polyclonal anti-Lamin B1	Abcam
Rabbit polyclonal anti-Lamin A/C	Santa Cruz
Rabbit polyclonal anti-Nesprin-1 (SpecII)	(Taranum et al., 2012)
Rabbit polyclonal anti-Pericentrin	Abcam
Mouse monoclonal anti-GFP (K3-184-2)	(Noegel et al., 2004)
Mouse monoclonal anti-Emerin (4G5)	Abcam
Mouse monoclonal anti-LAP2	BD Transduction Laboratories
Rabbit monoclonal anti-SUN1	Abcam
Rabbit monoclonal anti-SUN2	Abcam
Mouse monoclonal anti-NPC (Mab414)	Abcam
Mouse monoclonal anti-hnRNP F/H	ImmuQuest
Mouse monoclonal anti-hnRNP K/J	ImmuQuest
Mouse monoclonal anti-NXF1	Abcam
Mouse monoclonal anti-Nup153 (QE5)	Abcam

5.1.10 Secondary antibodies

Goat anti-mouse IgG, Alexa 488 conjugated	Life technologies™ Corp.
Goat anti-rabbit IgG, Alexa 488 conjugated	Life technologies™ Corp.
Goat anti-mouse IgG, Alexa 568 conjugated	Life technologies™ Corp.
Goat anti-rabbit IgG, Alexa 568 conjugated	Life technologies™ Corp.
Donkey anti-goat IgG, Alexa488 conjugated	Life technologies™ Corp.
Anti-mouse IgG, peroxidase conjugated	Sigma Aldrich Corp.
Anti-rabbit IgG, peroxidase conjugated	Sigma Aldrich Corp.

5.2 Molecular biological methods

5.2.1 Polymerase Chain Reaction (PCR)

The PCR is a powerful tool used in molecular biology to amplify DNA fragments from a template double stranded DNA (dsDNA). In order to perform PCR, one needs in addition to the template DNA, the DNA polymerase (Taq polymerase), deoxyribonucleotides (dNTPs), and primers. After denaturation of the template DNA at high temperature, the reaction mixture is cooled down to allow annealing of the primers. The Taq polymerase then extends the primers and synthesizes a complementary strand. These steps are repeated for many cycles. A “standard program” is presented below.

Standard PCR reaction set up

x µl template-DNA
2 µl forward primer (10 pmol/µl)
2 µl reverse primer (10 pmol/µl)
1 µl dNTP-mix (10 mM)
5 µl 10x PCR buffer
1 µl Taq polymerase (3-4 U)
ad 50 µl dH₂O

Standard PCR program

I. Initial denaturing	94°C, 5 min
Denaturing	94°C, 30 sec
Annealing	60-68°C, 30 sec
Extension	72°C, 1-5 min
II. Cycles	25-35
III. Final extension	2°C, 10 min
IV. Cooling to 4°C	forever

10x PCR buffer

0.15 M Tris/HCl, pH 8.0
0.5 M KCl
15 mM MgCl₂

5.2.2 Site-directed mutagenesis

The sequence of SUN1 corresponds to O94901 (NCBI), an isoform consisting of 812 amino acids. We used the plasmid human GFP-SUN1 full length (Lu et al., 2008) to produce the SUN1 mutant plasmids (GFP-SUN1A203V, GFP-SUN1A614V and siRNA resistant plasmid GFP-SUN1^R) according to a site-directed mutagenesis kit (Promega). The mutagenic oligonucleotide primers were designed individually according to the desired mutation (shown in 4.1). Mutant strand synthesis reaction was performed by PCR and the standard reaction mixture and program are shown below. After the amplification, 1 µl of the methylation sensitive Dpn I restriction enzyme (10 U/µl) was directly added to each reaction for digestion of the input DNA which is methylated whereas the newly synthesized DNA is not. The samples were incubated for 1 hour at 37°C. Transformation of XL1-Blue supercompetent cells was carried out afterwards.

Site-directed mutagenesis PCR

x µl (5-50 ng) template DNA
x µl (125 ng) forward primer
x µl (125 ng) reverse primer
1 µl dNTP-mix
5 µl 10x reaction buffer
1 µl *PfuUltra* HF DNA polymerase (2.5U/µl)
ad 50 µl dH₂O

Site-directed mutagenesis PCR program

I. Initial denaturing	95°C, 30 sec
Denaturing	95°C, 30 sec
Annealing	55°C, 1 min
Extension	68°C, 1 min/kb of plasmids length
II. Cycles	12-18
III. Final extension	68°C, 10 min
IV. Cooling to 4°C	forever

5.2.3 Agarose gel electrophoresis of DNA

Agarose gel electrophoresis was performed for separation and analysis of DNA fragments based on their size. Electrophoresis was performed with 0.7 %-1.2 % agarose gels in 1x TAE buffer with the fluorescent dye ethidiumbromide (2 µg/ml) which intercalates between bases of DNA. The gels were allowed to solidify and then submerged in a horizontal electrophoresis tank containing 1x TAE buffer. The DNA samples were mixed with 1/10 volume of a 10x DNA loading buffer and then pipeted into the sample wells. DNA size marker was always loaded along with the DNA samples and allowed to estimate the size of the resolved DNA fragments. The gels were visualized under UV light at 302 nm and photographed using a gel documentation system (Alpha Innotec).

1x TAE buffer

40 mM Tris (pH 7.6)

20 mM acetic acid

1 mM EDTA

DNA loading buffer

40 % sucrose

0.5 % SDS

0.25 % bromophenol blue in TE buffer, pH 8.0

5.2.4 Ligation of DNA fragments

Vector and fragment that were subjected to the same double digest were mixed in a final volume of 10 μ l Ligation mixture (the molar ratio of vector: fragment = 1:3) and incubated at 16°C overnight.

Ligation mixture

x μ l linearized vector DNA

x μ l DNA fragment

1 μ l 5x ligation buffer

1 μ l T4 Ligase (1 U/ μ l)

ad 10 μ l with ddH₂O

5x Ligation buffer

0.25 M Tris-HCl, pH 7.6

50 mM MgCl₂

5 mM ATP

5 mM DTT

25% polyethylene glycol-8000

5.2.5 Preparation of chemically competent *E. coli* cells

Chemically competent *E. coli* cells were prepared using the calcium chloride method. A single colony was selected from an LB plate and grown overnight in 5 ml LB-medium at 37°C with shaking (220 rpm). The pre-culture was added to 1 L LB-medium and grown to log-phase (OD₆₀₀ 0.4 - 0.6) at 37°C with shaking (220 rpm). The culture was chilled on ice for 30 min and then centrifuged for 10 min at 1,500 g at 4°C. All following steps were performed on ice. The pelleted cells were resuspended in 50 ml ice-cold transformation buffer and incubated on ice for 10 min. The cells were harvested, resuspended in 20 ml ice-cold transformation buffer and 1.5 ml DMSO was added with gentle shaking. Aliquots of 200 μ l cells were immediately frozen in liquid nitrogen and stored at -80°C until use.

Transformation buffer, pH 6.7

10 mM PIPES

15 mM CaCl₂

250 mM KCl

55 mM MnCl₂

5.2.6 Transformation of chemically competent *E. coli* cells

Transformation of competent *E. coli* cells with plasmid DNA was performed by heat shock at 42°C (Inoue et al., 1990). 200 µl of chemically competent cells were thawed on ice and mixed with plasmid DNA (10-40 ng) or ligation mixture. After 15 minutes incubation on ice, the cells were incubated at 42°C (heat shock) for 45 seconds then cooled down on-ice for 2 minutes. For ArcticExpress RIL *E. coli* cells, the heat shock was performed for only 20 seconds at 42°C. Afterwards, 800 µl preheated LB medium were added to the cells and incubation was at 37°C for 1 hour with shaking (220 rpm) without any antibiotics. Finally, the samples were centrifuged at 6,000 g for 2 min and 800 µl of the supernatant was discarded. The pelleted cells were resuspended and spread onto LB agar plates containing the appropriate antibiotic. Alternatively, for plasmid retransformation 50-100 µl of the cultured sample were directly spread on the LB agar plates. After overnight incubation at 37°C, colonies were picked for further analysis.

5.2.7 Blue-white selection of transformants

After cloning of the PCR-products into the pGEM-T Easy vector and transformation into *E. coli* XL1 Blue, cells were plated onto LB-ampicillin plates covered with 100 µl of LB-medium containing 20 µl of 2 % X-Gal solution and 10 µl of 1 M IPTG, and incubated at 37°C overnight. The next day, white positive colonies were selected for further analysis.

1 M IPTG solution

2.38 g IPTG
ad 10 ml with ddH₂O

2 % X-Gal solution

200 mg X-Gal
ad 10 ml with dimethylformamid

5.2.8 Colony PCR

Single bacterial colonies were picked and cultured in LB medium for 6 h or overnight, then 1 µl or 2 µl were taken as template for PCR with specific primers. The programme of the PCR reaction set up was as described in 4.2.1.

5.2.9 DNA-Mini-preparation from *E. coli* (Birnboim et al., 1979)

With this DNA isolation method plasmid DNA from small amounts (2 ml) of bacterial cultures was prepared. An overnight *E. coli* culture was centrifuged for 2 minutes (5000 g). The pellet was suspended in 300 µl B1, 300 µl B2 was added, mixed, incubated (5 min, RT),

Materials and Methods

300 µl B3 was added, mixed again and centrifuged for 15 minutes (14.000 g, RT). The supernatant was transferred to a new Eppendorf tube which contained 550 µl isopropanol for DNA precipitation. After 14.000 g centrifugation for 20 min at RT, the supernatant was discarded and the pellet air dried. Finally, the plasmid DNA was dissolved in 50 µl H₂O.

<u>B1</u>	<u>B2</u>	<u>B3</u>
50 mM Tris/HCl, pH 8.0	0.2 M NaOH	3 M KAc, pH 5.5
10 mM EDTA	1% SDS	
100 µg/ml RNase		

5.2.10 Restriction analysis of DNA

Restriction enzymes were purchased from New England Biolabs. 10 units enzyme were used for 50 ng - 1 µg of DNA and the digestions were usually performed in a final volume of 20 µl for 1-2 h at 37°C.

5.2.11 DNA-Midi/Maxi preparation-Pure Yield™ Plasmid System

For the large amount of DNA preparation, Pure Yield™ Plasmid System (Promega) was used and the buffer compositions are shown below.

Cell Suspension Solution

50 mM Tris/HCl, pH 8.0
10 mM EDTA
100 µg/ml RNase

Cell Lysis Solution

0.2 M NaOH
1% SDS

Neutralization solution

4.09 M Guanidinium hydrochloride
759 mM Potassium acetate
2.12 M Glacial acetic acid
0.04 mM EDTA

column wash

60% ethanol
60 mM Potassium acetate
8.3 mM Tris/HCl; pH 7.5

5.2.12 Measurement of DNA and RNA concentrations

Concentrations of DNA and RNA were estimated by determining the absorbance at a wavelength of 260 nm. A ratio of OD260/OD280 <1.8 (DNA) or <2 (RNA) indicates negligible protein contaminations. Protein contaminations were estimated from absorbance at 280 nm.

5.2.13 Isolation of total RNA with TRIzol®

Total RNA was extracted from cells using TRIzol (Invitrogen). Briefly, the cells with a confluency of 70-80% were trypsinised and centrifuged in ice cold PBS at 1200 rpm for 5 min. The pellet was suspended in 1 ml TRIzol per 50-100 mg cells and incubated at RT for 5 min. For each ml of TRIzol 200 µl chloroform were added, mixed and incubated at RT for 2-3 min followed by centrifugation at 12,000 g for 15 min. The aqueous phase was transferred into a new microcentrifuge tube. For each ml of solution 500 µl of isopropanol were added, mixed, incubated at RT for 10 min and centrifuged at 12,000 g for 10 min afterwards. The pellet was washed with 75% ethanol, vortexed and briefly centrifuged. After air drying, the pellet was dissolved in 50 µl of RNase-free water at 60°C for 10 min. Finally, the concentration and quality of the RNA was determined by Agilent Bioanalyser (Agilent Technologies) and stored at -80°C.

5.2.14 cDNA synthesis

First-strand cDNA synthesis was performed using the M-MLV reverse transcriptase RNase H Minus-kit (Promega). In brief, 1 µg of total RNA was mixed with 2 µl of random primers (50 µM pdN₆, Stratagene) and filled up to 15 µl with nuclease free water. After incubation for 5 min at 70°C and cooling down for 2 min on ice, 5 µl 5x reaction buffer (Promega), 1.25 µl dNTP's (10 mM, Stratagene), 1 µl RNase inhibitor (RNasin 40 U/µl, Promega), 1.75 µl nuclease free water and 1 µl M-MLV-RT (200 U/µl) were added to the sample. The mixture were incubated for 1 h at 37°C and stored at -20°C until use.

RT-Reaction Mix

15.0 µl incubation mix

5.0 µl 5x M-MLV reaction buffer

1.25 µl dNTP (10 mM)

1 µl RNase inhibitor RNasin (40 U/µl)

1 µl M-MLV-RT (200U/µl)

ad 25µl with ddH₂O

5.2.15 Quantitative Real Time PCR (qRT-PCR)

Quantitative real-time PCR analysis was performed with the Opticon II PCR machine (MJ Research) and Opticon Monitor (Version 3.1.32) program using the Quantitect™ SYBR® Green PCR kit. Gene-specific primers were selected with the program Primer 3.0 for product sizes of 200-400 bases. PCR was performed for 41 cycles at 95°C for 30 s (denaturation), 57°C for 45 s (annealing) and 68°C for 40 s (elongation). As quantification standard defined concentrations of the *annexin VII* gene (Doring et al., 1995) were used for amplification. For normalization, the expression of *GAPDH* was used. The primers are shown in 4.1.

Standard reaction set up (25 µl)

- 1.0 µl cDNA (1:10 diluted)
- 1.0 µl forward primer (10 pmol/µl)
- 1.0 µl reverse primer (10 pmol/µl)
- 12.5 µl 2x SYBR Green PCR Mix
- 9.5 µl H₂O

5.3 Mammalian cell culture methods and transfections

5.3.1 Cell culture and transfection

HeLa were routinely cultivated in DMEM (Dulbecco's Modified Eagle's Medium) medium supplemented with fetal bovine serum (10%), penicillin (100 U/ml) and streptomycin (100 µg/ml), L-glutamine (2 mM) and non-essential amino acids at 37°C and 5% CO₂. Human wild-type and patients primary fibroblasts were cultured in Eagle's DMEM supplemented with 20% FBS (Biochrom), 1 mM glutamine, 1% penicillin/streptomycin, 7.5% sodium bicarbonate and 10 mM HEPES (pH 7.5) at 37°C and 5% CO₂.

Human wild-type fibroblast cells were transfected by the CLB-Transfection™ System (Lonza) and HeLa cells were transfected by Lipofectamine 2000 (Invitrogen) according to the manufacturer's instructions. Cells transfected with plasmids were incubated for 24-48 h post-transfection.

5.3.2 Thawing cells

To thaw cells stored in cryogenic tubes at -80°C or in liquid nitrogen, 9 ml of prewarmed medium was filled into a 15 ml falcon tube. The cells were resuspended with this medium and

transferred into 15 ml falcon tubes. Thereby the concentration of toxic DMSO was reduced from 10% in the freezing medium to 1% in the falcon tube. After centrifugation for 5 minutes at 1,200 rpm, the DMSO-containing supernatant was discarded and the cells resuspended in an appropriate amount of medium and distributed onto cell culture dishes.

5.3.3 Freezing cells

To freeze cells, the cells were trypsinized and centrifuged. The supernatant was discarded and the cell pellet was resuspended in an appropriate amount (0.6-1 ml) of 1x freezing medium (20% FBS, 10% DMSO in medium). The cells were mixed with the freezing medium and transferred into a cryogenic tube. Cells were frozen at -80°C for a period of 2-3 weeks and then transferred to liquid nitrogen for longer storage.

5.3.4 RNAi

RNAi was performed as described (Turgay et al., 2014). Allstars negative control siRNA and SUN1 siRNA (5'-TTACCAGGTGCCTTCGAAA-3') were purchased from QIAGEN and Microsynth, respectively. 5×10^3 HeLa cells were seeded in 24-well plate for immunofluorescence analysis and 5×10^4 HeLa cells were seeded in 6-well plate for Western blot analysis. RNAi transfection was performed at a final siRNA concentration of 20 nM per target gene using transfection reagent (INTERFERin, Polyplus) according to the manufacturer's protocol. Cells were either fixed or harvested after 72 h transfection. For rescue experiments, HeLa cells were transfected with GFP-SUN1^R expression vector by Lipofectamine 2000 (Invitrogen) after 24 h siRNA treatment. Cells were processed for detection of poly(A)+RNA by in situ hybridization after 72 h siRNA treatment (Folkmann et al., 2013).

5.4 Cell biological assays

5.4.1 Cell proliferation, cell cycle and cell size measurements

For cell proliferation analysis, 1×10^5 cells of each patient and the wild-type were seeded at the same time. After every 48 h for a period of 6 days, cells were trypsinized and pelleted. After resuspending the cell pellets in 1 ml medium, cells were counted using a TC10™ Automated Cell Counter (Bio-Rad).

For cell cycle analysis, patient and wild-type cells were trypsinized and pelleted. After counting the cells, 5×10^5 cells each were taken and 2 μ l of cell permeable DNA specific dye Nuclear-IDTM Red DNA stain (Enzo life sciences) was added to the cell suspension (final concentration of 40 μ M, 500 μ l total volume). After incubation for 5 min at 37°C, the samples were analyzed by flow cytometry. The analysis was performed at the CMMC central facilities.

For determination of the cell size, patient and wild-type cells were trypsinized and pelleted. Then cells were resuspended in PBS and transferred to the plates. Examination was done by using bright field microscopy at 40x magnification. The size of 400 cells per strain was determined.

5.4.2 Senescence-associated β -galactosidase assay

Cells were seeded on coverslips one day before the assay was performed, washed with PBS and fixed with 2% (v/v) formaldehyde or 0.2% (w/v) glutaraldehyde (dissolved in PBS) (5 min, RT). Cells were washed three times with PBS and incubated with freshly prepared senescence-associated-Gal (SA-Gal) staining solution (van der Loo et al., 1998) for 6 to 8 h at 37°C without CO₂. The stained cells were imaged under bright field microscopy at 40x magnification.

SA- β -Gal staining solution

1 mg/ml 5-bromo-4-chloro-3-indolyl β -D-galactoside (X-Gal)
40 mM citric acid/sodium phosphate, pH 6.0
5 mM potassium ferrocyanide K₄Fe(CN)₆
5 mM potassium ferricyanide K₃Fe(CN)₆
150 mM NaCl
2 mM MgCl₂

5.4.3 Heat stress experiment

Wild-type and patient fibroblasts were seeded on 12 mm glass coverslips two days before the experiment and cultured at 37°C. For heat stress, cells were placed in a 45°C incubator for 30 min and fixed immediately after treatment with cold methanol at -20°C for 5 min, and then incubated with rabbit polyclonal anti-Lamin A/C antibodies to detect the nuclear envelope

and pericentrin specific polyclonal antibodies to detect the centrosome. Untreated wild-type and patient fibroblasts were used as control.

5.4.4 Cell migration analysis and wound-healing assay

Cell migration was studied by performing wound-healing assay using specific wound assay chamber (Ibidi, Munich, Germany). Cells were seeded at a density of 4×10^4 cells on each side of an Ibidi culture insert for live cell analysis and allowed to grow for 24 h. Inserts were then removed with sterile forceps to create a 500 μm space between the cells on each side of the well and incubation with fresh culture medium was continued. The cell migration into the defined cell free gap was followed over 20 h by live cell imaging using Leica DM IRE2 microscope. For analysis of single cell migration, cells were followed using the manual tracking software component of the Image J program. After tracking, the cell paths were analyzed using the “Chemotaxis and Migration Tool”.

5.5 Immunological and protein chemical methods

5.5.1 Immunofluorescence

Cultured cells grown on coverslips were fixed in 4% paraformaldehyde in PBS for 10 min followed by permeabilization with 0.5% Triton X-100 for 5 min for primary antibody staining. Alternatively, cells were fixed in cold methanol (-20°C) for 10 min. Subsequently, the fixed cells were washed three times with 1x PBS and incubated for 15 minutes with PBG blocking solution. After blocking, primary antibodies were diluted in PBG and incubated with the cells for 1 h at RT or overnight at 4°C . Subsequently the samples were washed three times (5 min each) with PBS and then incubated with required secondary antibodies (1:1.000 diluted in PBG) conjugated with Alexa Fluor 488, Alexa Fluor 568, Cy3, TRITC or FITC for one hour at RT. The nuclear DNA was counterstained with DAPI (4',6-Diamidino-2'-phenylindole), and the coverslips were mounted on glass slides with gelvatol. The stained cells were analyzed using confocal laser scanning microscopy (TCS-SP5, Leica).

Gelvatol

4.8 g Polyvinyl alcohol (87%-89%)
12 g Glycerol
+ 12 ml de-ionized water, stir (RT, 10 h)

PBG (pH 7.4)

5% BSA
0.45% fish gelatine
PBS

+ 24 ml 0.2 M Tris/HCl, pH 8.5
stir (50°C, 20-40 min)
centrifugation (15 min, 5000 g)
1.3 g Diazabicyclooctane (DABCO)
Aliquot-storage: – 20°C

5.5.2 Protein lysates from mammalian cells and western blotting

Cells grown to 80% confluency were trypsinized and pelleted down in 15 ml centrifuge tube. After washing with PBS, the cells were resuspended in modified radio-immunoprecipitation (RIPA) lysis buffer. Cell suspensions were passed through a 0.45 µm needle for 10 times and incubated for 15 min on ice, followed by 10 sec sonication. The lysates were cleared by centrifugation at 12,000 rpm for 10 min at 4°C. The supernatant of total cell lysates can be either directly heated in 5x SDS sample buffer (95°C, 5 min) for western blot analysis or incubated with GST fusion protein-coupled beads for pulldown experiment (described in 5.5.6).

For western blot analysis, proteins were resolved in 10%, 12% or 3–15% gradient SDS-PAGE and transferred to PVDF membrane with wet blot transfer buffer at 15 V for overnight or 48 h at 4°C. Transfer efficiency was confirmed by Ponceau staining. After blocking with 5% milk-powder in 1x NCP, the membrane was incubated with primary antibody diluted in 1x NCP buffer for 1 h at RT or overnight at 4°C. Following three washings, the secondary antibody (1:10,000) coupled with horseradish peroxidase (POD) was added for 1 h incubation. The membrane was washed again with 1x NCP and the signals were detected by using enhanced chemiluminescence (ECL) system.

RIPA lysis buffer

50 mM Tris/HCl, pH 7.5
150 mM NaCl
1% NP-40
0.5% Na-desoxycholate
Just add before use
1 mM dithiothreitol (DTT)
1 mM benzamidine
1 mM PMSF
Protease inhibitor cocktail

5x SDS loading buffer

3.12 ml 1M Tris/HCl, pH 6.8
10 ml 10% SDS
5 ml Glycerol
2 ml β-Mercaptoethanol
Pinch of Bromophenol blue

Transfer buffer

43.2 g Glycine
9 g Tris
ad ddH₂O to make 3 L

Ponceau staining solution

0.5 g Ponceau S
5 ml Acetic acid
ad ddH₂O to make 0.5 L

ECL solution

2 ml 1 M Tris/HCl, pH 8.0
200 µl 0.25 M Luminol in DMSO
89 µl 0.1 M p-coumaric acid in DMSO
20 ml dH₂O
6.3 µl 30% H₂O₂

10x NCP buffer

100 ml Tris/HCl, pH 8.0
87.5 g NaCl
6 ml Tween-20
ad ddH₂O to make 1 L

5.5.3 Subcellular fractionation

After RNAi transfection, HeLa cells were processed for subcellular fractionation as described (Suzuki et al., 2010). The cells grown in 6-well plate were washed, trypsinized and centrifuged in 1.5 ml centrifuge tubes (1000 rpm, 5 min at 4°C). After removing the supernatants, the cell pellets were resuspended in 450 µl fractionation buffer and triturated 5 times using a p1000 micropipette. Afterwards 150 µl of the lysate was removed and kept as the “whole cell lysate”. The rest samples were centrifuged with a table top microfuge (~10 sec), and then the supernatants were kept as the “cytosolic fraction”. Next the pellets were washed with fractionation buffer again and centrifuged as above. After removing the supernatants, the pellets were resuspended in 150 µl fractionation buffer and designated as the “nuclear fraction”. Finally, the “whole cell lysates” and the “nuclear fractions” were sonicated and heated along with the “cytosolic fraction” at 95°C for 5 min. Samples were resolved by SDS-PAGE and analyzed by western blotting with appropriate antibodies.

Fractionation buffer (freshly prepared on ice)

0.1% NP-40 dissolved in 1x PBS

5.5.4 Co-immunoprecipitation (Co-IP)

Precipitation by GFP polyclonal antibodies Wild-type fibroblasts were transfected with plasmids GFP-SUN1, GFP-SUN1A203V or GFP-SUN1A614V. The next day cells were scraped into RIPA buffer (50 mM Tris/HCl, pH 7.5, 50 mM NaCl, 1% NP-40, 1% Na-

deoxycholate) supplemented with 1 mM DTT, Benzamidine, PMSF and protease inhibitor cocktail (Roche), followed by sonication and centrifugation at 16,000 g and 4°C for 10 min. Lysates were precleared with protein A Sepharose (GE Healthcare) for 1 h and then incubated with 2 µg of antibody for 2 h at 4°C. Antibodies were precipitated by addition of protein A Sepharose for a further 1 h, pelleted at 1,000 g, and then washed in lysis buffer minus protease inhibitors. Samples were heated in SDS sample buffer (95°C, 5 min) and analyzed using 12% SDS -PAGE.

Precipitation by GFP-Trap beads Human fibroblasts cells were transfected with GFP, GFP-SUN1 or GFP-SUN2 encoding plasmids. The next day cells were scraped into lysis buffer (10 mM Tris/HCl, pH 7.5, 50 mM NaCl, 0.5 mM EDTA, 0.5% NP-40) supplemented with 1 mM DTT, Benzamidine, PMSF and protease inhibitor cocktail (Roche), followed by sonication and centrifugation at 16,000 g and 4°C for 10 min. Lysates were precleared with protein A Sepharose (GE Healthcare) for 1 h and then incubated with GFP-Trap beads (Chromotek) for 2 h at 4°C. Beads were pelleted at 1,000 g, and then washed several times with lysis buffer minus protease inhibitors. Samples were heated in SDS sample buffer (95°C, 5 min) and analyzed using 12% SDS-PAGE.

5.5.5 Purification of recombinant proteins from *E. coli*

For expression of recombinant proteins, a 20 ml pre-culture of LB-medium with appropriate antibiotics was inoculated with XL1-Blue or ArcticExpress RIL *E. coli* cells transformed with target plasmids and incubated at 37°C overnight with shaking at 220 rpm. The main-culture (500 ml) was inoculated at a ratio of 1/50 with the pre-culture and incubated at 37°C until the cells reached a density of OD600 ~ 0.5-0.6. Afterwards the recombinant protein expression was induced with 0.5-1 mM IPTG for 4 hours at 37°C or overnight at room temperature. Alternatively, the ArcticExpress RIL *E. coli* culture was incubated at 10°C for 24 h. Then, the cells were harvested by centrifugation at 6,000 g for 10 min and resuspended in 20 ml lysis buffer or frozen at -20°C for future use. After sonification (30 % amplitude, 15 s pulse, 10 s break, time 5 min), the soluble fraction of the bacterial lysate was obtained by centrifugation at 20,000 g for 30 min (4°C). The GST fusion protein was isolated from the supernatant by incubation with 300 µl of washed Glutathione Sepharose 4B beads (GE-Healthcare) under shaking for 3 hours or overnight at 4°C. And then the beads coupled with GST fusion proteins were washed 5 times with washing buffer. The purified GST fusion proteins were either directly used for pulldown experiment or incubated with cleavage buffer and specific enzyme (24-48 h, 4 °C) to remove the GST tag.

Washing buffer

50 mM Tris/HCl, pH 8.0
150 mM NaCl

Bacterial lysis buffer

washing buffer
Ad just before use
1 mM DTT
1 mM Benzamidin
1 mM PMSF
protease inhibitor

PreScission protease cleavage buffer

50 mM Tris/HCl, pH 7.4
150 mM NaCl
1 mM EDTA
1 mM DTT

Thrombin cleavage buffer

50 mM Tris/HCl, pH 8.0
150 mM NaCl
10 mM CaCl₂

5.5.6 GST pulldown assay

Expression of recombinant GST-CT-Lamin A/C, GST-SUN2-NT and GST-NXF1 polypeptide was induced in *E. coli* strain XL1-Blue. GST-SUN1-NT and all GST-Nup153 fragments polypeptide were induced in ArcticExpress RIL. Cells were lysed and the fusion proteins were isolated as described in 5.5.5. After several washing steps, the purified GST fusion proteins were incubated with human fibroblast or HeLa total cell lysates (lysate preparation is described in 5.5.2) for 1.5-3 h at 4°C. GST alone was used as negative control. Beads coupled with protein complexes were washed 3 times with RIPA buffer (500 g, 4°C, 1 min) and heated in 5x SDS sample buffer (95°C, 5 min). Samples were analyzed using 12% SDS-PAGE followed by western blotting.

5.5.7 Poly(A)+RNA isolation-Oligo (dT) pulldown assay

1.5x10⁷ HeLa cells were harvested for nuclear poly(A)+RNA immunoprecipitation essentially as described (Wickramasinghe et al., 2010), except Dynabeads[®] Oligo (dT)₂₅ were used instead of oligo(dT) cellulose. Briefly, the harvested HeLa cell pellet was washed in 1ml ice cold PBS and centrifuged at 1000 rpm for 2 min. The pellet was suspended in 1 ml PBS homogenization buffer and homogenized using a glass homogenizer (tight pestle). The nuclear fraction was isolated after 10 min centrifugation (2000 g, 4°C). After removing the supernatant (cytoplasmic fraction), the pellet was lysed in 450 µl PBS lysis buffer with 3

times (5 sec each) sonication and 10 min centrifugation (2000 g, 4°C) afterwards. The resulting supernatant was the soluble nuclear extract. Then the Dynabeads[®] Oligo (dT)₂₅ and 0.05% NP-40 were added and incubated with nuclear extract for 45 min at 4°C with gentle rotation. The Poly(A) + RNA was isolated after washing the beads thoroughly for 3 times (500 µl each) with PBS lysis buffer plus 0.1% NP-40 by placing on the magnet at room temperature. Samples were analyzed by SDS-PAGE followed by western blotting with relevant antibodies.

PBS homogenization buffer

137 mM NaCl
3 mM KCl
8 mM Na₂HPO₄
2 mM NaH₂PO₄, pH 7.2

Just add before use

0.2% NP-40

100 µg/ml PMSF

PBS lysis buffer

137 mM NaCl
3 mM KCl
8 mM Na₂HPO₄
2 mM NaH₂PO₄, pH 7.2

Just add before use

100 µg/ml PMSF

5 mM vanadyl ribonucleoside complex

0.2 U/µl of RNase OUT (Invitrogen)

5.5.8 In situ hybridization

HeLa cells were cultured and processed as described (Folkmann et al., 2013). To localize poly(A)+RNA in HeLa cells, 5x10³ cells were seeded in 24-well plate and fixed after 72 h RNAi transfection. For Leptomycin B (LMB) treatment, HeLa cells were treated with LMB at a final concentration of 7ng/ml (37°C, 2 h) after 72 h RNAi transfection. After fixation with 4% PFA for 15 min, the cells were permeabilized by 0.2% Triton X-100 in PBS for 5 min (RT). Between each step, the cells were washed 3 times (5 min each) with PBS. Then pre-hybridization was performed by incubating the cells with prehybridization buffer at 37 °C for 1h (in a tissue culture incubator). Then the poly(A)+RNA was localized by hybridization with diluted Cy3-conjugated Oligo d(T)₅₀ probe (1ng/µl) in prehybridization buffer at 37°C for 2 h (in tissue culture incubator). A series of washing steps followed afterwards. Washing was for 3 times (10 min each) in 2x SSC buffer at 37°C, 3 times (10 min each) in 1x SSC buffer at RT and 3 times (5 min each) in 1x PBS. The nuclear DNA was stained with DAPI diluted in 0.2% Triton X-100/PBS for 30 min at RT. The cells were washed in PBS and mounted with gelvatol. Images were acquired using confocal laser scanning microscopy (TCS-SP5, Leica) and processed with LAS AF Lite software (Leica). The mean Cy3 intensity was determined

Materials and Methods

for the nuclear and cytoplasmic distribution of 500 individual cells under each condition. Nuclear/cytoplasmic (N/C) ratios were calculated and plotted on line graphs for the indicated conditions.

Pre-hybridization buffer

(Prepare before use, for 1 ml)

2.5 μ l tRNA (50 mg/ml)

50 μ l herring sperm DNA (10 mg/ml)

100 μ l SSC (20x)

50 μ l BSA (20 mg/ml)

500 μ l formamide

5 μ l vanadyl ribonucleoside complexes (200 mM)

0.1 g dextran sulfate

289.5 μ l ddH₂O

20x SSC

175.32 g Sodium chloride

88.23 g Sodium citrate

ad ddH₂O to make 1 L

adjust pH to 7.0

6. Appendix

Table 1: Characteristics of patient fibroblasts

Characteristics	P1	P2	Laminopathy associated trait	SUN1 associated trait	Reference
Proliferation	↓	↑	↓	↓	(Chen et al., 2012; Pratt et al., 2011)
Cell cycle distribution	Less M-phase cells *	Normal	Anaphase delay	Sun1-/-Sun2-/- Less cells in G2/M, S phase arrest	(Lei et al., 2012; Pratt et al., 2011)
Cell size	↑***	Normal	Nuclear size↑	-	(Pratt et al., 2011)
Centrosome-nucleus distance	↑*	↓*	↑*	-	(Hale et al., 2008) (Taranum et al., 2012)
Senescence-associated β-galactosidase	↑***	↑*	↑**	-	(Chen et al., 2012; Le Dour et al., 2011; Taranum et al., 2012) (Ho et al., 2011) (Benson et al., 2010)
Sensitivity towards heat shock	↑	↑	↑	-	(Taranum et al., 2012) (Paradisi et al., 2005)
Single cell motility	↑**	Normal	↓	-	(Chancellor et al., 2010; Lee et al., 2007; Taranum et al., 2012)
Lamin B1 protein level	↓**	Normal	↓	-	(Liu et al., 2011)
SUN1 protein level	↓**	↓*	-	-	-
SUN2 protein level	Normal	↑***	-	-	-
LAP2 protein level	↓***	↓***	↓	-	(Liu et al., 2011)
Nesprin-2 protein level	↓**	Normal	-	-	-
Interaction between LaminA/C and SUN1	↓**	↓**	-	-	-

*Significance: * $p < 0.05$, ** $p < 0.01$, *** $p < 0.001$.

Table 2: Characteristics of wild-type fibroblasts expressing wild-type and mutant SUN1 proteins in immunofluorescence

Characteristics	SUN1	SUN1-A203V	SUN1-A614V
Lamin A/C	Localization	Nuclear envelope	Nuclear envelope
	Expression	Normal	Normal
Lamin B1	Localization	Nuclear envelope	Nuclear envelope
	Expression	Normal	Normal
Emerin	Localization	Nuclear envelope and aggregates	Nuclear envelope and aggregates
	Expression	↓	↓
SUN2	Localization	Nuclear envelope	Nuclear envelope
	Expression	↓	↓
LAP2	Localization	Nuclear envelope and dots	Nuclear envelope and dots
	Expression	↓	↓
Interaction with Emerin	Normal	↓	↓

7. Abbreviations

ATP	Adenosine triphosphat
bp	Base pair(s)
cDNA	Complementary DNA
CT	C-terminus
Da	Dalton
DAPI	4'-6-diamidino-2-phenylindole
DMSO	Dimethyl sulfoxide
DNA	Deoxyribonucleic acid
dNTP	Deoxynucleoside triphosphate
DTT	Dithiothreitol
<i>E. coli</i>	<i>Escherichia coli</i>
EDTA	Ethylene diamine tetraacetic acid
FBS	Fetal bovine serum
Fw	forward
g	Gramm
<i>g</i>	Relative centrifugation force
GAPDH	Glycerinaldehydephosphate dehydrogenase
GFP	Green fluorescent protein
GST	Glutathione S-transferase
h	Hour (s)
HEPES	4-(2-hydroxyethyl)-1-piperazineethanesulfonic acid
IgG	Immunglobulin G
IPTG	Isopropyl- β -Dithiogalactopyranoside
kb	Kilobases
KD	Knock down
kDa	kilodalton
LAP	Lamina-associated polypeptide
LC-MS	Liquid chromatography–mass spectrometry
MDa	Mega Dalton
min	Minute (s)
mM	Millimolar
mRNA	messenger ribonucleic acid

Abbreviations

NP-40	Nonidet P-40
NT	N-terminus
OD	Optical density
PBS	Phosphate buffered saline
PCR	Polymerase chain reaction
PFA	Paraformaldehyde
pH	negative decadic logarithm of protein concentration
PIC	Proteinase inhibitor cocktail
PMSF	Phenylmethanesulfonyl fluoride
PVDF	Polyvinylidene difluoride
qRT-PCR	Quantitative real time PCR
RIPA	Radioimmunoprecipitation assay
RNAi	RNA interference
rpm	Rotation per minute
RT	Room temperature
Rv	Reverse
SD	Standard deviation
SDS-PAGE	Sodium dodecyl sulfate polyacrylamide gel electrophoresis
Sec	Second (s)
siRNA	Small interfering RNA
SSC	Saline-sodium citrate
TAE	Tris-Acetate-EDTA
Taq	Thermophilus aquaticus
TE	Tris-EDTA
TEMED	N,N,N',N'-Tetramethylethylenediamine
Tris	Tris (hydroxymethyl) aminomethane
tRNA	Transfer-RNA
µg	Microgram
µl	Microliter
µM	Micromolar
UV	Ultraviolet light
WB	Western blot
WT	Wild type
X-gal	5-bromo-4-chloro-3-indolyl-D-galactopyranosid

8. References

- Aitchison, J.D., and Rout, M.P. 2012. The yeast nuclear pore complex and transport through it. *Genetics*. 190:855-883.
- Apel, E.D., Lewis, R.M., Grady, R.M., and Sanes, J.R. 2000. Syne-1, a dystrophin- and Klarsicht-related protein associated with synaptic nuclei at the neuromuscular junction. *J Biol Chem*. 275:31986-31995.
- Attali, R., Warwar, N., Israel, A., Gurt, I., McNally, E., Puckelwartz, M., Glick, B., Nevo, Y., Ben-Neriah, Z., and Melki, J. 2009. Mutation of SYNE-1, encoding an essential component of the nuclear lamina, is responsible for autosomal recessive arthrogyriposis. *Hum Mol Genet*. 18:3462-3469.
- Bachi, A., Braun, I.C., Rodrigues, J.P., Pante, N., Ribbeck, K., von Kobbe, C., Kutay, U., Wilm, M., Gorlich, D., Carmo-Fonseca, M., and Izaurralde, E. 2000. The C-terminal domain of TAP interacts with the nuclear pore complex and promotes export of specific CTE-bearing RNA substrates. *RNA*. 6:136-158.
- Ball, J.R., Dimaano, C., and Ullman, K.S. 2004. The RNA binding domain within the nucleoporin Nup153 associates preferentially with single-stranded RNA. *RNA*. 10:19-27.
- Bastos, R., Lin, A., Enarson, M., and Burke, B. 1996. Targeting and function in mRNA export of nuclear pore complex protein Nup153. *J Cell Biol*. 134:1141-1156.
- Bengtsson, L., and Wilson, K.L. 2006. Barrier-to-autointegration factor phosphorylation on Ser-4 regulates emerin binding to lamin A in vitro and emerin localization in vivo. *Mol Biol Cell*. 17:1154-1163.
- Benson, E.K., Lee, S.W., and Aaronson, S.A. 2010. Role of progerin-induced telomere dysfunction in HGPS premature cellular senescence. *J Cell Sci*. 123:2605-2612.
- Bokenkamp, R., Raz, V., Venema, A., DeRuiter, M.C., van Munsteren, C., Olive, M., Nabel, E.G., and Gittenberger-de Groot, A.C. 2011. Differential temporal and spatial progerin expression during closure of the ductus arteriosus in neonates. *PLoS One*. 6:e23975.
- Brachner, A., and Foisner, R. 2011. Evolvement of LEM proteins as chromatin tethers at the nuclear periphery. *Biochem Soc Trans*. 39:1735-1741.
- Brussino, A., Vaula, G., Cagnoli, C., Mauro, A., Pradotto, L., Daniele, D., Di Gregorio, E., Barberis, M., Arduino, C., Squadrone, S., Abete, M.C., Migone, N., Calabrese, O., and Brusco, A. 2009. A novel family with Lamin B1 duplication associated with adult-onset leucoencephalopathy. *J Neurol Neurosurg Psychiatry*. 80:237-240.

- Brussino, A., Vaula, G., Cagnoli, C., Panza, E., Seri, M., Di Gregorio, E., Scappaticci, S., Camanini, S., Daniele, D., Bradac, G.B., Pinessi, L., Cavalieri, S., Grosso, E., Migone, N., and Brusco, A. 2010. A family with autosomal dominant leukodystrophy linked to 5q23.2-q23.3 without lamin B1 mutations. *Eur J Neurol.* 17:541-549.
- Butin-Israeli, V., Adam, S.A., Goldman, A.E., and Goldman, R.D. 2012. Nuclear lamin functions and disease. *Trends Genet.* 28:464-471.
- Cai, M., Huang, Y., Ghirlando, R., Wilson, K.L., Craigie, R., and Clore, G.M. 2001. Solution structure of the constant region of nuclear envelope protein LAP2 reveals two LEM-domain structures: one binds BAF and the other binds DNA. *EMBO J.* 20:4399-4407.
- Cai, M., Huang, Y., Suh, J.Y., Louis, J.M., Ghirlando, R., Craigie, R., and Clore, G.M. 2007. Solution NMR structure of the barrier-to-autointegration factor-Emerin complex. *J Biol Chem.* 282:14525-14535.
- Capelson, M., Doucet, C., and Hetzer, M.W. 2010. Nuclear pore complexes: guardians of the nuclear genome. *Cold Spring Harb Symp Quant Biol.* 75:585-597.
- Carmody, S.R., and Wenthe, S.R. 2009. mRNA nuclear export at a glance. *J Cell Sci.* 122:1933-1937.
- Chancellor, T.J., Lee, J., Thodeti, C.K., and Lele, T. 2010. Actomyosin tension exerted on the nucleus through nesprin-1 connections influences endothelial cell adhesion, migration, and cyclic strain-induced reorientation. *Biophys J.* 99:115-123.
- Chang, W., Worman, H.J., and Gundersen, G.G. 2015. Accessorizing and anchoring the LINC complex for multifunctionality. *J Cell Biol.* 208:11-22.
- Chen, C.Y., Chi, Y.H., Mutalif, R.A., Starost, M.F., Myers, T.G., Anderson, S.A., Stewart, C.L., and Jeang, K.T. 2012. Accumulation of the inner nuclear envelope protein Sun1 is pathogenic in progeric and dystrophic laminopathies. *Cell.* 149:565-577.
- Chkheidze, A.N., Lyakhov, D.L., Makeyev, A.V., Morales, J., Kong, J., and Liebhaber, S.A. 1999. Assembly of the alpha-globin mRNA stability complex reflects binary interaction between the pyrimidine-rich 3' untranslated region determinant and poly(C) binding protein alphaCP. *Mol Cell Biol.* 19:4572-4581.
- Collier, B., Goobar-Larsson, L., Sokolowski, M., and Schwartz, S. 1998. Translational inhibition in vitro of human papillomavirus type 16 L2 mRNA mediated through interaction with heterogenous ribonucleoprotein K and poly(rC)-binding proteins 1 and 2. *J Biol Chem.* 273:22648-22656.

- Crisp, M., Liu, Q., Roux, K., Rattner, J.B., Shanahan, C., Burke, B., Stahl, P.D., and Hodzic, D. 2006. Coupling of the nucleus and cytoplasm: role of the LINC complex. *J Cell Biol.* 172:41-53.
- Culjkovic-Kraljacic, B., and Borden, K.L. 2013. Aiding and abetting cancer: mRNA export and the nuclear pore. *Trends Cell Biol.* 23:328-335.
- Culjkovic, B., Topisirovic, I., Skrabanek, L., Ruiz-Gutierrez, M., and Borden, K.L. 2006. eIF4E is a central node of an RNA regulon that governs cellular proliferation. *J Cell Biol.* 175:415-426.
- Daigle, N., Beaudouin, J., Hartnell, L., Imreh, G., Hallberg, E., Lippincott-Schwartz, J., and Ellenberg, J. 2001. Nuclear pore complexes form immobile networks and have a very low turnover in live mammalian cells. *J Cell Biol.* 154:71-84.
- Dechat, T., Pflieger, K., Sengupta, K., Shimi, T., Shumaker, D.K., Solimando, L., and Goldman, R.D. 2008. Nuclear lamins: major factors in the structural organization and function of the nucleus and chromatin. *Genes Dev.* 22:832-853.
- Denning, D.P., Patel, S.S., Uversky, V., Fink, A.L., and Rexach, M. 2003. Disorder in the nuclear pore complex: the FG repeat regions of nucleoporins are natively unfolded. *Proc Natl Acad Sci U S A.* 100:2450-2455.
- Dimaano, C., Ball, J.R., Prunuske, A.J., and Ullman, K.S. 2001. RNA association defines a functionally conserved domain in the nuclear pore protein Nup153. *J Biol Chem.* 276:45349-45357.
- Dimaano, C., and Ullman, K.S. 2004. Nucleocytoplasmic transport: integrating mRNA production and turnover with export through the nuclear pore. *Mol Cell Biol.* 24:3069-3076.
- Dittmer, T.A., and Misteli, T. 2011. The lamin protein family. *Genome Biol.* 12:222.
- Doring, V., Veretout, F., Albrecht, R., Muhlbauer, B., Schlatterer, C., Schleicher, M., and Noegel, A.A. 1995. The in vivo role of annexin VII (synexin): characterization of an annexin VII-deficient Dictyostelium mutant indicates an involvement in Ca(2+)-regulated processes. *J Cell Sci.* 108 (Pt 5):2065-2076.
- Dreyfuss, G., Kim, V.N., and Kataoka, N. 2002. Messenger-RNA-binding proteins and the messages they carry. *Nat Rev Mol Cell Biol.* 3:195-205.
- Dreyfuss, G., Matunis, M.J., Pinol-Roma, S., and Burd, C.G. 1993. hnRNP proteins and the biogenesis of mRNA. *Annu Rev Biochem.* 62:289-321.
- Ellis, J.A., and Shackleton, S. 2011. Nuclear envelope disease and chromatin organization. *Biochem Soc Trans.* 39:1683-1686.

- Enarson, P., Enarson, M., Bastos, R., and Burke, B. 1998. Amino-terminal sequences that direct nucleoporin nup153 to the inner surface of the nuclear envelope. *Chromosoma*. 107:228-236.
- Expert-Bezancon, A., Le Caer, J.P., and Marie, J. 2002. Heterogeneous nuclear ribonucleoprotein (hnRNP) K is a component of an intronic splicing enhancer complex that activates the splicing of the alternative exon 6A from chicken beta-tropomyosin pre-mRNA. *J Biol Chem*. 277:16614-16623.
- Fahrenkrog, B., Maco, B., Fager, A.M., Koser, J., Sauder, U., Ullman, K.S., and Aebi, U. 2002. Domain-specific antibodies reveal multiple-site topology of Nup153 within the nuclear pore complex. *J Struct Biol*. 140:254-267.
- Folkmann, A.W., Collier, S.E., Zhan, X., Aditi, Ohi, M.D., and Wentz, S.R. 2013. Gle1 functions during mRNA export in an oligomeric complex that is altered in human disease. *Cell*. 155:582-593.
- Fried, H., and Kutay, U. 2003. Nucleocytoplasmic transport: taking an inventory. *Cell Mol Life Sci*. 60:1659-1688.
- Frohnert, C., Schweizer, S., and Hoyer-Fender, S. 2011. SPAG4L/SPAG4L-2 are testis-specific SUN domain proteins restricted to the apical nuclear envelope of round spermatids facing the acrosome. *Mol Hum Reprod*. 17:207-218.
- Fukuda, T., Naiki, T., Saito, M., and Irie, K. 2009. hnRNP K interacts with RNA binding motif protein 42 and functions in the maintenance of cellular ATP level during stress conditions. *Genes Cells*. 14:113-128.
- Galy, V., Mattaj, I.W., and Askjaer, P. 2003. *Caenorhabditis elegans* nucleoporins Nup93 and Nup205 determine the limit of nuclear pore complex size exclusion in vivo. *Mol Biol Cell*. 14:5104-5115.
- Gao, J., Li, Y., Fu, X., and Luo, X. 2012. A Chinese patient with acquired partial lipodystrophy caused by a novel mutation with LMNB2 gene. *J Pediatr Endocrinol Metab*. 25:375-377.
- Gorjanacz, M., Klerkx, E.P., Galy, V., Santarella, R., Lopez-Iglesias, C., Askjaer, P., and Mattaj, I.W. 2007. *Caenorhabditis elegans* BAF-1 and its kinase VRK-1 participate directly in post-mitotic nuclear envelope assembly. *EMBO J*. 26:132-143.
- Griffis, E.R., Craige, B., Dimaano, C., Ullman, K.S., and Powers, M.A. 2004. Distinct functional domains within nucleoporins Nup153 and Nup98 mediate transcription-dependent mobility. *Mol Biol Cell*. 15:1991-2002.

- Gros-Louis, F., Dupre, N., Dion, P., Fox, M.A., Laurent, S., Verreault, S., Sanes, J.R., Bouchard, J.P., and Rouleau, G.A. 2007. Mutations in SYNE1 lead to a newly discovered form of autosomal recessive cerebellar ataxia. *Nat Genet.* 39:80-85.
- Grossman, E., Medalia, O., and Zwerger, M. 2012. Functional architecture of the nuclear pore complex. *Annu Rev Biophys.* 41:557-584.
- Gruter, P., Tabernero, C., von Kobbe, C., Schmitt, C., Saavedra, C., Bachi, A., Wilm, M., Felber, B.K., and Izaurralde, E. 1998. TAP, the human homolog of Mex67p, mediates CTE-dependent RNA export from the nucleus. *Mol Cell.* 1:649-659.
- Gundersen, G.G., and Worman, H.J. 2013. Nuclear positioning. *Cell.* 152:1376-1389.
- Guttler, T., and Gorlich, D. 2011. Ran-dependent nuclear export mediators: a structural perspective. *EMBO J.* 30:3457-3474.
- Habelhah, H., Shah, K., Huang, L., Ostareck-Lederer, A., Burlingame, A.L., Shokat, K.M., Hentze, M.W., and Ronai, Z. 2001. ERK phosphorylation drives cytoplasmic accumulation of hnRNP-K and inhibition of mRNA translation. *Nat Cell Biol.* 3:325-330.
- Hagan, I., and Yanagida, M. 1995. The product of the spindle formation gene *sad1+* associates with the fission yeast spindle pole body and is essential for viability. *J Cell Biol.* 129:1033-1047.
- Hale, C.M., Shrestha, A.L., Khatau, S.B., Stewart-Hutchinson, P.J., Hernandez, L., Stewart, C.L., Hodzic, D., and Wirtz, D. 2008. Dysfunctional connections between the nucleus and the actin and microtubule networks in laminopathic models. *Biophys J.* 95:5462-5475.
- Han, S.P., Tang, Y.H., and Smith, R. 2010. Functional diversity of the hnRNPs: past, present and perspectives. *Biochem J.* 430:379-392.
- Haque, F., Lloyd, D.J., Smallwood, D.T., Dent, C.L., Shanahan, C.M., Fry, A.M., Trembath, R.C., and Shackleton, S. 2006. SUN1 interacts with nuclear lamin A and cytoplasmic nesprins to provide a physical connection between the nuclear lamina and the cytoskeleton. *Mol Cell Biol.* 26:3738-3751.
- Haque, F., Mazzeo, D., Patel, J.T., Smallwood, D.T., Ellis, J.A., Shanahan, C.M., and Shackleton, S. 2010. Mammalian SUN protein interaction networks at the inner nuclear membrane and their role in laminopathy disease processes. *J Biol Chem.* 285:3487-3498.

- Harborth, J., Elbashir, S.M., Bechert, K., Tuschl, T., and Weber, K. 2001. Identification of essential genes in cultured mammalian cells using small interfering RNAs. *J Cell Sci.* 114:4557-4565.
- Hegele, R.A., Cao, H., Liu, D.M., Costain, G.A., Charlton-Menys, V., Rodger, N.W., and Durrington, P.N. 2006. Sequencing of the reannotated LMNB2 gene reveals novel mutations in patients with acquired partial lipodystrophy. *Am J Hum Genet.* 79:383-389.
- Herold, A., Teixeira, L., and Izaurralde, E. 2003. Genome-wide analysis of nuclear mRNA export pathways in *Drosophila*. *EMBO J.* 22:2472-2483.
- Ho, J.C., Zhou, T., Lai, W.H., Huang, Y., Chan, Y.C., Li, X., Wong, N.L., Li, Y., Au, K.W., Guo, D., Xu, J., Siu, C.W., Pei, D., Tse, H.F., and Esteban, M.A. 2011. Generation of induced pluripotent stem cell lines from 3 distinct laminopathies bearing heterogeneous mutations in lamin A/C. *Aging (Albany NY).* 3:380-390.
- Hocine, S., Singer, R.H., and Grunwald, D. 2010. RNA processing and export. *Cold Spring Harb Perspect Biol.* 2:a000752.
- Hoeltzenbein, M., Karow, T., Zeller, J.A., Warzok, R., Wulff, K., Zschesche, M., Herrmann, F.H., Grosse-Heitmeyer, W., and Wehnert, M.S. 1999. Severe clinical expression in X-linked Emery-Dreifuss muscular dystrophy. *Neuromuscul Disord.* 9:166-170.
- Honore, B., Rasmussen, H.H., Vorum, H., Dejgaard, K., Liu, X., Gromov, P., Madsen, P., Gesser, B., Tommerup, N., and Celis, J.E. 1995. Heterogeneous nuclear ribonucleoproteins H, H', and F are members of a ubiquitously expressed subfamily of related but distinct proteins encoded by genes mapping to different chromosomes. *J Biol Chem.* 270:28780-28789.
- Horn, H.F., Brownstein, Z., Lenz, D.R., Shivatzki, S., Dror, A.A., Dagan-Rosenfeld, O., Friedman, L.M., Roux, K.J., Kozlov, S., Jeang, K.T., Frydman, M., Burke, B., Stewart, C.L., and Avraham, K.B. 2013. The LINC complex is essential for hearing. *J Clin Invest.* 123:740-750.
- Houben, F., Willems, C.H., Declercq, I.L., Hochstenbach, K., Kamps, M.A., Snoeckx, L.H., Ramaekers, F.C., and Broers, J.L. 2009. Disturbed nuclear orientation and cellular migration in A-type lamin deficient cells. *Biochim Biophys Acta.* 1793:312-324.
- Hutten, S., and Kehlenbach, R.H. 2007. CRM1-mediated nuclear export: to the pore and beyond. *Trends Cell Biol.* 17:193-201.
- Inoue, H., Nojima, H., and Okayama, H. 1990. High efficiency transformation of *Escherichia coli* with plasmids. *Gene.* 96:23-28.

- Isermann, P., and Lammerding, J. 2013. Nuclear mechanics and mechanotransduction in health and disease. *Curr Biol.* 23:R1113-1121.
- Izaurrealde, E. 2002. A novel family of nuclear transport receptors mediates the export of messenger RNA to the cytoplasm. *Eur J Cell Biol.* 81:577-584.
- Izaurrealde, E., Jarmolowski, A., Beisel, C., Mattaj, I.W., Dreyfuss, G., and Fischer, U. 1997. A role for the M9 transport signal of hnRNP A1 in mRNA nuclear export. *J Cell Biol.* 137:27-35.
- Jaspersen, S.L., Martin, A.E., Glazko, G., Giddings, T.H., Jr., Morgan, G., Mushegian, A., and Winey, M. 2006. The Sad1-UNC-84 homology domain in Mps3 interacts with Mps2 to connect the spindle pole body with the nuclear envelope. *J Cell Biol.* 174:665-675.
- Kiledjian, M., Wang, X., and Liebhaber, S.A. 1995. Identification of two KH domain proteins in the alpha-globin mRNP stability complex. *EMBO J.* 14:4357-4364.
- Kohler, A., and Hurt, E. 2007. Exporting RNA from the nucleus to the cytoplasm. *Nat Rev Mol Cell Biol.* 8:761-773.
- Kracklauer, M.P., Banks, S.M., Xie, X., Wu, Y., and Fischer, J.A. 2007. Drosophila klaroid encodes a SUN domain protein required for Klarsicht localization to the nuclear envelope and nuclear migration in the eye. *Fly (Austin).* 1:75-85.
- Kudo, N., Wolff, B., Sekimoto, T., Schreiner, E.P., Yoneda, Y., Yanagida, M., Horinouchi, S., and Yoshida, M. 1998. Leptomycin B inhibition of signal-mediated nuclear export by direct binding to CRM1. *Exp Cell Res.* 242:540-547.
- Laguri, C., Gilquin, B., Wolff, N., Romi-Lebrun, R., Courchay, K., Callebaut, I., Worman, H.J., and Zinn-Justin, S. 2001. Structural characterization of the LEM motif common to three human inner nuclear membrane proteins. *Structure.* 9:503-511.
- Le Dour, C., Schneebeli, S., Bakiri, F., Darcel, F., Jacquemont, M.L., Maubert, M.A., Auclair, M., Jeziorowska, D., Reznik, Y., Bereziat, V., Capeau, J., Lascols, O., and Vigouroux, C. 2011. A homozygous mutation of prelamin-A preventing its farnesylation and maturation leads to a severe lipodystrophic phenotype: new insights into the pathogenicity of nonfarnesylated prelamin-A. *J Clin Endocrinol Metab.* 96:E856-862.
- Lee, J.S., Hale, C.M., Panorchan, P., Khatau, S.B., George, J.P., Tseng, Y., Stewart, C.L., Hodzic, D., and Wirtz, D. 2007. Nuclear lamin A/C deficiency induces defects in cell mechanics, polarization, and migration. *Biophys J.* 93:2542-2552.

- Lei, K., Zhu, X., Xu, R., Shao, C., Xu, T., Zhuang, Y., and Han, M. 2012. Inner nuclear envelope proteins SUN1 and SUN2 play a prominent role in the DNA damage response. *Curr Biol.* 22:1609-1615.
- Li, P., Meinke, P., Huong le, T.T., Wehnert, M., and Noegel, A.A. 2014. Contribution of SUN1 mutations to the pathomechanism in muscular dystrophies. *Hum Mutat.* 35:452-461.
- Libotte, T., Zaim, H., Abraham, S., Padmakumar, V.C., Schneider, M., Lu, W., Munck, M., Hutchison, C., Wehnert, M., Fahrenkrog, B., Sauder, U., Aebi, U., Noegel, A.A., and Karakesisoglou, I. 2005. Lamin A/C-dependent localization of Nesprin-2, a giant scaffold at the nuclear envelope. *Mol Biol Cell.* 16:3411-3424.
- Lin, F., Blake, D.L., Callebaut, I., Skerjanc, I.S., Holmer, L., McBurney, M.W., Paulin-Levasseur, M., and Worman, H.J. 2000. MAN1, an inner nuclear membrane protein that shares the LEM domain with lamina-associated polypeptide 2 and emerin. *J Biol Chem.* 275:4840-4847.
- Liu, G.H., Barkho, B.Z., Ruiz, S., Diep, D., Qu, J., Yang, S.L., Panopoulos, A.D., Suzuki, K., Kurian, L., Walsh, C., Thompson, J., Boue, S., Fung, H.L., Sancho-Martinez, I., Zhang, K., Yates, J., 3rd, and Izpisua Belmonte, J.C. 2011. Recapitulation of premature ageing with iPSCs from Hutchinson-Gilford progeria syndrome. *Nature.* 472:221-225.
- Liu, Q., Pante, N., Misteli, T., Elsagga, M., Crisp, M., Hodzic, D., Burke, B., and Roux, K.J. 2007. Functional association of Sun1 with nuclear pore complexes. *J Cell Biol.* 178:785-798.
- Lu, W., Gotzmann, J., Sironi, L., Jaeger, V.M., Schneider, M., Luke, Y., Uhlen, M., Szigyarto, C.A., Brachner, A., Ellenberg, J., Foisner, R., Noegel, A.A., and Karakesisoglou, I. 2008. Sun1 forms immobile macromolecular assemblies at the nuclear envelope. *Biochim Biophys Acta.* 1783:2415-2426.
- Luke, Y., Zaim, H., Karakesisoglou, I., Jaeger, V.M., Sellin, L., Lu, W., Schneider, M., Neumann, S., Beijer, A., Munck, M., Padmakumar, V.C., Gloy, J., Walz, G., and Noegel, A.A. 2008. Nesprin-2 Giant (NUANCE) maintains nuclear envelope architecture and composition in skin. *J Cell Sci.* 121:1887-1898.
- Lynch, M., Chen, L., Ravitz, M.J., Mehtani, S., Korenblat, K., Pazin, M.J., and Schmidt, E.V. 2005. hnRNP K binds a core polypyrimidine element in the eukaryotic translation initiation factor 4E (eIF4E) promoter, and its regulation of eIF4E contributes to neoplastic transformation. *Mol Cell Biol.* 25:6436-6453.

- Malone, C.J., Fixsen, W.D., Horvitz, H.R., and Han, M. 1999. UNC-84 localizes to the nuclear envelope and is required for nuclear migration and anchoring during *C. elegans* development. *Development*. 126:3171-3181.
- Margalit, A., Brachner, A., Gotzmann, J., Foisner, R., and Gruenbaum, Y. 2007. Barrier-to-autointegration factor--a BAFfling little protein. *Trends Cell Biol*. 17:202-208.
- Margalit, A., Segura-Totten, M., Gruenbaum, Y., and Wilson, K.L. 2005. Barrier-to-autointegration factor is required to segregate and enclose chromosomes within the nuclear envelope and assemble the nuclear lamina. *Proc Natl Acad Sci U S A*. 102:3290-3295.
- Martinez-Contreras, R., Fiset, J.F., Nasim, F.U., Madden, R., Cordeau, M., and Chabot, B. 2006. Intronic binding sites for hnRNP A/B and hnRNP F/H proteins stimulate pre-mRNA splicing. *PLoS Biol*. 4:e21.
- Matunis, M.J., Xing, J., and Dreyfuss, G. 1994. The hnRNP F protein: unique primary structure, nucleic acid-binding properties, and subcellular localization. *Nucleic Acids Res*. 22:1059-1067.
- Mejat, A., and Misteli, T. 2010. LINC complexes in health and disease. *Nucleus*. 1:40-52.
- Michael, W.M., Choi, M., and Dreyfuss, G. 1995a. A nuclear export signal in hnRNP A1: a signal-mediated, temperature-dependent nuclear protein export pathway. *Cell*. 83:415-422.
- Michael, W.M., Siomi, H., Choi, M., Pinol-Roma, S., Nakielny, S., Liu, Q., and Dreyfuss, G. 1995b. Signal sequences that target nuclear import and nuclear export of pre-mRNA-binding proteins. *Cold Spring Harb Symp Quant Biol*. 60:663-668.
- Molloy, A., Cotter, O., van Spaendonk, R., Siermans, E., and Sweeney, B. 2012. A patient with a rare leukodystrophy related to lamin B1 duplication. *Ir Med J*. 105:186-187.
- Moore, M.J., and Proudfoot, N.J. 2009. Pre-mRNA processing reaches back to transcription and ahead to translation. *Cell*. 136:688-700.
- Morimoto, A., Shibuya, H., Zhu, X., Kim, J., Ishiguro, K., Han, M., and Watanabe, Y. 2012. A conserved KASH domain protein associates with telomeres, SUN1, and dynactin during mammalian meiosis. *J Cell Biol*. 198:165-172.
- Mukhopadhyay, N.K., Kim, J., Cinar, B., Ramachandran, A., Hager, M.H., Di Vizio, D., Adam, R.M., Rubin, M.A., Raychaudhuri, P., De Benedetti, A., and Freeman, M.R. 2009. Heterogeneous nuclear ribonucleoprotein K is a novel regulator of androgen receptor translation. *Cancer Res*. 69:2210-2218.

- Nakielny, S., Shaikh, S., Burke, B., and Dreyfuss, G. 1999. Nup153 is an M9-containing mobile nucleoporin with a novel Ran-binding domain. *EMBO J.* 18:1982-1995.
- Natalizio, B.J., and Wentz, S.R. 2013. Postage for the messenger: designating routes for nuclear mRNA export. *Trends Cell Biol.* 23:365-373.
- Nichols, R.J., Wiebe, M.S., and Traktman, P. 2006. The vaccinia-related kinases phosphorylate the N' terminus of BAF, regulating its interaction with DNA and its retention in the nucleus. *Mol Biol Cell.* 17:2451-2464.
- Noegel, A.A., Blau-Wasser, R., Sultana, H., Muller, R., Israel, L., Schleicher, M., Patel, H., and Weijer, C.J. 2004. The cyclase-associated protein CAP as regulator of cell polarity and cAMP signaling in Dictyostelium. *Mol Biol Cell.* 15:934-945.
- Oeffinger, M., and Zenklusen, D. 2012. To the pore and through the pore: a story of mRNA export kinetics. *Biochim Biophys Acta.* 1819:494-506.
- Ostareck, D.H., Ostareck-Lederer, A., Shatsky, I.N., and Hentze, M.W. 2001. Lipoygenase mRNA silencing in erythroid differentiation: The 3'UTR regulatory complex controls 60S ribosomal subunit joining. *Cell.* 104:281-290.
- Ostareck, D.H., Ostareck-Lederer, A., Wilm, M., Thiele, B.J., Mann, M., and Hentze, M.W. 1997. mRNA silencing in erythroid differentiation: hnRNP K and hnRNP E1 regulate 15-lipoxygenase translation from the 3' end. *Cell.* 89:597-606.
- Padiath, Q.S., Saigoh, K., Schiffmann, R., Asahara, H., Yamada, T., Koeppen, A., Hogan, K., Ptacek, L.J., and Fu, Y.H. 2006. Lamin B1 duplications cause autosomal dominant leukodystrophy. *Nat Genet.* 38:1114-1123.
- Padmakumar, V.C., Abraham, S., Braune, S., Noegel, A.A., Tunggal, B., Karakesisoglou, I., and Korenbaum, E. 2004. Enaptin, a giant actin-binding protein, is an element of the nuclear membrane and the actin cytoskeleton. *Exp Cell Res.* 295:330-339.
- Padmakumar, V.C., Libotte, T., Lu, W., Zaim, H., Abraham, S., Noegel, A.A., Gotzmann, J., Foisner, R., and Karakesisoglou, I. 2005. The inner nuclear membrane protein Sun1 mediates the anchorage of Nesprin-2 to the nuclear envelope. *J Cell Sci.* 118:3419-3430.
- Paradisi, M., McClintock, D., Boguslavsky, R.L., Pedicelli, C., Worman, H.J., and Djabali, K. 2005. Dermal fibroblasts in Hutchinson-Gilford progeria syndrome with the lamin A G608G mutation have dysmorphic nuclei and are hypersensitive to heat stress. *BMC Cell Biol.* 6:27.
- Pinol-Roma, S., and Dreyfuss, G. 1992. Shuttling of pre-mRNA binding proteins between nucleus and cytoplasm. *Nature.* 355:730-732.

- Pinol-Roma, S., and Dreyfuss, G. 1993. hnRNP proteins: localization and transport between the nucleus and the cytoplasm. *Trends Cell Biol.* 3:151-155.
- Pratt, C.H., Curtain, M., Donahue, L.R., and Shopland, L.S. 2011. Mitotic defects lead to pervasive aneuploidy and accompany loss of RB1 activity in mouse LmnaDhe dermal fibroblasts. *PLoS One.* 6:e18065.
- Rashmi, R.N., Eckes, B., Glockner, G., Groth, M., Neumann, S., Gloy, J., Sellin, L., Walz, G., Schneider, M., Karakesisoglou, I., Eichinger, L., and Noegel, A.A. 2012. The nuclear envelope protein Nesprin-2 has roles in cell proliferation and differentiation during wound healing. *Nucleus.* 3:172-186.
- Razafsky, D., Wirtz, D., and Hodzic, D. 2014. Nuclear envelope in nuclear positioning and cell migration. *Adv Exp Med Biol.* 773:471-490.
- Rothballer, A., and Kutay, U. 2013. The diverse functional LINC of the nuclear envelope to the cytoskeleton and chromatin. *Chromosoma.* 122:415-429.
- Rothballer, A., Schwartz, T.U., and Kutay, U. 2013. LINCing complex functions at the nuclear envelope: what the molecular architecture of the LINC complex can reveal about its function. *Nucleus.* 4:29-36.
- Roux, K.J., Crisp, M.L., Liu, Q., Kim, D., Kozlov, S., Stewart, C.L., and Burke, B. 2009. Nesprin 4 is an outer nuclear membrane protein that can induce kinesin-mediated cell polarization. *Proc Natl Acad Sci U S A.* 106:2194-2199.
- Salpingidou, G., Smertenko, A., Hausmanowa-Petruciewicz, I., Hussey, P.J., and Hutchison, C.J. 2007. A novel role for the nuclear membrane protein emerin in association of the centrosome to the outer nuclear membrane. *J Cell Biol.* 178:897-904.
- Schirmer, E.C., Florens, L., Guan, T., Yates, J.R., 3rd, and Gerace, L. 2003. Nuclear membrane proteins with potential disease links found by subtractive proteomics. *Science.* 301:1380-1382.
- Schneider, M., Lu, W., Neumann, S., Brachner, A., Gotzmann, J., Noegel, A.A., and Karakesisoglou, I. 2011. Molecular mechanisms of centrosome and cytoskeleton anchorage at the nuclear envelope. *Cell Mol Life Sci.* 68:1593-1610.
- Schreiber, K.H., and Kennedy, B.K. 2013. When lamins go bad: nuclear structure and disease. *Cell.* 152:1365-1375.
- Schumacher, J., Reichenzeller, M., Kempf, T., Schnolzer, M., and Herrmann, H. 2006. Identification of a novel, highly variable amino-terminal amino acid sequence element in the nuclear intermediate filament protein lamin B(2) from higher vertebrates. *FEBS Lett.* 580:6211-6216.

- Schuster, J., Sundblom, J., Thuresson, A.C., Hassin-Baer, S., Klopstock, T., Dichgans, M., Cohen, O.S., Raininko, R., Melberg, A., and Dahl, N. 2011. Genomic duplications mediate overexpression of lamin B1 in adult-onset autosomal dominant leukodystrophy (ADLD) with autonomic symptoms. *Neurogenetics*. 12:65-72.
- Shan, J., Al-Rumaihi, K., Rabah, D., Al-Bozom, I., Kizhakayil, D., Farhat, K., Al-Said, S., Kfoury, H., Dsouza, S.P., Rowe, J., Khalak, H.G., Jafri, S., Aigha, II, and Chouchane, L. 2013. Genome scan study of prostate cancer in Arabs: identification of three genomic regions with multiple prostate cancer susceptibility loci in Tunisians. *J Transl Med*. 11:121.
- Shao, X., Tarnasky, H.A., Lee, J.P., Oko, R., and van der Hoorn, F.A. 1999. Spag4, a novel sperm protein, binds outer dense-fiber protein Odf1 and localizes to microtubules of manchette and axoneme. *Dev Biol*. 211:109-123.
- Shimi, T., Koujin, T., Segura-Totten, M., Wilson, K.L., Haraguchi, T., and Hiraoka, Y. 2004. Dynamic interaction between BAF and emerin revealed by FRAP, FLIP, and FRET analyses in living HeLa cells. *J Struct Biol*. 147:31-41.
- Shumaker, D.K., Lee, K.K., Tanhehco, Y.C., Craigie, R., and Wilson, K.L. 2001. LAP2 binds to BAF.DNA complexes: requirement for the LEM domain and modulation by variable regions. *EMBO J*. 20:1754-1764.
- Siddiqui, N., and Borden, K.L. 2012. mRNA export and cancer. *Wiley Interdiscip Rev RNA*. 3:13-25.
- Simon, D.N., and Wilson, K.L. 2011. The nucleoskeleton as a genome-associated dynamic 'network of networks'. *Nat Rev Mol Cell Biol*. 12:695-708.
- Simon, D.N., and Wilson, K.L. 2013. Partners and post-translational modifications of nuclear lamins. *Chromosoma*. 122:13-31.
- Sosa, B.A., Kutay, U., and Schwartz, T.U. 2013. Structural insights into LINC complexes. *Curr Opin Struct Biol*. 23:285-291.
- Sosa, B.A., Rothballer, A., Kutay, U., and Schwartz, T.U. 2012. LINC complexes form by binding of three KASH peptides to domain interfaces of trimeric SUN proteins. *Cell*. 149:1035-1047.
- Stains, J.P., Lecanda, F., Towler, D.A., and Civitelli, R. 2005. Heterogeneous nuclear ribonucleoprotein K represses transcription from a cytosine/thymidine-rich element in the osteocalcin promoter. *Biochem J*. 385:613-623.
- Stewart, C.L., Roux, K.J., and Burke, B. 2007. Blurring the boundary: the nuclear envelope extends its reach. *Science*. 318:1408-1412.

- Strambio-De-Castillia, C., Niepel, M., and Rout, M.P. 2010. The nuclear pore complex: bridging nuclear transport and gene regulation. *Nat Rev Mol Cell Biol.* 11:490-501.
- Stutz, F., and Izaurralde, E. 2003. The interplay of nuclear mRNP assembly, mRNA surveillance and export. *Trends Cell Biol.* 13:319-327.
- Sukegawa, J., and Blobel, G. 1993. A nuclear pore complex protein that contains zinc finger motifs, binds DNA, and faces the nucleoplasm. *Cell.* 72:29-38.
- Suzuki, K., Bose, P., Leong-Quong, R.Y., Fujita, D.J., and Riabowol, K. 2010. REAP: A two minute cell fractionation method. *BMC Res Notes.* 3:294.
- Talamas, J.A., and Hetzer, M.W. 2011. POM121 and Sun1 play a role in early steps of interphase NPC assembly. *J Cell Biol.* 194:27-37.
- Taranum, S., Vaylann, E., Meinke, P., Abraham, S., Yang, L., Neumann, S., Karakesisoglou, I., Wehnert, M., and Noegel, A.A. 2012. LINC complex alterations in DMD and EDMD/CMT fibroblasts. *Eur J Cell Biol.* 91:614-628.
- Topisirovic, I., Siddiqui, N., Lapointe, V.L., Trost, M., Thibault, P., Bangeranye, C., Pinol-Roma, S., and Borden, K.L. 2009. Molecular dissection of the eukaryotic initiation factor 4E (eIF4E) export-competent RNP. *EMBO J.* 28:1087-1098.
- Turgay, Y., Champion, L., Balazs, C., Held, M., Toso, A., Gerlich, D.W., Meraldi, P., and Kutay, U. 2014. SUN proteins facilitate the removal of membranes from chromatin during nuclear envelope breakdown. *J Cell Biol.* 204:1099-1109.
- Tzur, Y.B., Wilson, K.L., and Gruenbaum, Y. 2006. SUN-domain proteins: 'Velcro' that links the nucleoskeleton to the cytoskeleton. *Nat Rev Mol Cell Biol.* 7:782-788.
- van der Loo, B., Fenton, M.J., and Erusalimsky, J.D. 1998. Cytochemical detection of a senescence-associated beta-galactosidase in endothelial and smooth muscle cells from human and rabbit blood vessels. *Exp Cell Res.* 241:309-315.
- Vigouroux, C., Auclair, M., Dubosclard, E., Pouchelet, M., Capeau, J., Courvalin, J.C., and Buendia, B. 2001. Nuclear envelope disorganization in fibroblasts from lipodystrophic patients with heterozygous R482Q/W mutations in the lamin A/C gene. *J Cell Sci.* 114:4459-4468.
- Visa, N., Alzhanova-Ericsson, A.T., Sun, X., Kiseleva, E., Bjorkroth, B., Wurtz, T., and Daneholt, B. 1996. A pre-mRNA-binding protein accompanies the RNA from the gene through the nuclear pores and into polysomes. *Cell.* 84:253-264.
- Wagner, N., and Krohne, G. 2007. LEM-Domain proteins: new insights into lamin-interacting proteins. *Int Rev Cytol.* 261:1-46.

- Wang, W., Shi, Z., Jiao, S., Chen, C., Wang, H., Liu, G., Wang, Q., Zhao, Y., Greene, M.I., and Zhou, Z. 2012. Structural insights into SUN-KASH complexes across the nuclear envelope. *Cell Res.* 22:1440-1452.
- Wente, S.R., and Rout, M.P. 2010. The nuclear pore complex and nuclear transport. *Cold Spring Harb Perspect Biol.* 2:a000562.
- Wickramasinghe, V.O., McMurtrie, P.I., Mills, A.D., Takei, Y., Penrhyn-Lowe, S., Amagase, Y., Main, S., Marr, J., Stewart, M., and Laskey, R.A. 2010. mRNA export from mammalian cell nuclei is dependent on GANP. *Curr Biol.* 20:25-31.
- Wilhelmsen, K., Litjens, S.H., Kuikman, I., Tshimbalanga, N., Janssen, H., van den Bout, I., Raymond, K., and Sonnenberg, A. 2005. Nesprin-3, a novel outer nuclear membrane protein, associates with the cytoskeletal linker protein plectin. *J Cell Biol.* 171:799-810.
- Worman, H.J. 2012. Nuclear lamins and laminopathies. *J Pathol.* 226:316-325.
- Worman, H.J., and Gundersen, G.G. 2006. Here come the SUNs: a nucleocytoplasmic missing link. *Trends Cell Biol.* 16:67-69.
- Wu, J., Matunis, M.J., Kraemer, D., Blobel, G., and Coutavas, E. 1995. Nup358, a cytoplasmically exposed nucleoporin with peptide repeats, Ran-GTP binding sites, zinc fingers, a cyclophilin A homologous domain, and a leucine-rich region. *J Biol Chem.* 270:14209-14213.
- Xiong, H., Rivero, F., Euteneuer, U., Mondal, S., Mana-Capelli, S., Laroche, D., Vogel, A., Gassen, B., and Noegel, A.A. 2008. Dictyostelium Sun-1 connects the centrosome to chromatin and ensures genome stability. *Traffic.* 9:708-724.
- Yang, J., Bogerd, H.P., Wang, P.J., Page, D.C., and Cullen, B.R. 2001. Two closely related human nuclear export factors utilize entirely distinct export pathways. *Mol Cell.* 8:397-406.
- Yokoyama, N., Hayashi, N., Seki, T., Pante, N., Ohba, T., Nishii, K., Kuma, K., Hayashida, T., Miyata, T., Aebi, U., and et al. 1995. A giant nucleopore protein that binds Ran/TC4. *Nature.* 376:184-188.
- Zhang, Q., Ragnauth, C., Greener, M.J., Shanahan, C.M., and Roberts, R.G. 2002. The nesprins are giant actin-binding proteins, orthologous to *Drosophila melanogaster* muscle protein MSP-300. *Genomics.* 80:473-481.
- Zhang, X., Lei, K., Yuan, X., Wu, X., Zhuang, Y., Xu, T., Xu, R., and Han, M. 2009. SUN1/2 and Syne/Nesprin-1/2 complexes connect centrosome to the nucleus during neurogenesis and neuronal migration in mice. *Neuron.* 64:173-187.

- Zheng, R., Ghirlando, R., Lee, M.S., Mizuuchi, K., Krause, M., and Craigie, R. 2000. Barrier-to-autointegration factor (BAF) bridges DNA in a discrete, higher-order nucleoprotein complex. *Proc Natl Acad Sci U S A*. 97:8997-9002.
- Zhong, N., Radu, G., Ju, W., and Brown, W.T. 2005. Novel progerin-interactive partner proteins hnRNP E1, EGF, Mel 18, and UBC9 interact with lamin A/C. *Biochem Biophys Res Commun*. 338:855-861.
- Zhou, Z., Du, X., Cai, Z., Song, X., Zhang, H., Mizuno, T., Suzuki, E., Yee, M.R., Berezov, A., Murali, R., Wu, S.L., Karger, B.L., Greene, M.I., and Wang, Q. 2012. Structure of Sad1-UNC84 homology (SUN) domain defines features of molecular bridge in nuclear envelope. *J Biol Chem*. 287:5317-5326.

Acknowledgement

It's a great honor for me to express my sincere gratitude to all the people who helped me during my PhD study. To begin with, I would like to thank Prof. Angelika A. Noegel for offering me the opportunity to complete my PhD thesis in her institute. In the last years, she was always there to listen to problems, discuss results and cheer me up when things were not working in the way they should. I am very grateful for all her enthusiasm, constant support and excellent scientific guidance which provide me another opportunity to become a scientific worker. Her influences to my professional and personal career cannot be expressed in words. Thank you very much Prof. Noegel for everything.

My sincere thanks to Prof. Mirka Uhlirova, Prof. Michael Nothnagel and Prof. Ludwig Eichinger for becoming a part of my thesis committee. I also convey my genuine thanks to Prof. Manfred Wehnert (currently retired from Institute of Human Genetics and Interfaculty Institute of Genetics and Functional Genomics, Ernst-Moritz-Arndt-University, Greifswald, Germany) for giving us the patient fibroblasts; to Prof. Birthe Fahrenkrog (Institute for Molecular Biology and Medicine, Université Libre de Bruxelles, Charleroi, Belgium) and Prof. Stuart A Wilson (Department of Molecular Biology and Biotechnology, University of Sheffield, Sheffield, UK) for providing the Nup153 and NXF1 plasmids, respectively.

Everything is hard in the beginning, but I was helped a lot at that time. I would like to thank Eva V for introducing the interesting project to me and guiding me in the very beginning; deepest thanks to Napoleon for teaching and showing me the most experimental methods with great patience and being friendly with me all the time. I also want to give my thanks to Raphael for teaching me the cell migration experiment very patiently; to Marija Marko for helping me with the germen summary of my thesis and always giving suggestions whenever I need help.

Thanks to Rosi for introducing me the microscope; to Martina for showing me how to culture the patients' fibroblast and providing me the constructs what I required in my thesis; to Maria for solving my cloning problem which I tried many times, improving the organization in the lab which made us feel more comfortable and always helping and giving suggestions; to Berthold for telling me many stories about Germany and often bringing nice cakes to our office; to Rolf for helping me design the qRT-PCR primers and constructing the GFP-

Acknowledgement

CCDC87 plasmid in the beginning, and his exquisite cloning technology impressing me a lot. I extend my thanks to Budi and Gudrun for their computing assistance, to Dörte for her kind help concerning the official things which made life easy in this new city, to Sonja and Brigitte for helping with all the important reagents and media.

Many thanks to my dear friends who helped me at any time and spent enjoyable time with me whether inside or outside the institute. I convey my thanks to Sandra H for always nice to me and inviting us for coffee and visiting the top of the Dom; to Ilknur for involving me in many events and seeking pleasure amid the hardship with me when facing the difficulties; to Kurchi for talking and discussing the experiments with me no matter how long it takes and act as my "dictionary" when I need help; to Sandra S for keeping us at her place when we were homeless due to bomb excavating. Warm thanks to Anja, Liu, Carmen, Karthic, Salil, Carolin, Kosmas, Vivek, Atul, Emrah, Jan, Ramesh, Susanne, Roxana, Lin, Unni and Sarah for being so kind, friendly and helpful to me.

My deepest gratitude is dedicated to my parents and parents in law who supported and encouraged me at any time. Their love and trust made me much stronger in my PhD life. Very special thanks to my husband Qihong for his constant love, care, support, and understanding whether in work or life. I am very lucky to have his accompanying in these years which made my life colorful.

Finally, I would like to thank China Scholarship Council for the financial support and all the people who directly or indirectly helped me during my PhD study and my life in cologne.

Erklärung

Ich versichere, dass ich die von mir vorgelegte Dissertation selbständig angefertigt, die benutzten Quellen und Hilfsmittel vollständig angegeben und die Stellen der Arbeit - einschließlich Tabellen und Abbildungen -, die anderen Werken im Wortlaut oder dem Sinn nach entnommen sind, in jedem Einzelfall als Entlehnung kenntlich gemacht habe; dass diese Dissertation noch keiner anderen Fakultät oder Universität zur Prüfung vorgelegen hat; dass sie - abgesehen von der unten angegebenen Teilpublikation - noch nicht veröffentlicht ist, sowie, dass ich eine Veröffentlichung vor Abschluss des Promotionsverfahrens nicht vornehmen werde.

Die Bestimmungen dieser Promotionsordnung sind mir bekannt. Die von mir vorgelegte Dissertation ist von Prof. Dr. Angelika A. Noegel betreut worden.

Köln, 27.04.2015

(Ping Li)

Teilpublikation

Li, P., Meinke, P., Huong le, T.T., Wehnert, M., and Noegel, A.A. 2014. Contribution of SUN1 mutations to the pathomechanism in muscular dystrophies. *Hum Mutat.* 35:452-461.

Lebenslauf

Persönliche Daten

Name: Ping Li
Geburtsdatum: 06.11.1984
Nationalität: Chinesisch
Anschrift: Luxemburger str 124-136, 50939 Köln
E-mail: pli6@uni-koeln.de

Universitätsstudium

09.2004~06.2008 Bachelor in Bioscience
Studien an der Pädagogische Universität Shanxi, V.R. China

09.2008~06.2011 Magister in Biochemie und Molekular Biologie
Magisterstudium an der Shanxi Univeristät, V.R. China

Promotionsstudium

seit 10.2011 Promotion in Biochemie
Mathematisch-Naturwissenschaftliche Fakultät
Universität zu Köln,
Betreuerin: Prof. Dr. Angelika A. Noegel,
Institut Für Biochemie I, Medizinische Fakultät
Universität zu Köln, Köln, Deutschland

Publikation

Li, P., Meinke, P., Huong le, T.T., Wehnert, M., and Noegel, A.A. 2014. Contribution of SUN1 mutations to the pathomechanism in muscular dystrophies. *Hum Mutat.* 35:452-461.